NIAC 2013 Phase I Final Report

Biomaterials out of thin air: *in situ*, on-demand printing of advanced biocomposites

A New Materials Design and Production Technique using 3D-Printed Arrays of of Bioengineered Cells

Diana Gentry, NASA Ames Research Center (Co-I.) (diana.gentry@nasa.gov)
Ashley Micks, Stanford University (aemixx@stanford.edu)
Lynn Rothschild, NASA Ames Research Center (P.I.) (lynn.j.rothschild@nasa.gov)

June 3, 2014

Contents

1 Executive Summary

We have completed the proof of concept described in our Phase I proposal, a two-material array of non-structural proteins. We created an implementation of each step in our technology concept (Figure 7.1) and demonstrated its critical functionality (Table 7.2). The biological chassis and printing hardware we created as part of this work can be re-used for future work by inserting a material coding region upstream of the fluorescent tag. Overall, we showed that our technology concept is sound.

The mission benefit analyses, as described in our Phase I proposal, are complete and contained in this report. These calculations show that our technology can save hundreds of kilograms of upmass for a potential planetary human habit construction mission: the mass per habitat module can be reduced by approximately one third if the biomaterials are manufactured on Earth and included in the mission upmass, and the full 240 kg per module can be saved if the materials are derived entirely from *in situ* resources. Mass savings between these two extremes is expected for an actual mission, depending on the level of *in situ* resource extraction technology. We have shown that continued advancement of this technology concept for use in a space mission environment is justified.

Our survey of future development pathways proved extremely informative in light of the lessons learned from our proof of concept work and mission scenario analyses. For example, we were able for the first time to distinguish between the levels of functionality provided by production of structural proteins, other polymers such as polysaccharides, and true organic-inorganic composites such as bone and mineralized shell. This new information represents a significant advance in formulating specific applications, and key enabling technologies, for our proposed concept.

We surveyed potential collaborations with other projects and synergies with enabling technologies that are developing. We have received requests for collaboration from other institutions, including labs at Stanford University and Drexel University. We have also received visits from industry, including Organovo, a tissue engineering company, and Autodesk, a major 3D and materials design software company. Finally, we have been in touch with the team behind the 2013 NIAC Phase II 'Super Ball Bot - Structures for Planetary Landing and Exploration' and are planning to develop our biomaterial printing technology with the goal of enabling tensegrity-based rovers such as theirs to use lighter, more robust materials.

A smooth transition from TRL 2 to TRL 3 assumes that the implementations of the technology concept which demonstrate critical functionality are also pathways for future development; while this is the case for most hardware or software projects, the multidisciplinary nature of our project, particularly the biological aspect of it, means that this is not always true. For example, as part of this work we showed that although there are large number of known genetic parts that correspond to non-structural materials, this is not true for sequences for structural organic proteins, let alone biominerals. These realizations allowed us to further subdivide our concept into more detailed development areas, some of which are clearly established at TRL 3, others of which were newly identified sub-technologies moved from TRL 1 to TRL 2.

Similarly, although a single feasibility/benefit analysis is sufficient for advancement from TRL 2 to TRL 3, not all potential benefits to a technology concept as broad in scope as ours are apparent at TRL 2. Both our future pathways survey and our proof of concept work highlighted that the true mass savings potential of our technology concept cannot be quantified without modification of existing materials modelling tools to take into account the possibility of positional materials properties customization. Therefore, we have simultaneously both advanced one potential set of applications of our technology concept from TRL 2 to TRL 3 and also identified a previously unknown set of applications and advanced it from TRL 1 to TRL 2.

Overall, we have moved the original formulation of our concept forward from TRL 2 to TRL 3, and the

expanded formulation of it presented in this document has been advanced from a combination of TRL 1 and early TRL 2 to an overall late TRL 2. We have also identified the key areas necessary for both short-term and long-term advancement, and made recommendations for specific future work in the most promising directions. With future work on a 1–2 year timeframe to continue advancement to overall TRL 3, we will be well positioned to begin work on a specific space mission technology insertion path.

Concept

A 3D array of bioengineered living cells deposits materials, both biological and inorganic, that are bound into nonliving, microstructured finished products.

Potential applications:

- high-fidelity, low-overhead reproduction of existing biomaterials (food, wood, bone)
- flexible, just-in-time manufacturing and repair in on- and off-Earth environments
- rapid design and production of new, synthetic biomaterials
- opens up new frontiers in space missions, advanced manufacturing, and material science

Study Approach

Proof-of-concept:

- Optimize cell dispensing system for digitized materials
- Engineer S. cerevisiae cells to secrete material components
- Show successful cell secretion and material separation
- Produce a 2-material array from a digitized template

Feasibility/Benefit Study

- Determine effect of printing parameters on material yield
- Determine effect of printing parameters on material structure
- Identify key procedural parameters of technique
- Use results to determine potential upmass reduction of long-term Mars habitat

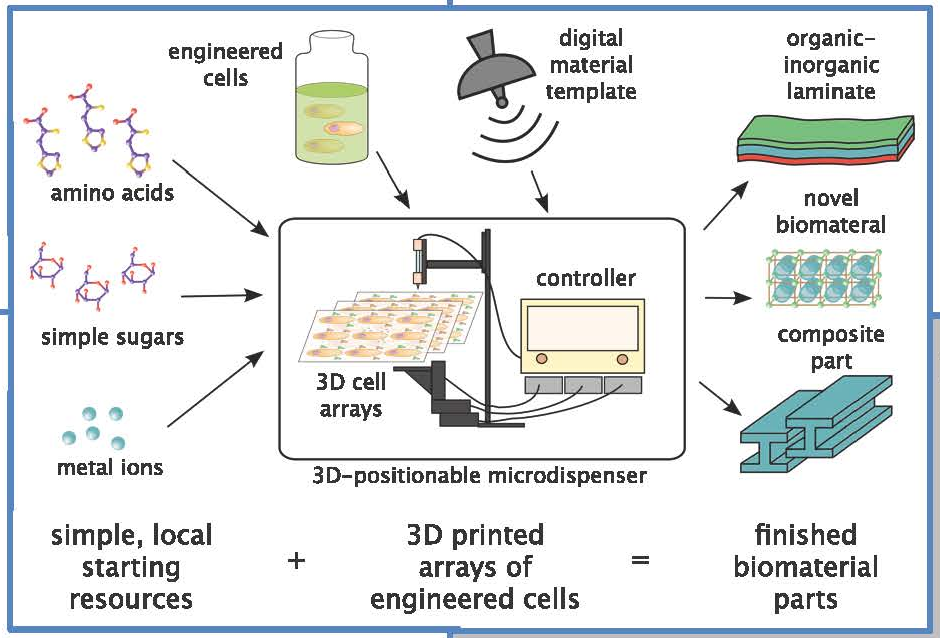

Benefits

Of the concept:

- drastically reduces upmass requirements of many current space missions
- greatly multiplies potential of off-planet in situ resource utilization
- enables new class of space missions currently precluded by material transport needs
- vast potential for exploration of novel, synthetic biomaterials and biocomposites

Of this study:

- given current progress, potential of approach can be established or dismissed in single year
- technology moved from TRL 2 to 3

Evaluation Notes

3 Introduction

3.1 Summary of Concept

Imagine a space mission structural module, whether lander frame, rover chassis, habitat support, or spacecraft hull, built from a single, continuous material. No pins, no bolts, no rivets; no joins, no welds, no laminates. The structural material's properties have been customized at a molecular level to allow it to be dense, rigid and load-bearing where necessary yet light and flexible wherever possible, drastically reducing total mass. The hierarchical microstructure of the material allows it to be far more fracture-resistant and energy-dissipating for its weight than traditional engineering materials, fundamentally altering the risk balance of planetary exploration.

Building further upon the mission concept, imagine that the structural material transitions seamlessly into a flexible gas barrier, creating functional unification between tensile, compressive, and pressurization support. Inherent 'joints', created by customizing directional material flexibility along particular axes, allow the entire structure to fold up like an umbrella into a smaller configuration when depressurized for reduced launch or re-entry volume. The open interior of the structure provides usable space for other mission functionality, including internal actuation, thermal protection, or radiation shielding. The ability to create a new class of biologically inspired materials customizable at this fine level will open up a new field of materials design for space applications.

Upmass requirements are the single most significant limitation of our current space mission capability. The limits of what we can economically launch and safely land severely restrict current missions and disqualify many others from consideration. For example, a lunar or Mars base would require heavy manufacturing equipment and construction materials far beyond our current transportation capacity. We believe that our proposed approach to structural materials manufacturing has the capability to both reduce upmass and allow the construction of a new category of strong, lightweight, multifunctional structures. It is a wide-ranging new synthetic material design and production technique, capable of creating novel biocomposites and laminates with customized physical properties; vastly increasing the use of extraterrestrial *in situ* resources in place of transported materials; and enabling just-in-time manufacturing of needed parts in off-Earth environments.

Our technique combines the emergent technologies of 3D live cell printing and synthetic biology. We will 3D print cells which have been genetically engineered to produce the constituent organic and inorganic phases of the desired synthetic biomaterial at rates under human control. Varying the internal self-assembly of the constituents at multiple spatial scales – ranging from the crystal lattice structure at the molecular scale to bonded 'plates' and 'scales' in the millimeter range – will enable the production of single-material, continuous structures with superior performance to any currently available. This technology will fundamentally invert the traditional relationship between materials and structural design. Given a set of structural requirements, designers currently must choose the shape of a structural element based on its material properties; under this new paradigm, designers need simply calculate the material properties necessary to suit the desired shape.

Specific applications include:

- *Reduced upmass requirements for space missions.* We can implement both just-in-time manufacturing of all needed materials from a small stock of basic resources and direct production of finished parts from digital templates, eliminating the need to bring most pre- and post-processing manufacturing equipment. The upmass requirements for everything from the ISS to, one day, a long-term lunar or Martian

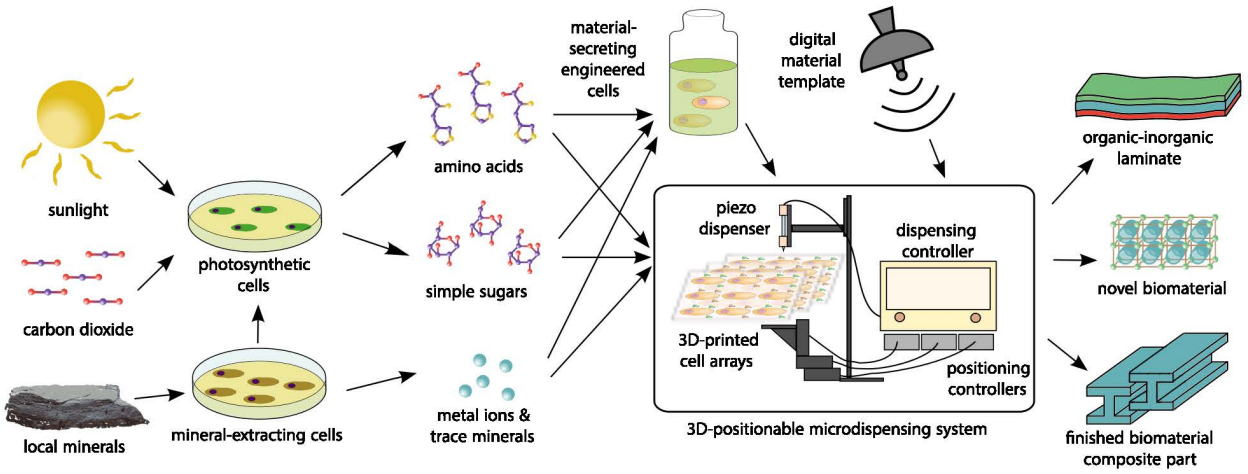

Figure 3.1: When combined with advances in in situ resource extraction and space synthetic biology, our technology concept has the potential to enable low-overhead, on-demand manufacturing of advanced, customized synthetic biomaterials in a space mission context.

base would be drastically reduced.

- Increased mission robustness for human exploration.With the ability to manufacture a wide range of materials and structures on an as-needed basis, astronauts can address unforeseen challenges using the best tools and materials for the job, regardless of whether those items were included in the payload.
- Increased use ofin situ resources in off-Earth environments.Since the cells make the biomaterial components of the finished product from basic molecules, a wide variety of materials – food, cloth, machine parts, construction materials – can be made from a very limited basic resource palette. In situ resources could replace transported ones in maintaining a long-term human space presence, building structures on other worlds, and even asteroid mining.
- Improved landing structures. The highly energy-absorbing properties of structural biomaterials allow them to withstand much greater loading conditions, particularly sudden shocks, than traditional engineering materials. They offer the possibility oflarge, lightweight landing structures, replacing mass-limited airbags or complex 'skyhook'-type approaches, that significantly increase the potential science payload of an MSL-type planetary exploration mission.
- Highly resilient exploration devices.The same energy-absorbing properties can be used to create chassis for planetary rovers that are extremely resilient to unexpected impacts such as falls or collisions. This greatly reduces the risk of remote or autonomous planetary exploration missions, particularly those with long time delay impeding supervisory control (e.g., Mars) or limited advanced sensing capabilities (e.g., Titan).

In short, this concept holds the potential to open up new frontiers in the human space presence, planetary exploration, advanced manufacturing, and materials science.

3.2 Review of Proposed Work

Our Phase 1 proposal had four objectives:

1. A feasibility and benefit analysis of this technology in two specific mission contexts. We proposed (1) a 'minimal working example' making a finished biomaterial part aboard the ISS, and (2) 'cradle-to-grave' use at a Mars human habitat. These analyses are presented in Section 6.

Table 3.1: TRL definitions as applied to our technology at the time of our Phase I proposal.

TRL	Definition	Status
'early' TRL 2	(a) technology concept formulated (b) documented speculative practical application	completed by Phase I white paper
TRL 2 exit	(a) feasibility/benefit analysis	Phase I Objective #1
'early' TRL 3	(a) proof-of-concept demonstration	Phase I Objective #2
'late' TRL 3	(a) analytical prediction of key parameters (b) laboratory validation of predictions	future work

2. *A proof-of-concept demonstration integrating all critical components of the biomaterial production technology.* A grid of two simple proteins, with a pattern demonstrated to correlate to the digital material template used to print the original cell array. Showing end-to-end critical functionality of each component part of our technology concept is necessary to validate the core technology concept. The process of implementing this demonstration and its results are included in Section 7.
3. *A proposed design of this technology for follow-on work.* We surveyed and provided recommendations for hardware, biological, and material implementations for the next stages of technology development. This objective complemented both #1 and #2, and is included in Section 8.
4. *A study of potential benefits of combining this technology with other concurrent, complementary studies.* We briefly survey potential synergies and collaborations between our technology concept and other current and emerging research topics. The conclusions are presented in Section 9.

As listed in our Phase I proposal, our goal was to produce, in a nine-month timeframe, the following: - a list of appropriate demonstration materials (Table 6.6, Table 6.2, and Table 6.3); - lines of cells expressing those material components (Figure 7.15); - a proof of concept demonstration created by printed arrays of these cells (Figure 7.26); - the results of microscopy that evaluate this proof of concept (Table 7.2); - estimates of the mass and energy cost for this system at the scale required for a Mars mission, along with the mass savings due to the use of this technology in place of traditional materials (Section 6).

All deliverables promised in our Phase I proposal are included, as listed above, in this report.

3.3 Technology Readiness Level Definitions

The established TRL categorical definitions require specification when applied to a particular technology. The formulation of the concept and the generalized aerospace potential applications in our Phase I Step A proposal met the criteria to establish the concept prior to our Phase I work as 'early TRL 2.'

To advance the TRL, two steps were required. The first, a feasibility/benefit analysis in a mission scenario, is the TRL 2 exit criterion. The second, a physical implementation of the technology idea sufficient to be a proof of concept, defines 'early TRL 3.' We include these definitions, the same as those in our Phase I proposal, in Table 3.1.

The purpose of including a proof-of-concept demonstration and mission feasibility/benefit analysis as part of TRL advancement is to answer those questions about cost and benefit that can be answered with the current state of knowledge and to bring to light those that cannot – in other words, to let us know what we do and don't know. Our technology is innovative, multidisciplinary, and extremely broad in potential scope; therefore, a significant part of both the proof of concept and the mission scenario analyses has been identifying the unknowns encountered raised and evaluating future paths to addressing them.

We completed the proof of concept described in our Phase I proposal (Objective #1), a two-material array of non-structural proteins. The biological chassis and printing hardware we created as part of this work can be re-used for a future structural proof of concept if one of the few structural proteins available as a

genetic part is used. However, our survey of available regulatory genetic parts (as part of Objective #3), particularly material delivery methods and coding regions for mineralization pathways, indicated that a significant amount of original synthetic biology work needs to be done before the biological system can be considered a general platform for structural material production.

The mission benefit analyses as described in our Phase I proposal (Objective #2) are contained in this report. As was appropriate for the information we had prior to the completion of the proof of concept, we focused on the benefits due to material substitution and *in situ* resource utilization. These calculations alone show that our technology can save hundreds of kilograms of upmass for a potential human habit construction mission, cutting the mass by one third if the biomaterials are manufactured on Earth and included in the mission upmass, and cutting the full 240 kg per module if the materials are derived entirely from *in situ* resources instead of aluminum and kevlar. However, as part of our proof of concept work, we showed that the true mass savings potential of our technology concept cannot be quantified without modification of existing materials modeling tools to take into account the possibility of positional materials properties customization. Development of these tools is within the scope of short-term (1–2 year) future work.

Taking these results of our Phase I work into account, we have defined the integral parts of our technology concept at a higher level of resolution – following the definition of the main different technology components shown in Figure 7.1, with some areas detailed further – and characterized each individual area in terms of its prior and current TRL. The results are shown in Table 3.2,

There are two major TRL advancements presented in this report. Firstly, the mission effects of applying our technology concept purely for its material substitution and on-site manufacturing capabilities show a clear benefit. Secondly, the proof of concept shows that there is at least one complete implementation of the concept that achieves all critical function in a non-structural material production run.

Beyond these advancements, we have added the mission effects of novel material design and material optimization as a new unknown and still TRL 2, as we cannot yet capture the technology concept's true potential without addressing them. We also list the organic/inorganic compositing aspect of our technology as advanced from TRL 1 to TRL 2, but pending future work on a second, structural proof of concept to reach TRL 3. We have listed our recommendations for this second proof of concept in Section 8.

3.4 Mission Scenarios Definitions

Due to the unusual breadth of potential aerospace applications of our technology concept, we decided to begin with two distinct mission concepts for our feasibility/benefit analysis. The two mission contexts were chosen to span different radiation, thermal, gravitational, and *in situ* resource availability regimes: (1) creating a structural replacement part aboard the International Space Station (ISS), and (2) providing a long-term Mars human habitat with construction materials, insulation, shielding, machine parts, and more. By examining the needed material functionality across at least two mission concepts, we were able to identify the types of missions and structures our concept is best suited to enable.

3.4.1 Structural Part Replacement, International Space Station

Our first mission scenario was chosen to emphasize the on-site manufacturing and material basis substitution potential of our concept. On the ISS, replacements for damaged parts must either be included as redundant mass in advance or sent up from Earth as needed. The first approach causes significant unused upmass, as parts which will not be needed must be sent up to ensure that there are sufficient replacements available for all critical components; the second approach risks time delays in providing critical functionality and may result in unused launch capacity. The ability to manufacture structural elements of a wide variety of materials, without having to bring all required base materials or limiting oneself to the types of feedstock compatible with current 3D printing techniques, would save both time and money while increasing mission robustness.

As a representative part that may need replacement, we chose a Nomex EVA tether with aluminum hooks,

Table 3.2: Summary of the components of our technology concept and their status before and after our Phase I work.

Obj.	Component	Pre-Phase I Status	Current Status
#1	material substition effects	2	3
#1	on site manufacturing effects	2	3
#1	novel material design effects	1	1
#1	material optimization effects	1	2
#2	host cell engineering	2	3
#2	plasmid backbone engineering	2	3
#2	biomaterial production	2	3
#2	structural material production	1	2
#2	material production control	2	3
#2	organic material delivery control	2	3
#2	inorganic material delivery control	1	2
#2	material binding control	2	2
#2	pint medium	2	3
#2	3D printing system	2	3
#2	print substrate	2	2
#2	2D material verification	2	3
#2	3D material verification	2	2

part number SED33104391–301 from the EVA Tools and Equipment Reference Book [1, p. 379]. A single-material part was chosen in order to provide a clear and straightforward comparison to the potential biomaterial-based alternatives. This is an element loaded in pure tension and consisting of a single material whose properties are constant along its length.

3.4.2 Long-Term Habitat Construction, Mars

Our second mission scenario was chosen to emphasize the *in situ* resource utilization and material form factor substitution potential of our concept.

In situ resource utilization is highlighted as key area for NASA due to its potential to reduce the upmass needed for planetary missions [52]. Our technique enhances this advantage, since with cell-based biomaterial production, the locally available carbon dioxide, sunlight, and regolith can be the raw materials needed to produce any number of structural materials.

We used the Human Exploration of Mars Design Reference Architecture 5.0 from NASAs Mars Architecture Steering Group [29] as a baseline mission architecture. As with the ISS mission scenario, we focused on a subset of needed structures to allow for a more in-depth materials breakdown. We chose habitats, as there is an long history of work on planetary habitat design (e.g., [13, 41, 71, 82]) and many of the constraints on planetary habitats are also applicable to spacecraft or space station modules [74]. We use the expandable habitat design from [71] as a specific material baseline where needed.

4 Technical Background

4.1 Definition of Structural Biomaterials

Biomaterials are the natural materials produced by and integrated into living systems, as well as artificial materials developed to mimic them [79]. (There is considerable debate over a precise definition of the term; we use it in its broadest possible useful sense here.) In size, they range from a single nanometer, for simple molecules like sugars, to micron-sized cell walls, to millimeter-sized sponge spicules, to meter-sized bones, to trees that can reach 100 m in height. In complexity, they range from largely amorphous soft matrices to highly structured, multi-layer composites of organic and inorganic constituents. There are many examples of naturally occurring materials showing all combinations of these characteristics (Figure 4.1); many proteins form highly ordered folded assemblies, and fist-sized sponge exoskeletons may be essentially bulk calcium carbonate deposits.

Our focus here is on *non-living, structural* biomaterials. In nature, these are the materials which are produced by, or integrated into, living systems to provide a physical, mechanical function – protection, leverage, support, and so on. The distinction between living tissue and non-living biomaterial is typically blurry in natural systems; an animal bone, for example, is a living organ that consists of active cells which have generated a complex, partially mineralized tissue, and it plays important hormonal and metabolic roles in addition to its mechanical one [89]. We define the structural biomaterial associated with bone as that extracellular part of the tissue which would, at least in theory, have essentially the same mechanical properties if all living cells were removed: a highly ordered composite of proteins (collagen, etc.) and biogenic minerals (calcium phosphate). Most structural biomaterials are rarely, if ever, found in a purely non-living state in nature; it is because our technology aims to create such forms of these materials that we term them 'synthetic biomaterials.'

Table 4.1 lists several examples of natural structural biomaterials and their most important constituents. A very common, though by no means dominant, type of arrangement consists of long-chain tough fibers such as collagen or keratin embedded in a softer and more compliant matrix. In some cases, such as spider silk, a single protein may fill both roles by alternating between different folding configurations; there are many more examples of composite materials in which the fibers and matrix are different material types. Most structural biomaterials are entirely organic, in the chemical sense of consisting of carbon-based compounds such as proteins, polysaccharides, and so forth. However, the most rigid structural biomaterials are those which have an additional inorganic component. These *biominerals* are formed through biologically-controlled crystallization of inorganic materials, such as calcium salts; this process of biomineralization is generally poorly understood [10], but there are known to be several different mechanisms involved in different species [6, 32, 86].

4.2 Properties of Structural Biomaterials

Naturally occurring structural biomaterials have several common traits relevant to our applications (see [61, 68, 105] for extensive reviews):

- *Hierarchical structure.* This, perhaps more than anything else, defines the class of biomaterials of most interest to us. Nacre, part of mollusk shell, is an excellent example (Figure 4.2): it has at least six different spatial scales of organization, with 'rods' bound together to form 'tiles', 'tiles' into 'shelves', and so on. The impressive toughness and resilience of many structural biomaterials emerge from their ability to distribute loading or impact energy between each of these microstructured levels.
- *Strong functional customization.* For example, the the non-living materials that compose insect [17] and

Table 4.1: Naturally occurring structural biomaterials may have compliant, rigid, organic, and inorganic components in any combination. It is worth noting how many different structures, with wildly differing mechanical properties, can be constructed from essentially the same basic components.

Structure	Example	Support (Matrix)	Structure (Organic)	Structure (Inorganic)	Notes
cytoskeletal fibers	all(?) cells	–	filamentous proteins	–	[60]
magnetosomes	bacteria	lipids, proteins	–	iron oxides or sulfides	[56]
frustrule	diatoms	silaffins	–	silica	[23]
microbial mats	microbial mats	polysaccharides	–	calcium carbonate	[42]
silk	silkworms	sericin	fibroin	–	[54]
silk	spiders	spidroin (amorphous)	spidroin (crystalline)	–	[76]
spicule	siliceous sponges	silicateins	–	silica	[87]
spicule	calcareous sponges	collagen	–	calcium carbonate	[86]
shell	crustaceans	resilin	chitin	calcium carbonate	[78, 102]
shell	mollusks	glycoproteins, polysaccharides	chitin	calcium carbonate	[61, 62]
feather	birds	unknown	keratin	–	[107]
tooth enamel	vertebrates	–	–	calcium phosphate	[33]
cartilage	animals	proteoglycans	collagen, elastin	–	[46]
horn, hoof	vertebrates	keratin (amorphous)	keratin (crystalline)	–	[101]
bone, scale	vertebrates	glycoproteins	collagen	calcium phosphate	[89, 107]
wood	plants	lignin	cellulose	–	

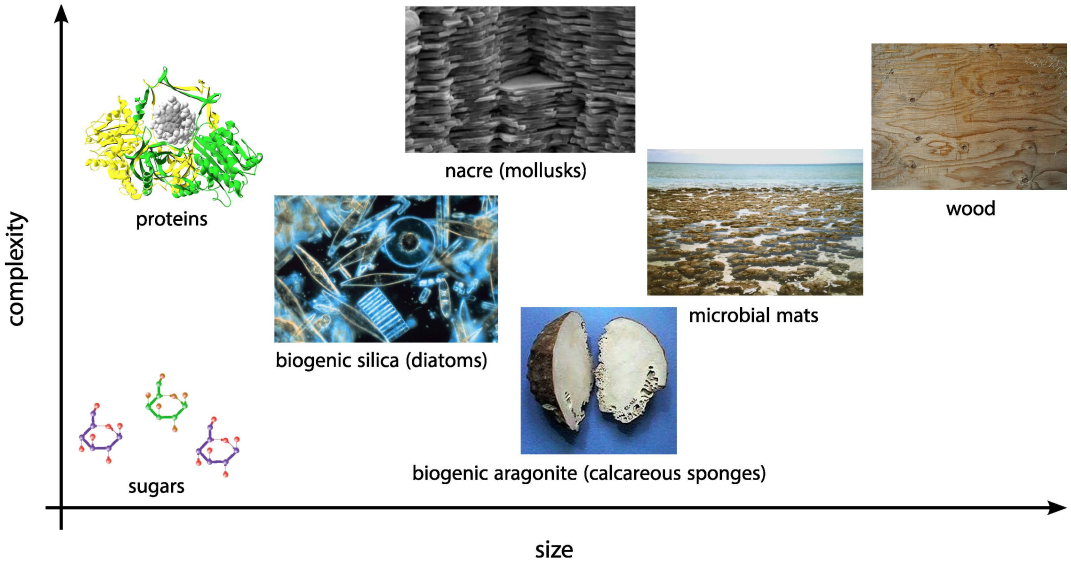

Figure 4.1: Biomaterials cover a wide range of size and complexity scales, ranging from simple biomolecules to macroscale organic-inorganic composites. (Non-original images are public domain.)

crustacean [78] exoskeletons are optimized at a molecular level to allow the structure to be dense, rigid and load-bearing where necessary yet light and flexible wherever possible; the outer surface transitions to a flexible vapor barrier, preventing dehydration; and the inner surface can transition to muscle or other attachments.

- Robust interfacing of distinct component materials. Many biominerals have organic and inorganic components interwoven in a highly ordered way on the molecular level. At a larger scale, many biological structures have continuous, gradient transitions between material phases [57, 106] – for example, the collagen fibers of rigid bone are essentially part of a continuous piece with the attached collagen-based tendons – which eliminates the weak points caused by seams, bolts, laminates, and so on in traditional human manufacture.
- Combinatorial complexity from basic molecular constituents. The basic building blocks of life are carbon, hydrogen, oxygen, nitrogen, phosphorus and sulfur. Proteins and polysaccharides have an astonishing array of properties despite having only a few dozen component monomers. There are relatively few inorganic components found in biomineralization – silica, calcium salts, and a few metals (primarily deposited by bacteria in sedimentary structures) comprise the vast majority. It is differences in the microstructures formed by these materials that are responsible for the incredible diversity of mechanical properties in structural biomaterials. This common material basis, combined with on-site manufacturing capabilities and the possibility of in situ resource extraction, makes biomaterials very mass-efficient to produce.
- Low mass. Structural biomaterials are near-universally less dense than traditionally-used manufacturing materials such as metals and ceramics. On many engineering measures – tensile strength, fracture resistance, elasticity, and so forth – they are also lighter for the same performance when tested under the directional loading conditions for which they are optimized (Table 6.2 , Table 6.3).
- Low energy manufacturing requirements. Biogenic materials are limited in manufacturing requirements by the amount of energy that can be spared by living systems. This is typically orders of magnitude lower than that required by, for example, casting metal or heat-molding plastic. This is achieved by, among others, use of catalysis, bottom-up 'self-assembly', and repeated use of naturally stable monomers. This is a potential advantage in low-energy environments such as the Moon and deep

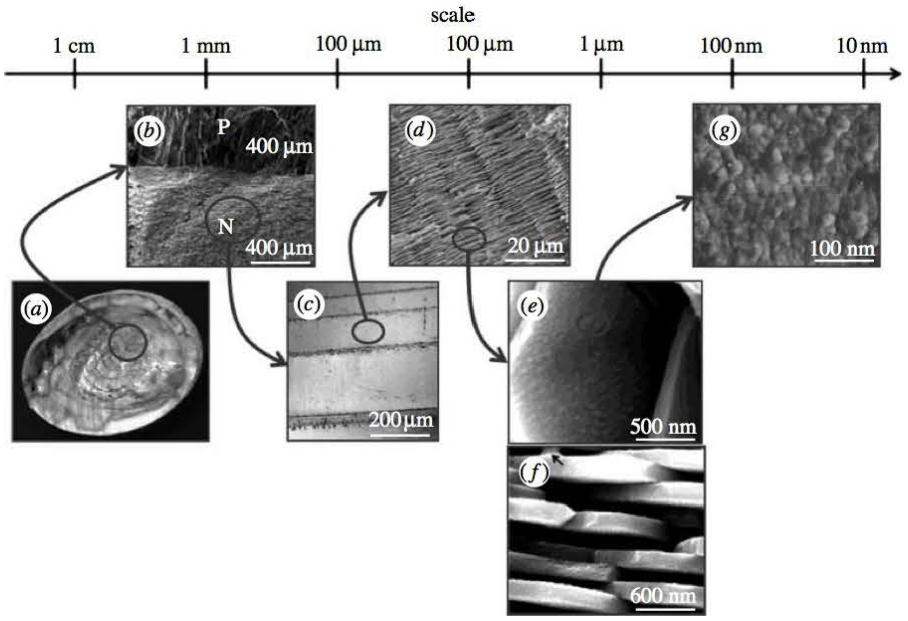

Figure 4.2: The macroscale mechanical properties of mollusk shell emerge from at least six different scales of structural organization, including 'bricks' and 'plates'. The shell material is an organic-inorganic composite whose primary components are calcium carbonate and chitin. Figure from [61].

space.

- Life-friendly environment manufacturing requirementsEssentially all biomaterials can be made at Earth-surface-normal pressure and temperature, near-neutral pH, moderate osmotic pressure, and so on (although cells may create internal microenvironments where the chemical environment can be quite different). This may be a disadvantage for materials which cannot be made in more space-typical environments during autonomous missions, but is an advantage on crewed space missions, as the manufacturing processes will pose no environmental risk to astronauts.

Beyond the already-discussed mollusk shell and arthropod cuticle, other light, tough, strong structural biomaterials include the feathers of birds [8], the bony plates of seahorse tails [77], and porcupine quills [69]. The ability of these natural structures to resist fracture and absorb impact or deformation energy has already been identified as highly desirable for human applications [17, 63, 65, 103].

So what prevents us from creating a large, multifunctional material structure using the same, non-living, biologically-derived constituents configured to suit human ends? There are three current roadblocks to human use of structural biomaterials:

- High production overheadNatural biomaterials are produced by living systems, which require a complete ecological support structure. Although this is only a moderate issue on Earth – raising a sheep to produce wool is, energetically speaking, absurdly expensive, but we generally have other reasons to raise sheep – it is an insurmountable barrier for use in space missions.
- Non-predictable microstructure. The process by which living systems fine-tune the microstructure of the materials they produce are poorly understood. We also lack the tools to predict the emergent mechanical properties of the overall material from its microstructure. Our inability to reproduce or predict the formation of these microstructures has led to an assumption that they make such materials unsuitable for human use.

- *Non-controllable macrostructure.* Life produces materials in the shape it needs. The enamel of tooth is found only in the shape of a tooth, the rachis of feather in the shape of a feather. Given the way the microstructures of the material are optimized to suit the function of the overall structure, the natural shape cannot simply be cut down to fit human needs without losing its mechanical benefits.

Our technology concept will eliminate all three of these drawbacks by allowing direct manufacture of synthetic biomaterials, treating the microstructure formation as a black box system to be empirically controlled, and allowing the materials to be produced in human-designed form factors.

5 State of the Art Review

5.1 3D Living Cell Printing

Additive manufacturing is a class of fabrication processes in which successive layers of material are laid down and bound together according to a 3D digital design. It comprises a variety of rapid prototyping and small-run manufacturing techniques, such as fused deposition modelling, powder sintering, and stereolithography; in recent years, some industrial firms have adapted the same approaches to larger scales. The term 3D printing, which originally referred to a specific subset of additive manufacturing technologies, is increasingly commonly used to refer to all additive manufacturing, particularly in the popular press; however, since we will be discussing several different additive manufacturing techniques in this section, we will stick to the more general term.

We will focus here on additive manufacturing techniques as they use, or are used for, biological and biomedical purposes; for a more general technical review, the reader is directed to a source such as [35].

Historically, additive manufacturing has been limited to either polymeric materials (plastics and waxes), which can be melted or photocured together, or thin sheets of materials like paper first cut and then bonded into laminates. More recent approaches have added metal and ceramics to the toolkit, primarily through techniques that deposit the materials in powdered form and then either fuse them to a secondary substrate or melt them together. Precision of material placement for these techniques varies with cost and implementation choices, but often approaches the microscale [84].

All of these approaches have two limitations relevant to our application. Firstly, the final material is made of the feedstock used – in other words, if the material laid down in layers is metal powder with a binding substrate, than the final piece will be made of porous metal mixed with binding substrate. Secondly, the material used must be relatively homogenous, as the process of fusing bulk smaller parts (whether powder particles, droplets of liquid, or solid laminate layers) into a larger whole is destructive to any internal material structure smaller than the scale of the parts. (Ceramics and metals do have small-grain crystalline structure, but these must re-form after powder fusion to be continuous; for this reason, fine temperature and positioning control during deposition, as well as post-processing with temperature treatments, are often necessary to prevent development of unplanned variation in the material properties of the final piece.) Thus, they cannot be used to make hierarchically structured materials such as the chitin and calcium carbonate complex of shell [32].

There have been two major drivers of the adoption of additive manufacturing technology for biological or bio-compatible materials over the past two decades. The first is the desire for microvolume cell or biomolecule spatial positioning, useful for compact and high-throughput biological or pharmaceutical assays [27, 58, 111, 113]. This approach tends to focus on single-cell precision and deposition speed, and is often only concerned with 2D spatial patterning. The second is the desire to construct replacement or testbed living tissues, a major goal of the field of tissue engineering [40] (also reviewed in [4, 28]). In this area, work typically focuses either on fabricating a non-living, biocompatible substrate onto which living cells can be seeded, in the hopes that they will grow over and bind into the substrate to form a 3D tissue, or on depositing layers of 'activated' cell clusters and stimulating them to form attachments to each other, a closer mimicry of natural tissue growth [49, 97].

A third, more recent driver is the discovery that the three-dimensional structure of groups of cells, both unicellular microbial cultures [18, 104] and multicellular tissues and tumors (reviewed in [55]), has a profound effect on their behavior. These techniques have hewed closely to those developed for tissue engineering, primarily creating biocompatible scaffolds – typically a combination of hydrogel [2], support proteins such

as collagen or its derivative gelatin [22, 96], and sometimes synthetic polymers [26] – seeded with cells to create 3D living cell clusters for purposes of testing environmental and pharmaceutical effects. Various depositional technologies have been developed for these scaffolds and cells, including optical gel cross-linking [22], chemical hydrogel cross-linking [92], liquid jet-based methods (reviewed in [80]), and laser thermal/photomechanical ejection [5].

The primary limitation of these 'bioprinting' technologies, where our application is concerned, is the lack of integration between single-cell resolution deposition and and biocompatible substrate construction. Although some hydrogel-based tissue engineering approaches can embed single cells, or small cell clusters, in a substrate [110], living tissues are not spatially organized on a single-cell level. In tissue engineering, therefore, the goal is to encourage cell-cell binding and production of extracellular matrix among functional units of cell clusters, and the cells' ability to proliferate over and migrate into the scaffold is often considered an important feature. Although much of the work on substrate printing is directly applicable to our work, in existing systems typically no provision is made for fine-level control over the structure of the final cell array, which is necessary for our technique.

5.2 Synthetic Biology for Material Production

Synthetic biology is the creation of new, designed systems using biological parts – biomolecules, cells, tissues, and organisms [85]. Although the boundaries of the field have expanded in recent years to include subjects previously considered independent, such as protein engineering and functional genomics, a common synthetic biology application involves re-ordering and re-linking DNA sequences to form a new gene or set of genes, inserting the modified sequences into cells, and characterizing and make use of the resulting change in cell functionality.

The combination of synthetic biology and material production has largely focused on engineering microorganisms to increase their production of bulk biomolecules, such as pharmaceuticals (e.g., [19, 21]), biofuels [20, 44], and biopolymers which can be processed into so-called 'bioplastics' [72]. The goal may be to increase the rate at which the microorganisms make the desired biomolecule, to increase their ability to excrete it into solution (reducing the amount of post-production work to isolate the target product), to increase their survival at high levels of the target compound, or any other improvement to the final product yield.

Application of synthetic biology to tissue engineering (which, as discussed in section 5.1, has been the primary area of development for 3D printing of living cells) has been sparse. Some work has been done, similar to the biomolecule production approaches above, on making microorganisms produce supporting protein ingredients for tissue scaffolds [37]; these proteins are purified and mixed into a gel substrate to produce the final scaffold material. A slightly different use is engineering microorganisms to produce regulating or signalling proteins; when these proteins are purified and distributed within a scaffold, they can be used to stimulate or otherwise control biological growth after the scaffold is seeded with cells [39].

The closest work in the existing field of synthetic biology to our concept is the use of spatially structured arrays of cells to regulate gene expression. In this approach, cells are spatially patterned along with physical cues or causes of changed cell behavior as a means of creating spatial differentiation in function. This technique has been implemented with cells and gene-vector viruses [64, 75], patterns of two different cell types [7], and cells and plasmids [116].

The use of synthetic biology to enable spatially controlled, non-living, macroscale material production has been essentially unexplored prior to our work.

5.3 Biomimetic Materials

As mentioned above, there are two major factors that distinguish structural biomaterials from traditional human-made materials. One is the many levels of hierarchical organization. The other is the micro-level integration of different, molecularly complex constituent materials. Much current materials research focuses

on 'biomimetic materials', a term which encompasses two related goals.

The first goal is reproduction of the mechanical properties of structural biomaterials; this is the usage common in materials science and engineering, and work in this area tends to focus on producing hierarchical organization using non-biogenic materials (see [9, 83] for reviews). Examples include designs for new mixed-phase reinforced ceramics based on the structure of sponge spicules [63] and structuring the fiber grain directions of glass-fiber resin composites to match the directionality of chitin fibers in insect cuticle [16].

One intriguing set of techniques in this area has been the direct use of biogenic materials as templates for additional material assembly. Titanium dioxide structures formed by coating and then burning away butterfly wing scales have been shown to be effective photoanodes [114]; a similar approach was used to antireflective structures from fly eyes [45]. More unusually, carbon nanotubes have been shown to self-assemble into honeycomb structures directly onto butterfly wings, resulting in composite biogenic-artificial material structures with unusual thermal and electrical characteristics [70].

The second goal is production of biocompatible materials that can substitute for or supplement the function of natural materials; this is the usage common in tissue and biomedical engineering, and work in this area tends to focus on producing one or two levels of structural function using existing biogenic materials. An example is the formation of collagen-based scaffolds for tissue engineering focusing on porosity in the 10^{-4} m range [57].

More interdisciplinary work includes the creation of new composites of existing biogenic materials. For instance, silk fibers have been integrated with hydroxyapatite, the key mineral in bone, to create a human-designed composite biomaterials mimicking the bone/ligament interface [43, 112]. Such work establishes that there is a desire for techniques which can create novel biomaterial composites; our technology concept aims to provide a general framework for this application, rather than the collection of *ad hoc* techniques used in existing work.

More directly relevant to our technology concept, self-assembling structures of viruses genetically engineered to be crystallization nuclei have been used to control the orientation of microstructures formed by hydroxyapatite in solution [109]. Here, genetic engineering is used to create what is, in essence, a scaffold providing a template for material self-assembly. This is highly relevant to the substrate design section of our work, and offers a potential path for future development.

6 Mission Context Feasibility/Benefit Analyses

6.1 Introduction

One of the major objectives of our Phase I study was a feasibility and benefit analysis of this technology in two specific mission contexts. This milestone, along with the proof-of-concept demonstration (Section 7), will move the concept from TRL 2 to TRL 3 (Table 3.1).

As a new tool for *in situ* resource utilization, 3D bioprinting would be useful for long-term missions either in space or on a planetary surface. As we described in our proposal, this analysis covers two mission contexts: we chose to focus on the ISS as a representative space setting, and Mars as a planetary setting.

6.2 An ISS Replacement Part

6.2.1 Mission Description and Assumptions

On the ISS, replacement parts currently need to be sent from Earth as needed, so the ability to 3D print these parts on the station would save both time and money. The ability to replace certain materials with biomaterials which are lighter and stronger would save launch mass and energy. 3D bioprinting in particular would combine these advantages: the material type is not limited to what has already been sent up to the station, as cells can be engineered to produce only the amount and type of material that is needed.

As this mission concept was chosen to look at the use of our technology concept in a minimal context, we assume that the original part was manufactured on Earth and launched as part of the original ISS module placement. We also assume that all of the infrastructure necessary to implement on-site use of our technology for replacement parts was sent up in advance, and that the necessary material design template files for making the replacement part – created during the on-Earth manufacturing process – are stored locally rather than having to be sent up via radiocommunication.

Further, we assume that the repair infrastructure includes cells already engineered to make all desired biomaterials. This eliminates the need to include the tools necessary to make new cell lines for new material types in launch mass. Although this process, based on the trajectory of existing technology, will likely be automated to the point where it could be performed remotely from Earth in five to ten years, we decided not to include that feature in this mission scenario, as we wanted to focus specifically on near- or immediate-term benefits and use cases.

This reduces the use of our technology concept to simply making a replacement part.

Additionally, we assume that the incubators, freezers, and refrigerators used for the biological work associated with this technology will be similar in mass and power requirements to those used on Earth. Finally, we assume that training astronauts to do the synthetic biology work will not take significantly longer than it takes, for example, a new intern to learn the analogous protocols in a biology lab.

As shown in the subsequent sections, the use of biologically derived materials can reduce the mass of a typical replacement part by half, while the mass of the equipment needed for the synthetic biology work is about 380 kg. Most of this mass is due to the 80 °C freezer used for cryostock and competent cell storage, so if a smaller, tabletop version of this freezer could be developed, this mass could go down to around 100 kg. The bioprinter would then need to produce 100 kg of parts at half the mass of their traditional material counterparts in order for there to be a net mass savings for an ISS mission or other mission without *in situ* resource utilization. Alternatively, if a bioprinter on Earth manufactures the same parts prior to the mission, their masses could be reduced by half without the cost of flying the synthetic biology equipment. The main

benefit of flying this equipment is the versatility it provides to address the missions needs on demand.

6.2.2 Target Materials Types and Form Factors

As a representative part that may need replacement, we chose a Nomex EVA tether with aluminum hooks, part number SED33104391–301 from the EVA Tools and Equipment Reference Book [1, p. 379]. This is an element loaded in pure tension and consists of a single material in the form of a long, compliant band whose properties are constant along its length.

6.2.3 Feasibility, Costs and Benefits

Mass & Energy Requirements

The purpose of this section is to compare the mass and energy required to use traditional engineering materials, as opposed to synthetic biomaterial alternatives, to acquire a replacement part aboard the ISS – which is to say, flying up a new tether versus printing one. The existing tether design consists of aluminum hooks at either end of a Nomex strap (2.45 cm wide, 214.63 cm long when fully extended), and weighs 0.42 kg (0.93 lbs). The Nomex is initially folded up and held by stitching that breaks under a 34 kg (75 lbs) load, and after these stitches break, the tether has a load limit of 635 kg (1400 lbs). In comparison, as shown below, a tether constructed from biogenic materials can meet the same load requirements with less mass, while also providing more versatility in terms of the types of repairs that could be made through bioprinting, starting from the same biological raw materials.

While the biological materials discussed here can save upmass for a given repair, the printing process has its own equipment and energy requirements that need to be taken into account. Specifically:

- A freezer for cryostocks of engineered cells.
- A refrigerator for liquid growth medium and print substrate constituents, and cell cultures.
- An incubator to regulate the temperature of the printed cells during material deposition, if the species used does not grow fast enough at the ambient temperature on the ISS.
- The dry chemical supplies necessary to make liquid media and print substrate.
- Automated microfluidics to reconstitute the frozen cells and mix the dry chemical supplies, so that astronauts do not need to attempt to do wet lab work in microgravity.
- The printer itself, designed with microgravity in mind (droplet velocity from the dispenser head, as well as the print media and substrate, adjusted so that the droplet gels to the substrate with minimal splash).

This is a conservative scenario, assuming that all equipment needs to be on board the ISS to allow on-site engineering of cells to produce specific materials. The power requirements, in particular, can be reduced significantly if the bioengineering takes place on Earth and a battery of cryostocks of cells corresponding to all needed materials are sent up instead.

Although the items listed above are additional mass that would need to be taken to the ISS, and the electrical components would require power aboard the ISS, all of these items can be used to fill a variety of needs. They have value outside of the one tether that might need to be supplied or replaced. The incubator, freezer, and refrigerator, as well as the printer itself, would be used repeatedly for all replacement parts or new parts produced through bioprinting, so the cost of their mass and power requirements is offset by the sum of the mass and power savings due to all of the items that will be printed during the lives of these pieces of equipment.

Table 6.2 compares a range of biologically-derived materials to Nomex 410 and aluminum 6061-T6. The original tether design weighs 0.36 kg, so if we assume the aluminum accounts for two-thirds of that weight and the Nomex for the rest, replacing aluminum with pine and Nomex with cellulose (likely as part of a

Table 6.1: Conservative mass and power estimates for the equipment required for on-site synthetic biology and storage of cell cultures for use in the bioprinter.

Item	Always on?	mass (kg)	power (W)
refrigerator (storage)	yes	18.0	120.0
freezer (storage, cryostocks)	yes	300.0	2300-4400
incubator (cell culture)	yes	70.0	236.0
Microfluidics setup	no	1.5	36.0
Bioprinter, dispensing	no	5.0	50.0
Bioprinter, positioning	no	1.2	1.8
system control computer (incl. user interface)	no	2.0	50.0
Total (estimated)		379.7	493.8

composite to provide form to the cellulose, but assuming the cellulose itself is the primary mass contribution) reduces the part mass to 0.15 kg, less than half its previous weight. Pine is mentioned for the tether hooks because its the material that could do the job with the least mass, not considering materials that would deform too much to be practical replacements for a hook. If a similar technique were applied for other everyday parts on the ISS, the mass savings would add up.

Labor & Effort Requirements

Astronauts would need to be trained to use the bioprinting equipment: how to grow up cultures and load them into the printer. In microgravity, the wet lab work would largely be done by automated microfluidics.

The astronauts would need to be trained to select the appropriate cells to thaw and grow up, which could be done simply by consulting a database, and then to load the cells into the printing system. The growth and loading process could be designed to be a sealed cartridge interface. Assuming the astronaut training required for the use of this technology is similar to that required for a new intern in a biology lab to learn the analogous on-Earth protocols, 10 hours of training and repetitive practice would be required to master each protocol, and about 1 hour per week per protocol to keep the procedure fresh in the trainees mind. For the handful of protocols that would be involved, the total would be approximately 50 hours of training per person and 5 hours per week to stay in practice. This training would only be relevant for the two or three crewmembers whose job it would be to use the printer, and not necessarily the entire crew.

This is additional labor that the astronauts would not need to perform if a replacement part were flown up from Earth. The labor associated with bioprinting would be minimal, however, since most of the fabrication process would be automated, just as machinist labor is not required when existing (non-biological) 3D printers are used to manufacture parts.

Other Considerations

In addition to the mass, energy, and labor effects of applying our technology concept to this mission concept, there are other factors to take into account. One that we intend to explore in future work is the applicability of other unique properties of biomaterials, beyond simple strength criteria. For instance, many biomaterials are far more fracture resistant (tough) than traditional engineering materials for their mass. They may also have unusual deformation responses or failure modes.

Other factors include:

- *Versatility.* A replacement tether can only meet one need, and may require an additional flight to bring it to the ISS if no spare part specific to this need was already flown. Raw materials for bioprinting, on the other hand, can meet a variety of needs depending on which ones arise.
- *Packing.* Tethers and other replacement parts have specific dimensions, and therefore have more con-

Table 6.2: Table comparing Nomex 410 and aluminum 6061-T6 to alternative materials, including biogenic and traditional engineering materials, for the purpose of a load-bearing tether.

Material	tensile strength (Pa)	p (kg/m ^{3})	Al area ratio	Al mass ratio	Nomex area ratio	Nomex mass ratio
aluminum (6061-T6)	2.80×10^8	2700	1.00	1.00	0.43	1.13
Nomex 410	1.21×10^8	1030	2.32	0.88	1.00	1.00
silk (max)	3.00×10^9	1340	0.09	0.05	0.04	0.05
cellulose (max)	2.00×10^9	1500	0.14	0.08	0.06	0.09
carbon fiber in epoxy	1.73×10^9	1600	0.16	0.10	0.07	0.11
silicon carbide	3.44×10^9	3210	0.08	0.10	0.04	0.11
cellulose (min)	1.00×10^9	1500	0.28	0.16	0.12	0.18
silk (min)	3.00×10^8	1340	0.93	0.46	0.40	0.52
pine (along grain)	9.40×10^7	550	2.98	0.61	1.28	0.69
titanium (alloy)	7.30×10^8	4510	0.38	0.64	0.17	0.72
oak (along grain)	1.09×10^8	750	2.57	0.71	1.11	0.81
bone mineral (compact)	1.10×10^8	1850	2.55	1.74	1.10	1.97
aluminum oxide	1.70×10^8	3800	1.65	2.32	0.71	2.62
steel (AISI 1045)	3.10×10^8	7850	0.90	2.63	0.39	2.97
nylon-6	4.50×10^7	1150	6.22	2.65	2.68	3.00
polypropylene	3.30×10^7	1070	8.48	3.36	3.66	3.80
lignin	2.17×10^7	1300	12.90	6.21	5.57	7.03
copper	7.00×10^7	8960	4.00	13.27	1.73	15.01
rubber, small strain (max)	7.00×10^6	1522	40.00	22.55	17.26	25.50
kevlar	3.62×10^6	1440	77.35	41.25	33.37	46.65
brick	2.80×10^6	1900	100.00	70.37	43.14	79.58
rubber, small strain (min)	1.00×10^6	1522	280.00	157.84	120.79	178.49
concrete	1.40×10^6	2400	200.00	177.78	86.28	201.04

straints in terms of how they can be packed for a flight to the ISS, as opposed to the bioprinting raw materials, which are not constrained to a specific large-scale shape: they are liquid solutions, chemical powders, and small, inch-long tubes containing cell cultures or DNA.

- *Robustness.* The mission is more robust because it can make replacement parts to heal an injured mission.
- *Efficiency.* If a bioprinted part is no longer needed, its material can be broken down and used as feedstock to produce a new part, which means additional mass savings.

6.2.4 Summary

Overall, the use of biologically derived materials, printed into the desired forms, can reduce the mass of parts used in ISS or other in-orbit missions by half or more, depending on the materials to be replaced. Not all silk or cellulose is exactly the same in composition or material properties, which is why maximum and minimum values were specified in Table 6.2, but the entire range for both materials provides the same load-bearing ability as aluminum with a fraction of the mass: between 5 and 50% depending on the variety of silk or cellulose (between 5.2 and 52% of the mass when compared to Nomex). What brings these two compounds to the high end of their capacity for tensile strength is worthy of investigation, as is the potential to use them in composites with other materials, but the first step is determining how easily and efficiently these materials can produced in a lab by cells that can then be deposited into the desired configuration by the bioprinter.

These mass savings can be applied directly if the parts are manufactured on Earth and flown as usual, or the mission can take advantage of the flexibility provided by a bioprinter on-site, manufacturing parts on an as-needed bases. The mass cost of the latter scenario would be an additional 100 to 300 kg, depending on the size of the incubator, freezer, and refrigerator used for cell culture growth and storage of biological supplies.

6.3 A Long-Term Mars Habitat

6.3.1 Mission Description and Assumptions

On Mars, *in situ* resource utilization can reduce the upmass needed for the mission, and with 3D bioprinting, the local CO_2, sunlight, and regolith can be the raw materials needed to produce any number of biomaterials. Here, we use Human Exploration of Mars Design Reference Architecture 5.0 from NASAs Mars Architecture Steering Group as a baseline mission architecture [29].

A prominent manufacturing concern when it comes to accommodating astronauts on Mars is the construction and repair of habitats. A Mars habitat must fulfill several requirements at once – it must be airtight, it must provide thermal insulation, it must provide radiation shielding, it must be puncture resistant, it must withstand the mechanical stresses placed on it – and any given traditional material will typically not be optimal for more than one of these requirements. It is for this reason that EMU suits and ISS modules have several layers: fiberglass, aluminum, and stainless steel for structural support, neoprene bladder for airtightness, Dacron restraint for the bladder, aluminized Mylar insulation, and the orthofabric outer layer (a mix of Gore-Tex, Kevlar, and Nomex) for thermal insulation and puncture resistance [1].

Biomaterial composites, on the other hand, can incorporate the properties of multiple materials into a single layer tailored to the desire form factor, or simply replace layers of traditional material with biologically derived alternatives that meet the same requirements with less mass. It was demonstrated in the previous section on ISS applications that biomaterials can meet a given tensile load requirement with less mass than would be required of aluminum or Nomex, and here the comparison is applied to the construction of Mars habitats. Specifically, a design is considered in which high-tensile-strength materials provide the skin over a frame made of high-compressive strength materials. The comparison of material tensile strengths can be found in the previous section, in Table 6.2, and the comparison of material compressive strengths can be found below in Table 6.3.

Table 6.3: Table comparing aluminum 6061-T6 to alternative materials, including biogenic and traditional engineering materials, for the purpose of a compressive load-bearing part.

Material	compressive strength (Pa)	ρ (kg/m^3)	Al area ratio	Al mass ratio
aluminum (6061-T6)	3.86×10^8	2700	1.00	1.00
aluminum oxide	2.95×10^9	3800	0.13	0.18
titanium (alloy)	9.70×10^8	4510	0.40	0.66
mollusk shell	3.00×10^8	2900	1.29	1.38
bone mineral (compact)	1.70×10^8	1850	2.27	1.56
enamel	2.00×10^8	3000	1.93	2.14
brick	8.00×10^7	1900	4.83	3.40
steel, max	3.10×10^8	7850	1.25	3.62
steel, min	1.70×10^8	7850	2.27	6.60
pine (along grain, dry)	8.27×10^6	550	46.65	9.50
oak (along grain, dry)	7.93×10^6	750	48.68	13.52
cork	7.00×10^5	175	551.43	35.74
concrete	7.00×10^6	2400	55.14	49.02

Table 6.4: *In situ* resource grades.

Grade	Definition
A	directly available *in situ*
B	present *in situ*, extractable
C	present *in situ*, not extractable
D	not present *in situ*

Table 6.5: Material compatibility grades.

Grade	Definition
A	standardized genetic part
B	naturally occurring, non-standardized gene
C	theoretical *de novo* genetic part
D	not producible by cells

The most straightforward method of *in situ* radiation shielding would be to construct the habitat far enough underground that the local regolith provides sufficient shielding. In this case, the habitat would need to withstand the load of the regolith above it, with materials optimized for compressive loading. For this reason, the focus of this preliminary analysis is tensile and compressive load strength as opposed to radiation shielding.

The primary type of habitat considered here is the expandable habitat, a concept which has demonstrated several benefits over rigid structures for aerospace applications [13]:

- The flexibility of expandable structures means that they can be packaged more compactly and in a wider variety of geometries, and can therefor be launched in smaller, cheaper vehicles.
- Expandable structures lend themselves to the thin sheet form factor, which is better suited to composite weaves and other materials that have higher strength to weight ratios than traditional rigid materials.
- Expandable composite structures can be tailored such that the composition of the material varies from one point to another, concentrating the strength of the system where needed and saving mass elsewhere.
- Expandable structures are flexible, and can therefore be more damage tolerant, giving instead of breaking as a rigid system might. Structural supports, rigid or also inflatable, can of course be positioned as needed to ensure that the structure supports itself.
- In prior studies, expandable alternatives have consistently proven lower in development and manufacturing costs than their rigid counterparts.

For this mission scenario, we assume that our technology concept is being used to create a habitat modelled after the study done by Nowak on inflatable lunar habitats [71]. We assume that the regolith densities of

Table 6.6: Material compatibility, with synthetic biology and utilization, for the materials used in our mission scenarios. Also included are grades for many other options, both biogenic and traditional engineering materials, that we investigated.

Material	Bioengineering Compatibility	*In Situ* Availability
silk	B+	B
oak	B	B
pine	B	B
cellulose	B	B
lignin	B	B
bone mineral	B	B
rubber	B	B
cork	B	B
mollusk shell	B	B
enamel	B	B
kevlar	C	D
polypropylene	C	D
nylon	C	D
carbon fiber in epoxy	C	C
silicon carbide	C	B
Nomex	C	D
aluminum (6061-T6)	D	B
concrete	D	A
brick	D	A
copper	D	D
aluminum oxide	D	A
steel (AISI 1045)	D	B
titanium (alloy)	D	B

Mars and the Moon are comparable [3, 67], and that wherever the density is lower, the regolith will be layered thicker to achieve the same level of shielding, so the the regolith mass per unit area is estimated to be the same for both the Moon and Mars.

Mass savings are calculated both for a scenario where the biologically derived materials are manufactured entirely from *in situ* resources, and a scenario where no *in situ* resources are used and the biologically derived materials have to be flown from Earth. These two cases provide best and worst case scenarios in terms of mass savings.

6.3.2 Target Materials Types and Form Factors

In this habitat design, compressive members are modelled as circular-cross-section columns supporting the habitat dome from inside. All columns are the same distance from the center of the dome, so they are all the same length and support the same load. The dome is pressurized to 1 Earth atmosphere. Therefore, our mission scenario requires two material types and form factors: columns loaded in compression, and sheets (the covering 'skin' of the dome) loaded in tension.

As described in our Phase I proposal, we have graded the materials used in our mission scenario in terms of both their correspondence to known genetic parts (Table 6.5) and compatibility with known *in situ* resource extraction techniques (Table 6.4). The results, along with those for several other materials we investigated, are shown in Table 6.6.

None of the most promising target materials have already been standardized as genetic parts, a fact which reflects the innovation of our combination of synthetic biology and structural material production. How-

Table 6.7: Table comparing the required mass for tensile elements for the above mission scenario using different materials, some traditional, some biologically derived.

Material	tensile strength (Pa)	ρ (kg/m^3)	σ_t (Pa)	t_m (m)	mass (kg)
silk (max)	3.00×10^9	1340	2.00×10^9	1.05×10^{-4}	3.30×10^1
cellulose (max)	2.00×10^9	1500	1.33×10^9	1.58×10^{-4}	5.54×10^1
carbon fiber in epoxy	1.73×10^9	1600	1.15×10^9	1.82×10^{-4}	6.83×10^1
silicon carbide	3.44×10^9	3210	2.29×10^9	9.18×10^{-5}	6.89×10^1
cellulose (min)	1.00×10^9	1500	6.67×10^8	3.16×10^{-4}	1.11×10^2
silk (min)	3.00×10^8	1340	2.00×10^8	1.05×10^{-3}	3.30×10^2
pine (along grain)	9.40×10^7	550	6.27×10^7	3.36×10^{-3}	4.32×10^2
titanium (alloy)	7.30×10^8	4510	4.87×10^8	4.32×10^{-4}	4.56×10^2
oak (along grain)	1.09×10^8	750	7.27×10^7	2.90×10^{-3}	5.08×10^2
Nomex 410	1.21×10^8	1030	8.05×10^7	2.61×10^{-3}	6.29×10^2
aluminum (6061-T6)	2.80×10^8	2700	1.87×10^8	1.13×10^{-3}	7.12×10^2
bone mineral (compact)	1.10×10^8	1850	7.33×10^7	2.87×10^{-3}	1.24×10^3
aluminum oxide	1.70×10^8	3800	1.13×10^8	1.86×10^{-3}	1.65×10^3
steel (AISI 1045)	3.10×10^8	7850	2.07×10^8	1.02×10^{-3}	1.87×10^3
nylon-6	4.50×10^7	1150	3.00×10^7	7.02×10^{-3}	1.89×10^3
polypropylene	3.30×10^7	1070	2.20×10^7	9.57×10^{-3}	2.39×10^3
lignin	2.17×10^7	1300	1.45×10^7	1.45×10^{-2}	4.42×10^3
copper	7.00×10^7	8960	4.67×10^7	4.51×10^{-3}	9.45×10^3
rubber, small strain (max)	7.00×10^6	1522	4.67×10^6	4.51×10^{-2}	1.60×10^4
kevlar	3.62×10^6	1440	2.41×10^6	8.72×10^{-2}	2.94×10^4
brick	2.80×10^6	1900	1.87×10^6	1.13×10^{-1}	5.01×10^4
rubber, small strain (min)	1.00×10^6	1522	6.67×10^5	3.16×10^{-1}	1.12×10^5
concrete	1.40×10^6	2400	9.33×10^5	2.25×10^{-1}	1.27×10^5

ever, spider silk receives a slightly higher grade than the others; one of its major component proteins has been cloned and produced in *E. coli* with demonstrated function [108], an important first step.

6.3.3 Feasibility, Costs and Benefits

Mass & Energy Requirements

The loads that our habitat design would face when covered with a layer of regolith are calculated, using those studied in the context of lunar habitats [71] as a baseline, as described below. For the habitat skin in tension, the required material thickness is given by:

$$t_m = \frac{p_s R}{2\sigma_t} \tag{6.1}$$

where σ_t is the allowable material tensile stress, R is the radius of the habitat dome, p_s is the internal pressure of the habitat, and t_m is the thickness of the skin material. So for a given habitat radius and internal pressure, the thickness (and therefore the mass for a given material density) is inversely proportional to the max allowable stress, which will be the yield stress multiplied by a factor of safety. So for a radius of curvature of 6.1 m (20 ft) and an internal pressure of 69 kPa (10 psi), the mass of each material required to cover the $2\pi(6.1\text{ m})^2 = 233.8\text{ m}^2$ surface of the dome, with a factor of safety of 1.5, is shown in Table 6.7.

The compressive members are modelled as columns supporting the habitat dome from inside, all placed at the same distance from the center of the dome so that they are all the same length and support the same

Table 6.8: Table comparing the required mass for the compressive elements (columns) of the habitats described above, some traditional, some biologically derived.

Material	compressive strength (Pa)	ρ (kg/m^3)	σ_c (Pa)	A (m^2)	mass (kg)
aluminum oxide	2.95×10^{9}	3800	1.96×10^{9}	3.48×10^{-4}	3.97×10^{0}
titanium (alloy)	9.70×10^{8}	4510	6.47×10^{8}	1.06×10^{-3}	1.43×10^{1}
aluminum (6061-T6)	3.86×10^{8}	2700	2.57×10^{8}	2.65×10^{-3}	2.15×10^{1}
mollusk shell	3.00×10^{8}	2900	2.00×10^{8}	3.42×10^{-3}	2.97×10^{1}
bone mineral (compact)	1.70×10^{8}	1850	1.13×10^{8}	6.03×10^{-3}	3.34×10^{1}
enamel	2.00×10^{8}	3000	1.33×10^{8}	5.12×10^{-3}	4.61×10^{1}
brick	8.00×10^{7}	1900	5.33×10^{7}	1.28×10^{-2}	7.30×10^{1}
steel (max)	3.10×10^{8}	7850	2.07×10^{8}	3.30×10^{-3}	7.78×10^{1}
steel (min)	1.70×10^{8}	7850	1.13×10^{8}	6.03×10^{-3}	1.42×10^{2}
pine (along grain, dry)	8.27×10^{6}	550	5.52×10^{6}	1.24×10^{-1}	2.04×10^{2}
oak (along grain, dry)	7.93×10^{6}	750	5.29×10^{6}	1.29×10^{-1}	2.91×10^{2}
cork	7.00×10^{5}	175	4.67×10^{5}	1.46×10^{0}	7.68×10^{2}
concrete	7.00×10^{6}	2400	4.67×10^{6}	1.46×10^{-1}	1.05×10^{3}

load. In the Nowak study, the gravity load of the 3.3 m thick regolith radiation shielding and the structural dead load was estimated for the lunar scenario to be 297 kN per column for a 6.1 m radius structure with four columns per dome [71]. Gravitational acceleration on the surface of Mars is 2.3 times that on the surface of the moon, so approximating the regolith densities to be roughly the same, the loading on Mars would be 683 kN per column. The compressive stress is:

$$\sigma_c = \frac{F_c}{A} \tag{6.2}$$

where F_c is the compressive load in units of force and A is the columns cross-sectional area. The columns in this design study are 3 m long. The mass per column required for each material to support this load with a 1.5 factor of safety is shown in Table 6.8.

Of the materials considered here, the most mass-efficient options for the compressive and tensile elements of the structure are aluminum oxide (ceramic) and silk, respectively. Cellulose is a close second to silk; given its higher elastic modulus, it would provide greater rigidity [105]. A composite of silk and cellulose is a promising option through the use of bioprinting.

Mollusk shell is a relatively low-mass option for the compressive members, and although its columns would only be the fourth lightest of the materials considered, it has the benefit of being manufacturable *in situ*, meaning that only a fraction of that mass would need to come from Earth. The minerals in the shell could be derived from regolith, and the organic components of the shell could be formed by engineered cell cultures using CO_2 in the Martian atmosphere and water. Some of the water may come from Earth, but some of it could also be harvested locally [29], meaning that this material option could have the lowest required upmass of the compressive materials considered, depending on which local materials the mission is equipped to harvest *in situ*.

For a direct comparison, if a cellulose skin is chosen (55–110 kg), and the load-bearing columns are made of mollusk shell (4 columns, each 29.7 kg), the total for one habitat module is 173.8–228.9 kg depending on the quality of cellulose. Using a traditional kevlar skin (154 kg) and aluminum columns (4 at 21.5 kg each), one module would be 240 kg. So in the worst case, where all biologically derived materials need to be flown from Earth, there is still a savings of 11.1–66.2 kg per habitat module. But with the *in situ* CO_2 in the atmosphere, energy from the sunlight, minerals from the regolith, and the possibility of extracting

local water, a typical mission is expected to acquire at least some of the material for bioprinting on site. In the best scenario where all biologically derived material comes from local resources, the full 240 kg is saved per module, with a one-time mass cost of 100–300 kg for the necessary equipment (as described in subsection 6.2.3).

Labor & Effort Requirements

In addition to the synthetic biology training mentioned in the Labor & Effort section of the ISS mission analysis, a Mars mission would require the astronauts to oversee the use of the printed materials to construct the habitat modules, or any other structures that might use these materials. The construction could be done robotically, or in a partially automated fashion where certain steps are done robotically, but in any scenario, the astronauts would need to understand the procedure so that they can step in as needed troubleshoot, and take care of the non-automated steps. In terms of the time required, training for this type of procedure should be comparable to the training that would be required to construct the same structures using traditional materials, since the structures to be built would be no different in complexity even if the materials are different.

Other Considerations

Given the low surface temperatures on Mars, about $-50\,^{\circ}\mathrm{C}$ on average [51], it may be possible to reduce the power and mass of insulation material required for low-temperature storage of synthetic biology supplies. Instead of keeping refrigerators and freezers fully inside of the climate controlled astronaut habitats, they could be installed either outside the habitat, or more practically, partially outside, extending out through the habitat wall to take advantage of the low temperatures outdoors. If these storage units open to the inside of a habitat but have most of their volume outside the habitats thermal insulation, then their contents would be both readily accessible and easier to keep cold.

In terms of how this mass translates into launch costs, even at the low end of the price range, the ability to save a kilogram is significant. SpaceX proposes to take 13,150 kg to LEO or 4,850 kg to GTO per \$56.5M launch [25], which is \$11,649.48/kg to GTO and \$4,296.58/kg to LEO. Even if we assume minimal acceleration and therefore minimal fuel spent during most of the journey to Mars, the cost savings become significant when the mass reduction is on the order of hundreds of kilograms. The cost per kg is especially high if an additional launch is required to send necessary parts that weigh less than the max payloads listed above.

This mission scenario assumes simple material substitution using an existing habitat design. It is very likely that the mass savings for a structure designed to take full advantage of synthetic biomaterials' properties, particularly microscale material gradients and customization, would be much higher. Although designing a new mission concept from scratch to address this question, first identified by our Phase I results, is beyond the scope of this report, it is a promising avenue for follow-on work. To give a preliminary idea of what the difference might be, we repeated our mass saving calculation using a proposed space mission tensegrity structure, the 2013 NIAC Phase II project 'Super Ball Bot - Structures for Planetary Landing and Exploration'. Human-scale tensegrity structures share many features with the biomaterial microstructures, such as inherent tensile-compressive load balancing and whole-structure passive energy dissipation, so they are a good fit for biomaterials' natural strengths.

We chose materials with high compressive and tensile strength per unit mass for the distinct compressive and tensile elements of the structure. Looking at the loads that the compressive and tensile elements of this tensegrity structure were designed for [12, 81], Table 6.9 and Table 6.10, and Table 6.11 compare the masses needed for a range of traditional and biologically derived materials.

For the compressive elements, buckling rather than compressive yield proved to be the limiting factor. The compressive elements are modelled as hollow tubes with circular cross-sections and inner diameters of 3 mm. In terms of buckling, the wood-type biomaterials appear the most mass-efficient, with mollusk shell falling just behind them. In terms of tension, silk and cellulose remain the most mass efficient. Cellulose

Table 6.9: Table comparing the required mass for the compressive elements of a tensegrity-based rover using different materials, some traditional, some biologically derived. The compressive strength is in Pascals, ρ is the density, σ_c is the compressive yield strength, A is the cross-sectional area of the material required to keep the max expected loading below the compressive yield strength by a safety factor of 1.5, and the mass listed is for a compressive element with this cross-section. The struts are 1 m in length.

Material	compressive strength	ρ (kg/(m^3))	σ_c (Pa)	A (m^2)	mass (kg)
aluminum oxide	2.95×10^{9}	3800	1.96×10^{9}	4.07×10^{-7}	1.55×10^{-3}
titanium (alloy)	9.70×10^{8}	4510	6.47×10^{8}	1.24×10^{-6}	5.58×10^{-3}
aluminum (6061-T6)	3.86×10^{8}	2700	2.57×10^{8}	3.11×10^{-6}	8.39×10^{-3}
mollusk shell	3.00×10^{8}	2900	2.00×10^{8}	4.00×10^{-6}	1.16×10^{-2}
bone mineral (compact)	1.70×10^{8}	1850	1.13×10^{8}	7.06×10^{-6}	1.31×10^{-2}
enamel	2.00×10^{8}	3000	1.33×10^{8}	6.00×10^{-6}	1.80×10^{-2}
brick	8.00×10^{7}	1900	5.33×10^{7}	1.50×10^{-5}	2.85×10^{-2}
steel, max	3.10×10^{8}	7850	2.07×10^{8}	3.87×10^{-6}	3.04×10^{-2}
steel, min	1.70×10^{8}	7850	1.13×10^{8}	7.06×10^{-6}	5.54×10^{-2}
pine (along grain, dry)	8.27×10^{6}	550	5.52×10^{6}	1.45×10^{-4}	7.98×10^{-2}
oak (along grain, dry)	7.93×10^{6}	750	5.29×10^{6}	1.51×10^{-4}	1.14×10^{-1}
cork	7.00×10^{5}	175	4.67×10^{5}	1.71×10^{-3}	3.00×10^{-1}
concrete	7.00×10^{6}	2400	4.67×10^{6}	1.71×10^{-4}	4.11×10^{-1}

will allow less deformation for a given load, since its Youngs modulus is over two orders of magnitude higher than that of silk [105]; the importance of this criterion is another unknown that must be addressed in future work through the use of improved soft-body modelling tools (as described in section 8.3).

6.3.4 Summary

Of the materials considered here, the most mass-efficient options for the compressive and tensile elements of the structure are aluminum oxide (ceramic) and silk, respectively, though cellulose is a close second to silk. A composite of silk and cellulose is a promising long-term future application for investigation.

Mollusk shell is a relatively low-mass option for the compressive members, and although its columns would only be the fourth lightest of the materials considered, it has the benefit of being manufacturable *in situ*, meaning that only a fraction of that mass would need to come from Earth. The minerals in the shell could be derived from regolith, and the organic components of the shell could be formed by engineered cell cultures using CO_2 in the Martian atmosphere and water. Some of the water may come from Earth, but some of it could also be harvested locally [29], meaning that this material option could have the lowest required upmass of the compressive materials considered, depending on which local materials the mission is equipped to harvest *in situ*.

Even without *in situ* resource utilization, the use of biologically derived materials still reduces the upmass required for the mission, and the use of bioprinting provides the versatility needed repair or replace damaged parts as needed, or meet new demands if the mission needs to change for any reason. With full use of *in situ* resources, however, the mass savings are considerable, potentially saving hundreds of kilograms per habitat module.

6.4 Conclusions

Overall, for both the ISS scenario and the Mars scenario, the use of bioprinting offers a net benefit in terms of mass savings as well as the ability to dynamically address mission needs.

For the ISS, bioprinting on Earth prior to the mission has the greatest benefit, reducing the mass of typical

Table 6.10: Table comparing the required mass for the compressive elements, subject to buckling, of a tensegrity-based rover using different materials, some traditional, some biologically derived. ρ is the density, I is the area moment of inertia required to keep the max expected loading below the buckling point by a safety factor of 1.5, r is the outer radius of the cross-section, and A is the cross-sectional area. The geometry of the cross-section is assumed to be a circular tube with an inner diameter of 0.3 cm. The struts are 1 m in length.

Material	**elastic modulus (Pa)**	ρ **(kg/(m^3)**	I **(m^4)**	r **(m)**	A **(m^2)**	**mass (kg)**
aluminum oxide	3.50×10^{11}	3800	1.39×10^{-9}	6.41×10^{-3}	1.01×10^{-4}	3.83×10^{-1}
pine (along grain, dry)	9.00×10^{9}	550	5.40×10^{-8}	1.62×10^{-2}	7.95×10^{-4}	4.37×10^{-1}
oak (along grain, dry)	1.10×10^{10}	750	4.42×10^{-8}	1.54×10^{-2}	7.17×10^{-4}	5.37×10^{-1}
aluminum (6061-T6)	6.90×10^{10}	2700	7.05×10^{-9}	9.71×10^{-3}	2.68×10^{-4}	7.24×10^{-1}
mollusk shell	7.00×10^{10}	2900	6.95×10^{-9}	9.68×10^{-3}	2.66×10^{-4}	7.71×10^{-1}
titanium (alloy)	1.13×10^{11}	4510	4.32×10^{-9}	8.58×10^{-3}	2.03×10^{-4}	9.16×10^{-1}
enamel	5.00×10^{10}	3000	9.73×10^{-9}	1.05×10^{-2}	3.20×10^{-4}	9.61×10^{-1}
bone mineral (compact)	1.80×10^{10}	1850	2.70×10^{-8}	1.36×10^{-2}	5.54×10^{-4}	1.02×10^{0}
brick	1.70×10^{10}	1900	2.86×10^{-8}	1.38×10^{-2}	5.71×10^{-4}	1.08×10^{0}
steel (AISI 1045)	2.05×10^{11}	7850	2.37×10^{-9}	7.36×10^{-3}	1.42×10^{-4}	1.12×10^{0}
concrete	1.70×10^{10}	2400	2.86×10^{-8}	1.38×10^{-2}	5.71×10^{-4}	1.37×10^{0}
cork	1.00×10^{7}	175	4.86×10^{-5}	8.87×10^{-2}	2.47×10^{-2}	4.32×10^{0}

Table 6.11: Table comparing the required mass for tensile elements of a tensegrity-based rover using different materials, some traditional, some biologically derived. Tensile strength is in Pascals, ρ is the density, σ_t is the tensile yield strength, A is the cross-sectional area of the material required to keep the max expected loading below the tensile yield strength by a safety factor of 1.5, and the mass per unit length listed is for a tensile element with this cross-section.

Material	Tensile Strength	ρ (kg/(m^3))	σ_t (Pa)	A (m^2)	mass (kg/m)
silk, max	3.00×10^{9}	1340	2.00×10^{9}	5.00×10^{-8}	6.70×10^{-5}
cellulose, max	2.00×10^{9}	1500	1.33×10^{9}	7.50×10^{-8}	1.13×10^{-4}
carbon fiber in epoxy	1.73×10^{9}	1600	1.15×10^{9}	8.67×10^{-8}	1.39×10^{-4}
silicon carbide	3.44×10^{9}	3210	2.29×10^{9}	4.36×10^{-8}	1.40×10^{-4}
cellulose, min	1.00×10^{9}	1500	6.67×10^{8}	1.50×10^{-7}	2.25×10^{-4}
kevlar	6.90×10^{8}	1440	4.60×10^{8}	2.17×10^{-7}	3.13×10^{-4}
silk, min	3.00×10^{8}	1340	2.00×10^{8}	5.00×10^{-7}	6.70×10^{-4}
pine (along grain)	9.40×10^{7}	550	6.27×10^{7}	1.60×10^{-6}	8.78×10^{-4}
titanium (alloy)	7.30×10^{8}	4510	4.87×10^{8}	2.05×10^{-7}	9.27×10^{-4}
oak (along grain)	1.09×10^{8}	750	7.27×10^{7}	1.38×10^{-6}	1.03×10^{-3}
Nomex 410	1.21×10^{8}	1030	8.05×10^{7}	1.24×10^{-6}	1.28×10^{-3}
aluminum (6061-T6)	2.80×10^{8}	2700	1.87×10^{8}	5.36×10^{-7}	1.45×10^{-3}
bone mineral (compact)	1.10×10^{8}	1850	7.33×10^{7}	1.36×10^{-6}	2.52×10^{-3}
aluminum oxide	1.70×10^{8}	3800	1.13×10^{8}	8.82×10^{-7}	3.35×10^{-3}
steel (AISI 1045)	3.10×10^{8}	7850	2.07×10^{8}	4.84×10^{-7}	3.80×10^{-3}
nylon-6	4.50×10^{7}	1150	3.00×10^{7}	3.33×10^{-6}	3.83×10^{-3}
polypropylene	3.30×10^{7}	1070	2.20×10^{7}	4.55×10^{-6}	4.86×10^{-3}
lignin	2.17×10^{7}	1300	1.45×10^{7}	6.91×10^{-6}	8.99×10^{-3}
copper	7.00×10^{7}	8960	4.67×10^{7}	2.14×10^{-6}	1.92×10^{-2}
rubber, small strain (max)	7.00×10^{6}	1522	4.67×10^{6}	2.14×10^{-5}	3.26×10^{-2}
brick	2.80×10^{6}	1900	1.87×10^{6}	5.36×10^{-5}	1.02×10^{-1}
rubber, small strain (min)	1.00×10^{6}	1522	6.67×10^{5}	1.50×10^{-4}	2.28×10^{-1}
concrete	1.40×10^{6}	2400	9.33×10^{5}	1.07×10^{-4}	2.57×10^{-1}

replacement parts by half. On-site bioprinting could still be worthwhile to quickly address needs without waiting for the next flight to deliver a certain part, particularly if all needed materials are itemized in advance and the needed cell stocks are already created. The benefit to on-site construction depends on assumptions about part failure rates and launch costs; these can be further quantified in follow-on work.

On Mars, material substitution (that is, using materials manufactured on Earth without use of *in situ* resources) offers a mass reduction of approximately one-third for a habitat construction mission. The use of *in situ* resources has the potential to dramatically reduce upmass by using local sources of carbon, minerals, and even water to fabricate biologically derived materials with high tensile or compressive strength relative to their density. Theoretically, the upmass cost of the construction materials can be reduced to zero using our technology, although there will be an offset, estimated conservatively to be the equivalent of one habitat unit, due to the need to bring biomaterial construction equipment. Additionally, as with the ISS scenario, there is a significant mission robustness benefit to being able to produce newly designed parts on demand without waiting for resupply. The overall benefit to on-site construction depends on assumptions about the state of ISRU technology; these can be further quantified in follow-on work.

In addition to these quantitative results, performing this mission scenario analysis also produced some conceptual insights. We identified three key unknowns in the process of this analysis. The first is the performance of our potential synthetic biomaterials in a space environment. The second is the lack of good compliant materials models. The third is the lack of materials optimization design tools.

Although the mechanical behavior of natural structural biomaterials at non-Earth-standard temperatures and other conditions is largely unexplored (silk being a notable exception [76]), it has been hypothesized that it will be significantly different (e.g., [38]), particularly since many biomaterials' properties are highly sensitive to their water content [68]. This is an unknown that can be addressed directly with environmental tests on natural samples.

Many biomaterials are more fracture-resistant than traditional engineering materials because they are able to absorb energy through non-destructive bending, deformation, or other types of physical compliance. This behavior is poorly represented in traditional materials modeling and analysis and consequently is often ignored in standard design tools and approaches. Addressing this unknown will require modification of existing models or development of entirely new software tools.

Lastly, the most powerful potential advantage our technology concept offers is the ability to do micron-scale material property customization. Traditional materials design analysis tools tend to assume fixed, and spatially constant, material properties, and solve for maximum loading conditions. Our technology concept, one day, may be able to turn this philosophy on its head by providing the necessary material properties at each point in a desired structure to support a given range of loading conditions with minimized mass. Needless to say, the design tools to do this 'reversed' calculation have not yet been created, and so we cannot yet say what the maximum possible benefit of our technology concept might be under ideal conditions. Addressing this unknown will require modification of existing specialized software tools or re-implementation of traditional solving methods (e.g., finite element analysis) using existing general systems.

7 Proof of Concept

7.1 Introduction

One of the major objectives of our Phase I study was a proof-of-concept demonstration of our technology. This milestone, along with the mission context feasibility/benefit analyses (Section 6), moves the concept from TRL 2 to TRL 3 (Table 3.1).

As part of the work on our technology concept completed prior to our Phase I proposal, we created preliminary implementations of two parts of the concept (see Figure 7.1 for an explanation of how the components fit together). The first, the 3D printing hardware and software, is breadboard-level 3D-positionable microdispensing hardware (Figure 7.16) consisting of commercial off-the-shelf (COTS) components, our own integration hardware frame, and our own integration software communications. The second, the genetically engineered cell, are two strains of the yeast *Saccharomyces cerevisiae* engineered to secrete two different-color fluorescent proteins, red (RFP) and green (GFP).

The remaining necessary steps of our proof of concept were as follows:

1. *Choose an appropriate demonstration.* We needed to choose a two-material digital template pattern that demonstrates the functionality of both the printer and the engineered cells.
2. *Demonstrate critical functionality of all components.* The two remaining key components were the print medium and the print substrate.
3. *Demonstrate and characterize end-to-end functionality of the integrated system.* After verifying each individual component, we needed to integrate them all into a complete system and characterize the system's performance parameters.
4. *Proof-of-concept demonstration.* Our proof of concept, following the workflow in Figure 7.1, required printing an array of our cells from the digital template pattern and stimulating the cells to secrete the corresponding material onto the binding substrate.
5. *Analyze the material properties.* We needed to characterize the finished cell-made material to show that its structure was correlated to the original digital template.

We review in this section the necessary technical background of the concept, the current state of the art, and the results of our proof-of-concept demonstration.

As described in our Phase I proposal, our technology concept has several distinct functional stages drawn from widely varying fields (Figure 7.1). To achieve a proof of concept demonstration, one of the two requirements necessary to advance our concept's Technology Readiness Level, the following steps were necessary:

- identify a suitable implementation choice for each component stage;
- choose an appropriate demonstration material pattern;
- demonstrate critical functionality of all components;
- integrate the functional components into a complete system;
- demonstrate functionality of the complete system; and
- analyze the performance of the complete system, including correlation of the final material product to the original material pattern.

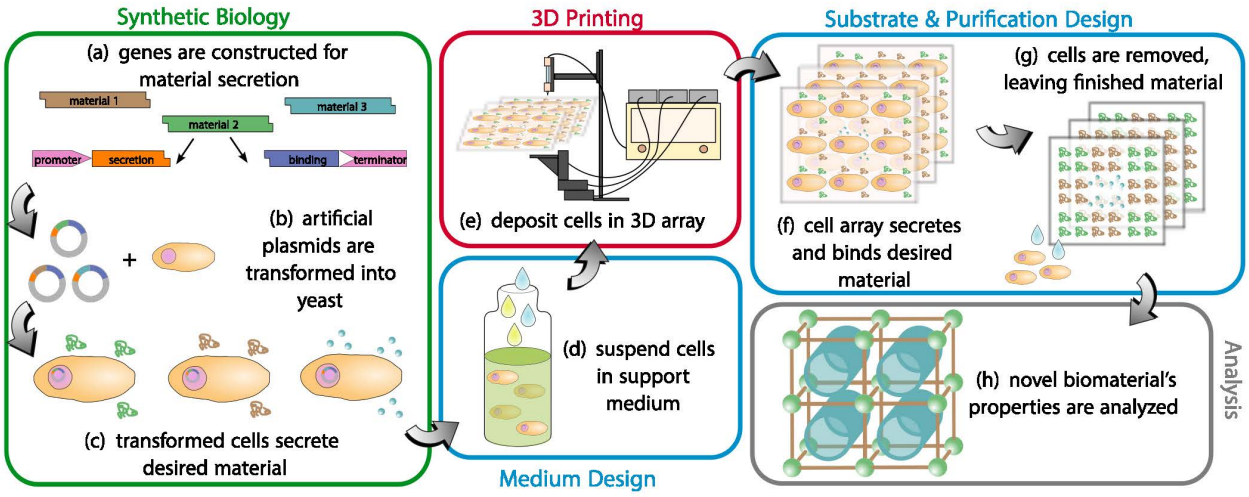

Figure 7.1: Our technology concept has components drawn from many different disciplines. Each component can be implemented in different ways; the 'best' implementation of each will be application-dependent.

We derived two sets of performance metrics for our system. The first, the minimum values, come from the need to distinguish between cell-expressed and extracellular, bound material and to verify that the material has a pattern correlated to the print template. The second, the desired values, come from those in the literature for related applications; the references for these are those cited in Section 5.

This section details the following:

- the implementation choices we identified for each component stage;
- our reasons for choosing the implementations we used;
- the characterizations of each implementation we performed;
- our end-to-end integration of each component; and
- the results of our end-to-end functional demonstration.

We have identified the cell engineering as by far the most labor-intensive and complex part of our technology concept's implementation. It requires choosing a host cell to be printed, a material to be deposited, and identifying and assembling genetic parts for the material, material stimulus, material delivery, and material binding. As such, the cell engineering implementation has its own subsections below detailing each of these individual steps. The other components are the print medium, the print substrate, and the 3D printing system.

Our final proof of concept demonstration was a two-material (non-structural) pattern: a "checkerboard" pattern of red and green fluorescent proteins. Overall, we demonstrated that each component technology had at least one feasible implementation. The information provided by our identification and characterization of available implementations not only answered key questions necessary for our mission feasibility/benefit analysis (Section 6), but also identified several unknowns that will be need to be quantified in future work.

Table 7.1: The performance metrics we derived for our proof of concept.

Metric	Minimum	Desired
positioning precision	1 cell diameter $\sim 10\ \mu$m	$1\ \mu$m
dispensing volume	$\leq 1000\ \frac{\text{cells}}{\text{“voxel”}}$	$\sim 1\ \frac{\text{cell}}{\text{“voxel”}}$
“voxel” size	enc. 1000 cells = 1 nL	10 pL
cell survival	50%	90%
pattern completion	75%	95%

7.2 Cell Engineering

7.2.1 Host Cell Strain Selection

We initially identified two primary desired qualities for our host cell strain. The first was size-driven; we wanted the functional cellular units (either single cells, as unicellular organisms, or activated clusters of cells with a unified function, as in multicellular tissues) to be no smaller than our printing system's resolution. This constraint allows us to achieve one functional cellular unit (FCU) per voxel resolution in constructing our cellular arrays. Being able to control FCU spacing as an independent variable is necessary to determine whether our ultimate goal of using the spatial pattern of the cell array to control the formation of material microstructure is possible. Although the Phase I work was limited to a non-structural proof of concept, we wanted to ensure that the same system could be used for follow-on work.

The second initial desired quality for our host cell strain was that have a history of established use. At a minimum, this would be a cell type which can be easily cultured in the laboratory; ideally, this would be a cell type with a strong history in molecular biology and genetic engineering. This criterion was particular important given the short timeline of the Phase I work; we would not be able to develop new plasmid backbones or other support biological tools.

A third criterion was identified after we had drawn up our list of potential material types. Nearly all of the most promising structural materials are made by multicellular organisms, all of whom are eukaryotes; the internal genetic machinery of eukaryotes is substantially different from that of prokaryotes. Although genetic engineering of prokaryotes is generally much simpler, and there is a longer history of established tools for it, we decided that we wanted our initial cell strain to be eukaryotic; this avoided the eventuality of having to re-implement our genetic engineering from prokaryotes to eukaryotes when moving to structural materials after the Phase I work.

Investigation of available microdeposition systems showed that the typical minimum droplet size of commercial systems is in the picoliter range, which corresponds very roughly to a droplet diameter of 10 μm. This is substantially larger than typical prokaryotes (around 1 μm for *E. coli*), on the small side for single-celled eukaryotic species, and much smaller than cells from most multicellular organisms.

The combination of these three criteria narrowed down our potential cell strains to existing unicellular eukaryote model organisms. We examined the following options:

- *Saccharomyces cerevisiae.* A common, spherical yeast approximately $5 - 10\ \mu$m in diameter Figure 7.2. It grows very quickly, is robust under standard laboratory conditions, and has an extensive history in genetic engineering. This was our final selection.
- *Schizosaccharomyces pombe.* Another common yeast, very similar to *S. cerevisiae.* We did not choose it due to its rod-like shape, which makes it exceed our size criterion along one dimension (although not in total volume).
- *Thalassiosira pseudonana.* An often-studied diatom. It was a promising option due to its natural deposition of silica, which would have given us immediate material production. However, the ability to

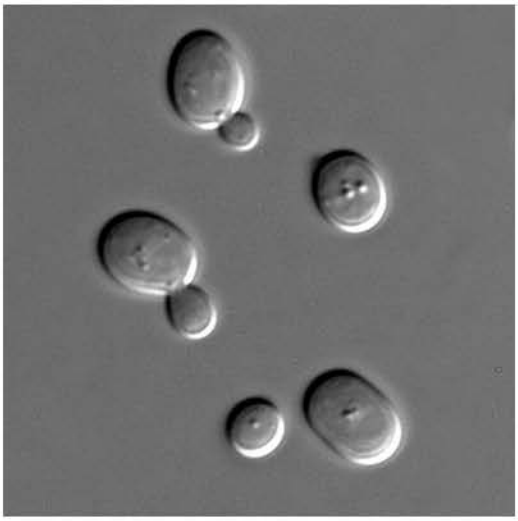

Figure 7.2: *Saccharomyces cerevisiae* under 1000x DIC magnification. The cells are roughly spherical, although they will elongate prior to division. (Public domain image.)

control the cells' silica deposition, and suppress it in order to introduce genes for other materials, is not established. We did not choose it for our initial study because (as with our prokaryotic options) it would have required re-implementing our genetic engineering later to add additional materials.

The most promising choice was clearly *Saccharomyces cerevisiae*. Our selection was cemented by the discovery of a commercially available plasmid backbone, pYES2.1 (Life Technologies), which is specialized for use in *S. cerevisiae* and included several other features necessary for our work (see details in subsection 7.2.5). This saved us a substantial amount of time in getting to our final proof of concept.

Our final choice was a *S. cerevisiae ura3* strain, meaning that the strain lacked the ability to synthesize its own uracil (one of the basic amino acids). Making the strain dependent on user-supplied uracil is a contamination and selection control.

7.2.2 Material Selection

As with choosing our host cell strain, when examining materials to implement for our proof of concept, we wanted one with an established history of implementation in genetic engineering. For material choice, this meant that it corresponded to a known genetic part, or coding DNA sequence. After deciding that we needed to work with two materials (see section 7.6 for more details), this criterion was expanded to include that both materials should be expressible using the same plasmid backbone. Being able to do all of our genetic engineering on a single plasmid greatly simplified our workflow.

Our other primary criterion was ease of verification. We wanted to ensure that we would be able to use the facilities we already had access to to analyze our material product, as the Phase I budget and timeline did not allow us to acquire new training or instrumentation. Most structural biomaterials, in their natural state, can only be identified and studied with electron microscopy, which we did not have low-cost access to. We did, however, have high-quality optical and fluorescence microscopy tools, as well as spectrophotometry and fluorometry.

Our last major decision, after establishing these criteria, was whether to use a protein directly as our material. Broadly speaking, genes within a cell code for proteins; some of these proteins are structural in and of themselves, such as keratin and collagen, but others work indirectly to cause the formation of non-protein-based structural materials, such as polysaccharides (chitin, cellulose, etc.), inorganic crystalline materials (silica, calcium carbonate) or even sequestered metal ions (Figure 7.3). The number of secondary materials with established genetic parts was relatively low, and there were even fewer secondary materials whose

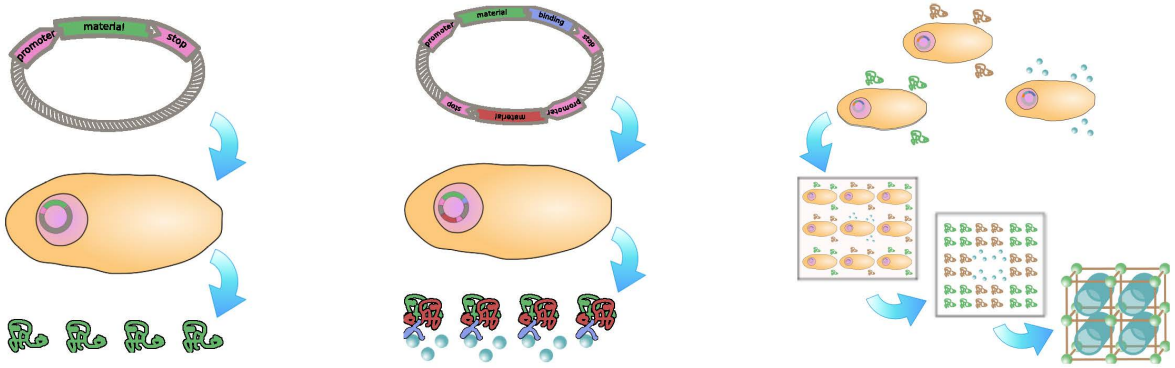

Figure 7.3: Assuming that the material is made by a cell and is dependent on a genetic part, there are multiple levels of complexity available. The simplest (l) is a protein-based material encoded by a single gene. Some protein-based materials have multiple subunits controlled by different genes (c). At the highest level of complexity (r), a composite biomaterial may consist of multiple protein-based materials as well as inorganic materials deposited by the cell.

presence and placement could be quantified in situ with our instrumentation.

We therefore decided to use two differently-colored fluorescent proteins for our proof of concept. We used several DNA sequence registries, including GenBank and the Registry of Standard Biological Parts, to search for coding sequences that were appropriate for our host cell strain. Our final selections were yeGFP, a green fluorescent protein modified slightly from that presented in [24] to enhance expression in S. cerevisiae, and and yeRFP, a red fluorescent protein modified similarly from that presented in [53]. The final sequences used are included in Appendix B .

An additional advantage to this material choice is that that GFP and RFP can be 'fused' to the end of other, non-fluorescent proteins to provide optical verification of their placement. Thus, when we move to work with structural proteins, we can use the same RFP/GFP implementation as fluorescent tags to improve our material analysis.

This literature search and downselection process brought to light the dependence of our technology concept on future advancement in genetic sequencing and functional identification.

7.2.3 Material Stimulus Method Selection

Our technology concept requires the ability to control the production of material by the cells. For our proof of concept, at a minimum, we need to prevent material production prior to printing, in order to ensure that the final material product is truly the result of the cells' activity in the array. However, ultimately, we will need to be able to regulate material production on a fine-grained level to be able to characterize its effect on material structure formation.

Although gene expression regulation can be complex, particularly in eukaryotes such as our host cell strain, its basis is the part of the gene known as the promoter(Figure 7.4). There are many established promoter sequences for S. cerevisiae in the literature. The first choice is whether to use a constitutive promoter, or one whose effect is determined by external stimuli; if the latter, the second choice that must be made is what the external stimuli is to be.

We reviewed a significant number of promoters available in yeast (see overviews in [14, 73, 94], among others). We quickly determined that there was no advantage to choosing a constitutive promoter, as there are equally strong or stronger inducible promoters and the additional process overhead added by needing to time printing to avoid accumulation of secreted material in the print medium was a significant cost.

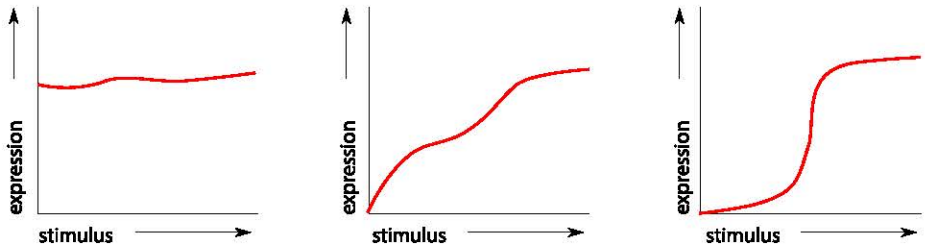

Figure 7.4: Broadly speaking, promoters are the part of a gene which control expression. The simplest type is (l) a constitutive promoter, which is essentially insensitive to environmental conditions. Many promoters are (c) inducible, controlling expression of their linked coding regions in response to a particular stimulus. Some are also (r) repressible, allowing for an effect like a programmable dimmer switch.

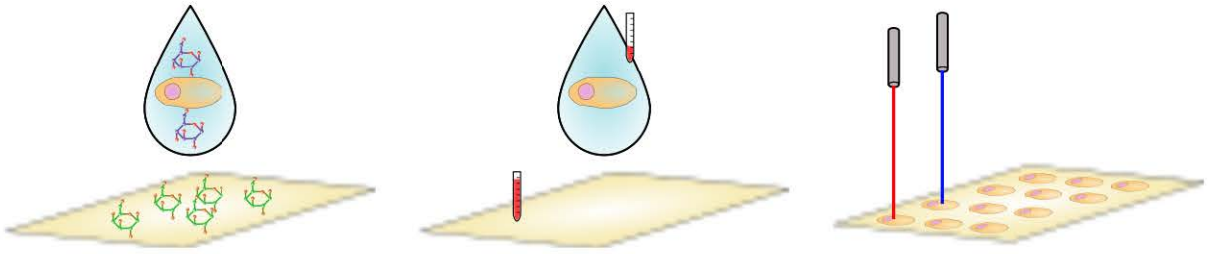

Figure 7.5: Material production can be triggered via, among other choices: (l) chemical stimulus, which can be implemented by adding the trigger to the print substrate; (c) thermal stimulus, in which an exogenous temperature change after printing is used; and (r) optical, in which post-printing cells are exposed to different intensities or wavelengths oflight.

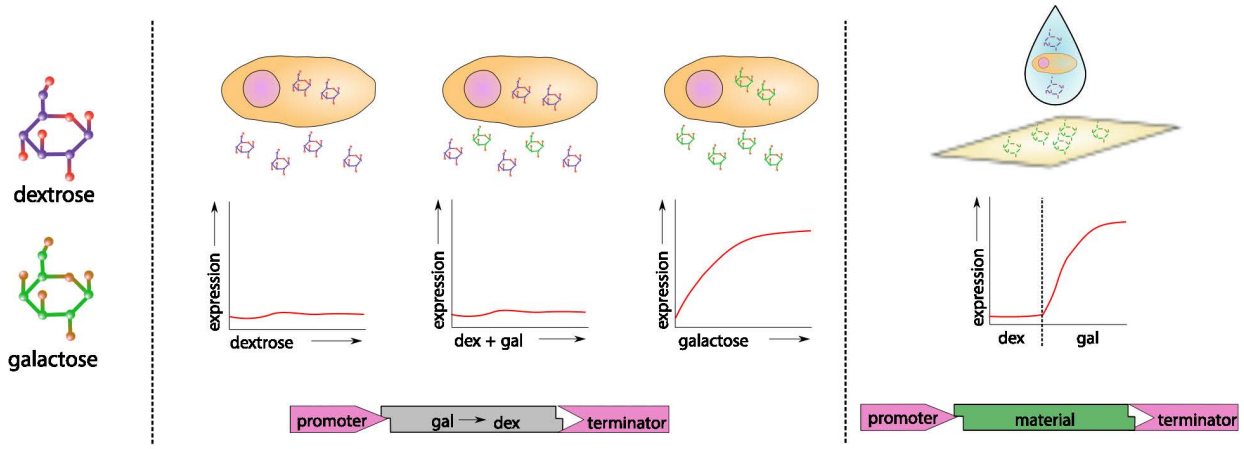

Figure 7.6: In nature, the GAL1 promoter is attached to the gene that makes an enzyme involved in metabolism of galactose, a sugar that provides less energy than dextrose; the promoter has two methods of response, both suppressing expression in the presence of dextrose and promoting expression in the presence of galactose.

Having decided to use an inducible promoter, the next key question was what type of stimulus to use (Figure 7.5). We examined the function of promoters which are controlled by heat, different wavelengths of light, and a wide variety of chemical stimuli (phosphates, alcohols, metal ions, and sugars, among others). We discounted thermal stimulus because of the undesirable effects of changes in temperature on the viscosity of our printing solution and print substrate. Optical stimulus had several attractive features, including the potential of finest-scale control over material production, but both optical gene regulation systems we examined [88, 93] were extremely complex and not feasible to implement on a Phase I timeline. We therefore decided to use a chemical-based stimulus.

A key realization from this examination of promoters was that the type of stimulus best suited to a particular implementation of our technology concept would vary based on the form factor of the material being produced. A material that does not require small-scale variation in material properties – for instance, a structural element in tension – can be produced at much lower cost and effort using thermal or chemical stimulus; a more specialized piece, such as a gear or buckle, might require a scanning laser optical stimulus system to be fully optimized. Table 8.2 summarizes our conclusions.

Of the remaining promoters, the GAL1 promoter, pGAL1 , offered several notable features. It is well-studied, and its peak expression effect is so strong that it is sometimes used as a baseline for comparing the effectiveness of other promoters [14, 73]. In nature, pGAL1 regulates galactose metabolism. Galactose is a sugar that requires more energy to break down (i.e., is less desirable as a food source) than common dextrose. pGAL1 represses expression in the presence of dextrose and induces expression in the presence of galactose, leading to preferential consumption of dextrose (Figure 7.6). Placing pGAL1 upstream of our material coding region would therefore allow us to suppress material production by placing the cells in a dextrose-containing medium, then stimulate it by printing the cells onto a galactose-containing substrate. This functional unification between the act of printing and the act of material production stimulus eliminated several potentially costly development steps in our Phase I workflow.

We therefore chose inducible chemical stimulus, implemented by pGAL1 and dextrose/galactose presence, as our material stimulus method. The depth of the connection between printing process control and material stimulus method, and the importance of achieving functional unification wherever possible, was another key aspect of our technology concept identified here.

7.2.4 Material Delivery Method Selection

Material delivery method is the means by which the final material products (proteins, secondary materials, etc.) are removed from the cell. For materials which are manufactured within the cell, there are two broad approaches to delivering it to the external environment. One class of approach to material delivery is to use existing cellular mechanisms; cells have many ways of transporting proteins and other biomolecules outside of themselves (Figure 7.7). The other class of approach is to forcibly remove the material, typically by killing and rupturing the cells. Some secondary materials, such as metal ions sequestered by surface-expressed proteins, are deposited entirely outside of the cell to begin with, making production and delivery unified into a single function.

Initially, our primary criterion was simply to use an established method of material delivery, as the Phase I timeline did not allow for the extensive additional protocol development. Having already decided to use a protein as our end material (see subsection 7.2.2 for details), sequestration was not a relevant approach, although it remains of interest for future work involving secondary materials. A review of existing work on related methods of biomolecule production (section 5.2) showed that, of the remaining possibilities, cell rupture was typically used for large biomolecules and fibers, such as silk and 'plastic' polymers, whereas genetic parts for secreting smaller proteins in yeast have been used in the production of pharmaceuticals for decades [15, 117].

Given the size of the protein choice we made, secretion was a natural choice. However, this stage of the proof of concept served to strongly emphasize that the choice of implementation for material delivery method is deeply intertwined with the selection of target material. The results of our initial survey are shown in Table 8.3; this is an area that will require further characterization and development.

Having chosen secretion as our delivery method, we had to determine how to implement it in our host strain and given our choice of material coding region. The secretory mechanisms of eukaryotes are much more complex than those of prokaryotes, and secretion often requires several different genetic mechanisms to work in concert. Fortunately, we were able to identify a consensus artificial 'secretion signal' protein section that had been proven to work for a wide variety of proteins in our host organism [21]. This 'header' (pre-pro-peptide) attaches to the material protein of interest and signals the cell that it should be secreted; the header sequences is cleaved as part of the secretion process, leaving the desired protein deposited intact in the extracellular environment. The DNA sequence corresponding to this amino acid sequence was modified slightly to account for limitations of our synthesis capabilities and inserted upstream of our material coding region. The sequence is included in Appendix B.

7.2.5 Material Binding Method Selection

Once the material has been extracted from the cell, via secretion or another delivery method, it must be bound either to other deposited material (as in material self-assembly) or to the print substrate. This is necessary both to ensure a continuous material product and to enable the cells to be removed prior to material analysis.

The mechanisms used in nature to cause continuous macroscale material growth appear to involve fine control of the cells' immediate microenvironment (pH, chemical composition, and so forth), but are currently poorly characterized. One of the key strengths of our technology concept is that it treats this function as a 'black box'; we do not need to understand how it works now as long as we can stimulate the cell to reproduce the desired behavior, and when the genetic tools are developed in the future to allow us to customize the behavior, our technology's potential will only be expanded. Therefore, although this part of our technology concept is theoretically the most wide-open in terms of potential implementations, for our proof of concept, we limited ourselves to the simplest material binding methods currently well-understood.

There were three criteria on which we made our binding method selection. The first, as with our previous choices, was that it correspond to an established genetic part, a necessity given our timeframe and budget. The second was that it not interfere with material production or delivery. The last was that it require

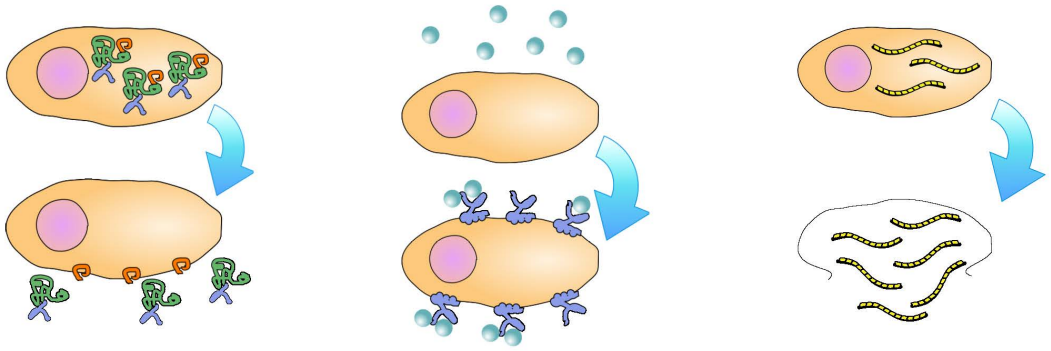

Figure 7.7: The material can be delivered by to the external environment via, among other choices: (l) secretion, in which the material has a self-cleaving tag that causes the cell to export it outside its membrane; (c) sequestration, in which the cell expresses a protein that causes it to gather a material present in the external environment close to itself; and (r) lysing, in which the cell has to be exogenously broken open to release the desired material.

minimal pre- and post-processing, as reducing the overhead of biomaterial production is a key selling point of our technology concept.

The natural place to start was by surveying existing protein purification methods, as the choices already made regarding material selection, stimulus method, and delivery method, simplified the material binding step of our proof of concept to separating a secreted protein from its parent cell. We quickly identified the concept of protein affinity tags – short protein sequences added to a 'main' protein that bind to a specific complementary substance – as a suitable implementation.

Our initial choice was a polyhistidine tag, which binds to nickel or cobalt ions. We implemented this as an additional DNA sequence downstream of our material coding region. We achieved detectable binding with this method (full results in section 7.7); however, cytotoxicity assays showed that the presence of nickel ions in our print substrate had a significant negative effect on material production due to stress on the printed cells. We therefore re-implemented this step with a second type of affinity tag, an antibody-binding tag (V5 epitope); this approach borrows from the technique of western blotting. Characterizing the binding efficiency of this new implementation is not yet complete.

As with material stimulus and delivery achieved earlier, the implementation of 'on contact' affinity tags as our material binding choice lets the act of printing also be the trigger for material binding. In our proof of concept, therefore, printing is the trigger for all three downstream steps. This functional unification is a significant advantage of our chosen implementation, and highlights the need to address all steps of the technology concept simultaneously when making implementation decisions for future work.

7.2.6 Assembly and Testing

With all of these choices of genetic sequences made, the final step was to assemble each of these parts and test the efficiency of the final engineered cell strain.

With five genetic parts to combine (Figure 7.9), we used several different established methods. Our first, partial plasmids, containing only the target material genes, were assembled using TOPO TA cloning kits (Life Technologies). We then added the secretion tag and other parts using Golden Gate assembly [31]; this resulted in several partial plasmids, which later became useful as controls. After our first implementation, using the GFP and RFP sequences provided in [24, 53] proved to have relatively low fluorescence, we adjusted the sequences in software to re-balance their codon frequency and had the new sequences synthesized from scratch; these new sequences were again inserted into the plasmid using TOPO cloning. After our first binding method proved to be of marginal efficiency, we realized that we would need to express

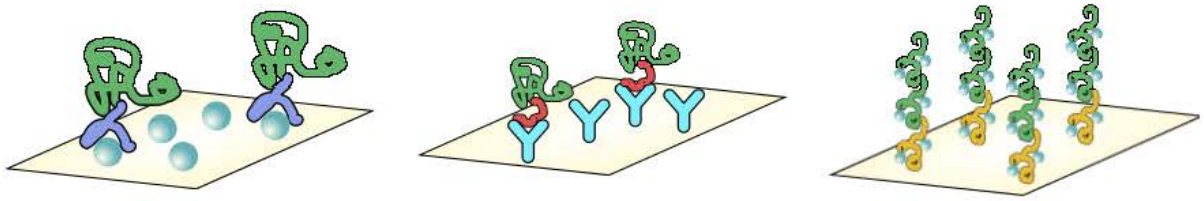

Figure 7.8: Protein-based materials can be given an 'affinity tag' which binds to a substance present in the print substrate. Polyhistidine tags (l) bind to certain kinds of metal ions, such as nickel or cobalt; antibody-epitope tags (c) bind to specific antibodies. A more advanced option is (r) is self-assembly, in which a 'seed' material is embedded in the substrate to allow self-assembling protein or other biomolecule constructions to form.

the gene construct in E. coli as well to provide a baseline for protein quantification; we therefore added a consensus ribosome binding site (used in [30], sequence given in [90]) first with the Flexi digestion/ligation system (Promega), and then re-done with site-directed plasmid mutagenesis [59] after the restriction site scar from the Flexi system proved problematic.

We tested the functionality of our engineered cell strain first qualitatively, by fluorescence microscopy (Figure 7.10). Both RFP and GFP expression were clearly much higher in the strains grown in galactose medium than in glucose medium, although there was (as expected) a low level of 'leakage' expression in the glucose cultures.

The next test was to quantify the expression and to demonstrate secretion. RFP and GFP cultures were grown in either dextrose or galactose for 7 days. Each day, their density (number of cells per mL) and fluorescence (relative to a standard) were measured and recorded. Dividing the fluorescence by the cell density gives an average measure of fluorescent protein produced per cell. Each day, an aliquot of cells from the culture was spun down and the supernatant (remaining liquid free of cells) was also measured for fluorescence; this provided a measure of how much fluorescent protein was being secreted into the culture medium, rather than simply contained within the cells. As these tests were done in conjunction with the final print medium and substrate tests, the results are shown in Figure 7.15 .

To demonstrate the effectiveness of material binding, we extracted and purified the RFP and GFP made by our cells. These purified protein solutions were mixed inside of microcenterfuge tubes with small pieces of our substrate that had different concentrations of nickel, as well as a few other materials we had examined for use. After a brief period ofincubation to ensure the proteins had time to bind fully, the substrates were washed with distilled water to remove any unbound protein. The substrates were then stained with Coomassie Brilliant Blue (Sigma-Aldrich), a blue dye which binds to protein, and washed to remove unbound dye. The dyed substrates were then measured for blue light absorption to quantify the amount of bound protein (Figure 7.11 .)

The results show that the presence of nickel in our substrate has a clear protein-binding effect. However, the lowest level of nickel at which binding was observed was also, in our post-printing expression tests, the highest level of nickel at which detectable material expression occurred.

These results show that our target choice of material is easily detectable; that its expression is strong and our stimulus method provides adequate control; and that our delivery method is effective. The binding efficiency was detectable, which was our minimum bar, but required further investigation in combination with our specific print substrate (subsection 7.5.3).

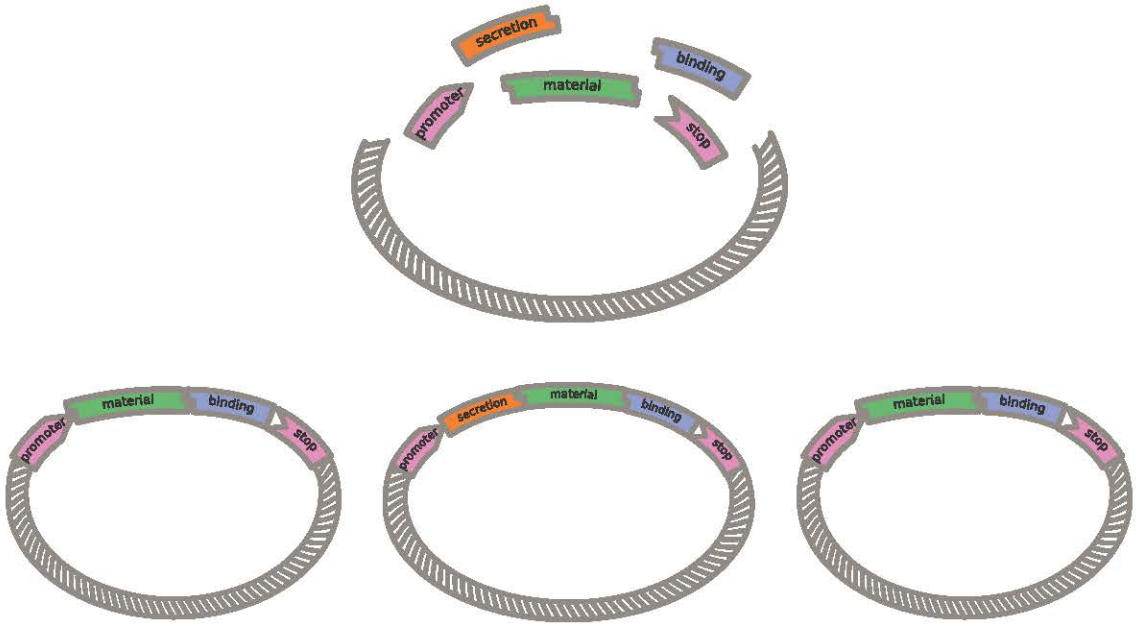

Figure 7.9: Our final plasmid design had five distinct parts (top). Through a variety of assembly methods, we generated several partial plasmids (l,r) as well as the complete plasmid (c).

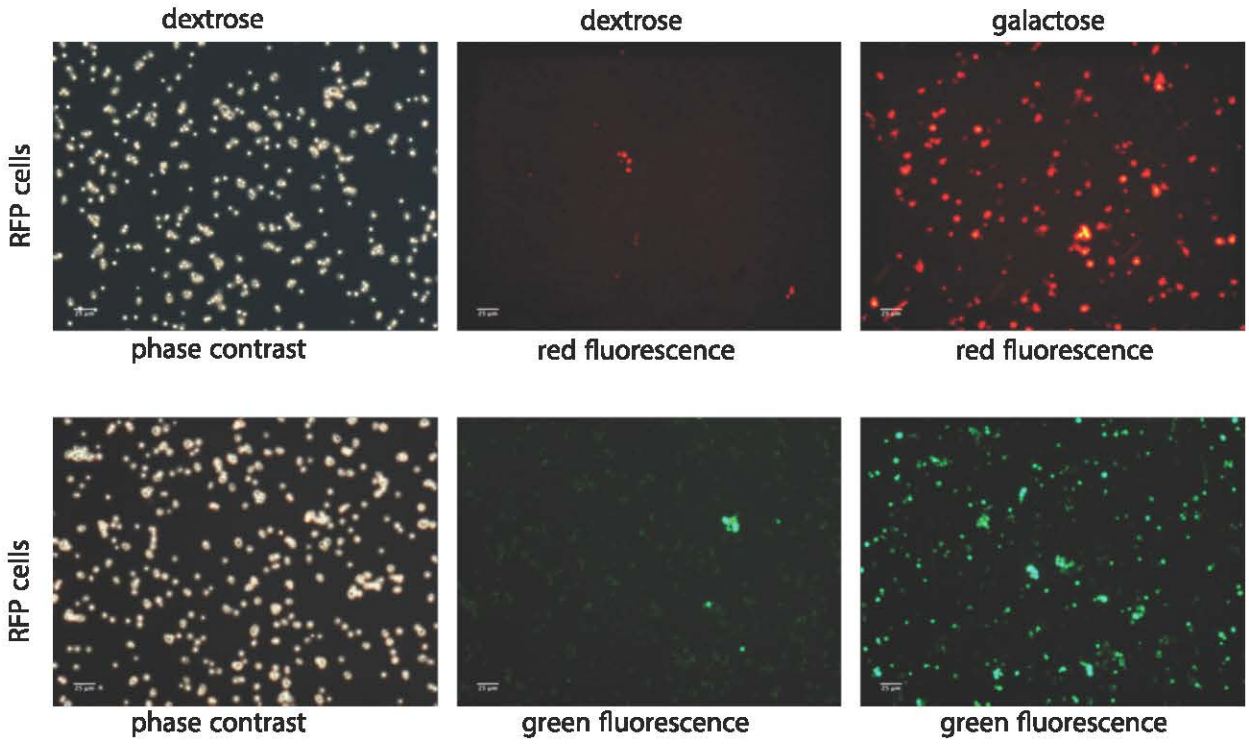

Figure 7.10: The RFP and GFP cells both show strong expression in galactose medium and minimal expression in dextrose medium. The non-fluorescence (phase contrast) micrographs are included to give a sense of overall cell density.

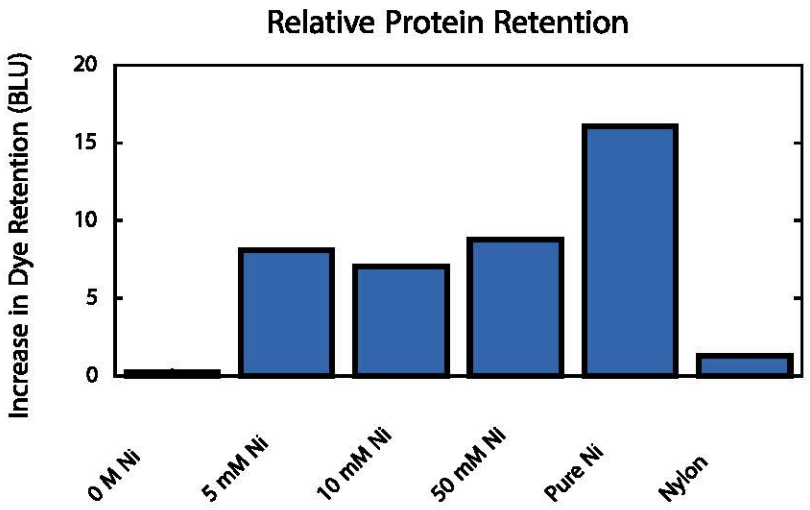

Figure 7.11: A simple test using a blue dye which binds to proteins was used to test the differences in protein retention on several different substrates with the same surface area. The amount of dye bound was quantified by blue light absorption.

7.3 Print Medium

7.3.1 Medium Basis Selection

The printing medium must keep the cells alive and in a non-material-producing state prior to printing; provide protection during printing; not interfere with cell expression post-printing; and work together with the print substrate to form a physical support structure for the cells and to minimize cell motion (drift or migration) after printing.

Given our choice of host cell strain, the printing medium needed to be an aqueous solution containing all the elements of a yeast minimal growth medium, minus uracil. Given our choice of material stimulus control, it needed to include dextrose as a carbon source, to prevent material production prior to printing. (This is an excellent illustration of how the implementation choices of this technology concept are interdependent.) We also included ampicillin, an antibiotic which does not affect fungi such as yeast, as a control against bacterial contamination. The remaining choice was only whether the print medium would contribute to the physical support structure, meaning have a gelling basis, or not.

Our microdispensing system had a viscosity limit of 10 cP (= 10 mPa ·s), which means that the print medium must be printed in a close to liquid state. If the print medium was to contribute to the physical support structure, it would have to be triggered to gel after after printing. As discussed in section 5.1, a number of biocompatible printing support scaffold materials have been developed. Since the ingredient used as the gelling basis had by far the largest effect on total print medium viscosity, we tested all of our potential bases at different concentrations under varying temperature conditions (Figure 7.12).

Both agarose and alginate, the two materials with the most suitable viscosities in the range of concentrations that suit our application, are polysaccharides. Agarose gels below a certain threshold temperature; alginate gels in the presence of calcium ions. We chose alginate as our print medium basis, as adding temperature control to our printing process was not feasible given our setup at the time. Because the calcium exposure can be provided by printing the medium onto a calcium-containing substrate, this choice also provides functional unification between the act of printing and the substrate gelling, further simplifying our workflow.

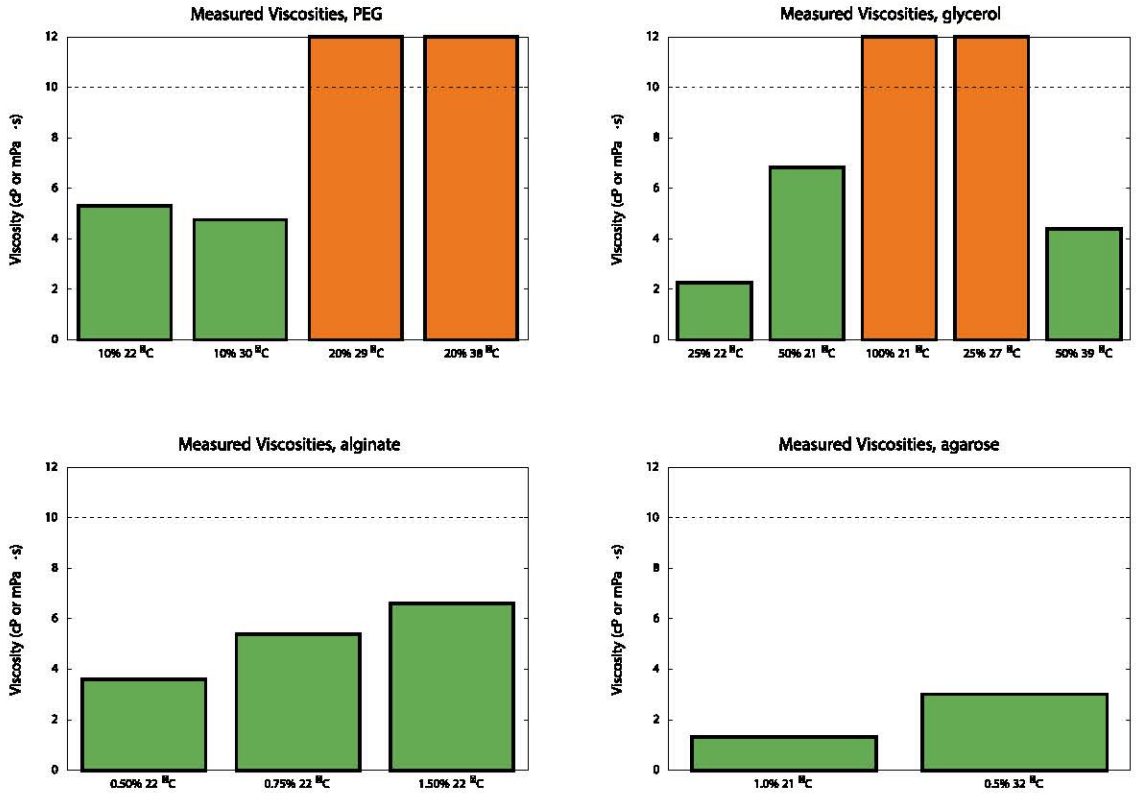

Figure 7.12: We tested four different gel bases under a variety of concentration and temperature conditions. The dashed line represents the limit of our microdispensing system.

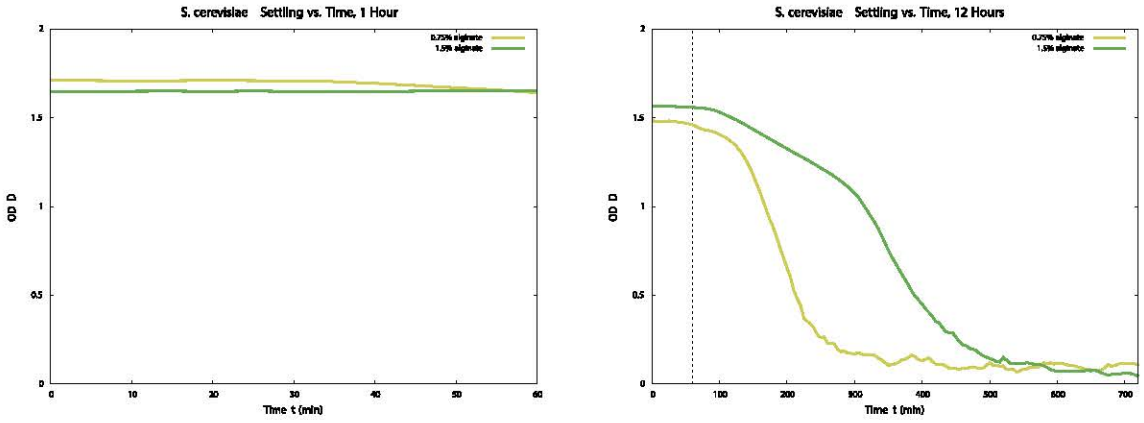

Figure 7.13: We tested cell settling in our alginate-based medium on 1-hour (l) and 12-hour (r) timeframes. The y-axis is in optical density, which is proportional to absorbance on a log scale.

The final recipe for our print medium is included in Appendix B .

7.3.2 Anti-Aggregation Performance

Our microdispensing system had a particulate limit of 10 µm in diameter; we found that it was very sensitive to the presence of particles larger than this size and frequently clogged, sometimes requiring expensive replacement of the nozzle, if the solution to be printed was not passed through a 10 µm filter immediately prior to loading. Given that our target print solution was a cell suspension, and yeast cells fairly rapidly form aggregates, the rate of yeast cell settling in the print medium was a parameter of high importance.

The workspace of our micropositioning system is one cubic centimeter (1 $\times 10^{-6}$ m^3). Combining this figure with a desired minimum resolution of one cell diameter per droplet and the maximum droplet production rate of our nozzle gave us a maximum print run time estimate of one hour.

We tested the settling rate of yeast cells in our medium by filling a transparent container with a cell suspension of our target density and continually measuring the absorbance at a fixed level near the top of the liquid level. Absorbance, in this type of setup, is proportional to cell density, so as more cells begin to drift downward, the measured density at the top of the solution should decrease.

We tested two different concentrations of alginate in our print medium (Figure 7.13), and determined that 0.75% alginate was sufficient to meet all of our criteria.

7.3.3 Cell Growth and Expression

To determine whether our print medium design had any negative affect on cell growth, we grew the RFP-expressing cells, the GFP-expressing cells, and the original unaltered cell strain in our print medium for a week and measured the cell density (Figure 7.14). Neither the print medium nor the presence of the genetic modifications appeared to affect growth.

To determine whether the print medium formulation was sufficient to fully suppress material production, and whether the equivalent galactose concentration in the print substrate would stimulate it, the cell strains were grown in either our print medium, which contains dextrose, or a modified version containing galactose. The effect of dextrose and galactose is very clear (Figure 7.15). Also worth noting is that the GFP is approximately twice as bright as the RFP, which can be seen by comparing the levels of the background 'leakage' expression, and that the RFP appears to be more stable than the GFP, as it takes longer to accumulate to a steady level.

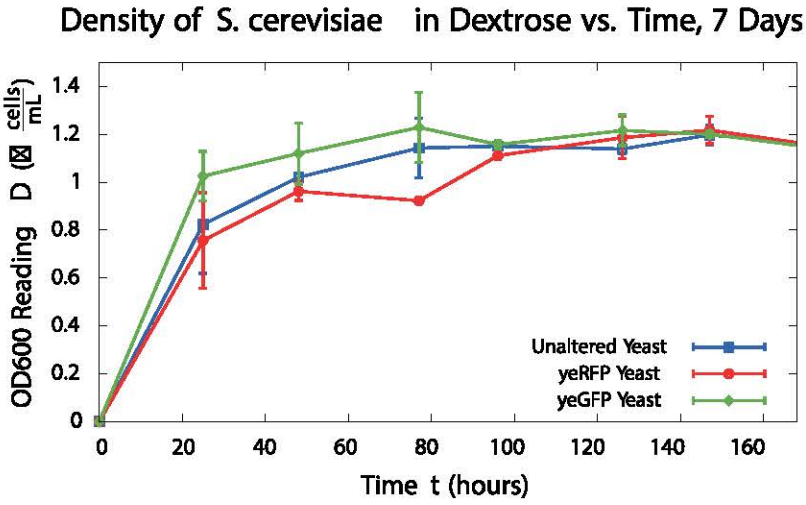

Figure 7.14: Cell density measured over a week for our unmodified host cell strain, our RFP-expressing cells, and our GFP-expressing cells in our print medium. The modifications necessary to enable material production do not appear to affect cell growth when the cells are not actively producing. Compare with Figure 7.21 .

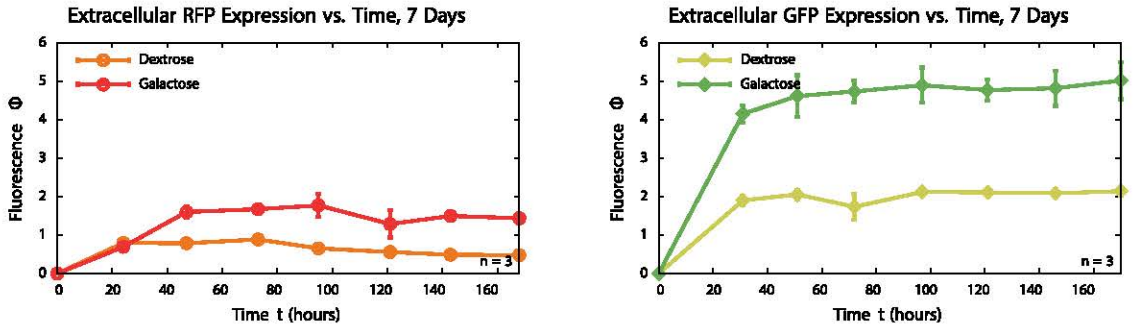

Figure 7.15: We quantified the amount of secreted fluorescent protein by measuring the fluorescence of the supernatant after the cells had been gently spun down. This measurement was normalized to a fluorescent standard and then divided by the number of cells present in the original solution to create Φ, a measure of the average amount of secreted fluorescence per cell.

These results clearly show that we have established the functionality of our print medium and its integration with our cell strain, an important step towards our proof of concept demonstration. They also established that a typical timeframe for material deposition is on the order of 2 days, a parameter that allowed us to add a section on time costs and savings to our mission feasibility/benefit analysis.

7.3.4 Cell Drift and Gelling Measurements

As the positioning of the cells is one of the primary control variables for our technology concept, quantifying and reducing the uncertainty in it is key. In keeping with our 'one cell per voxel' ideal resolution criterion, we wanted to keep cell drift after printing to within one cell diameter, or 10 μm for our *S. cerevisiae* cell strain.

A short qualitative demonstration comparing cell motion in ordinary aqueous medium to that in different gelling bases (glycerol, agarose, and alginate with and without calcium) on an agar substrate was conducted in order to determine the amount of post-printing cell drift likely to occur. Videos taken at 200x magnification showed that the baseline cell drift, for cells printed in aqueous medium, was on the order of several hundreds of microns. Agarose reduced this to essentially zero, as it gelled completely upon cooling. Glycerol reduced to drift by approximately an order of magnitude; alginate's effect without calcium was barely noticeable. Alginate with calcium, like agarose, gelled upon printing and reduced cell drift to a largely undetectable level. (Video files are available upon request.)

This short demonstration indicated that our alginate-based print medium reduced cell drift to within acceptable parameters.

7.4 3D Printing System

7.4.1 Hardware & Software Design

Additive manufacturing systems typically consist of two major parts: a dispensing subsystem, which handles feeding the material at the appropriate rate and time, and a positioning subsystem, which . In some designs, the positioning subsystem is physically integrated with the dispenser and moves it relative to a stationary build platform on which the finished piece is deposited; in others, the positioning subsystem moves the build platform, the dispenser head is stationary, and only software integration is required between the two.

As reviewed in Section 5, there are a number of commercially available microdispensing systems capable of printing living cells at picoliter resolution, which corresponds very roughly to a droplet diameter of 10 μm. Spatial resolution of positioning systems is typically finer: on the order of 1–2 μm for DC-motor-based solutions and into the nanometers for piezo-based systems.

We created a concept cell printing run consisting of a double-walled cylinder with an outer diameter of 1 cm. This form factor was chosen as a simplified version of several load-bearing elements found in animals, including sponge spicules and small vertebrate bones. Based on this concept print run, we derived the set of performance parameters for our micropositioning and microdispensing subsystems used in our market search. These parameters are reproduced below.

Printing system requirements: A combination of motion positioners, motion verification sensors (encoders), controller/driver electronics, and software, some or all of which may be integrated with each other, sufficient to allow commanded positioning to the following specifications:

- Range of motion in X direction (along print substrate surface) $\geq$ 10 mm
- Range of motion in Y direction (along print substrate surface, perpendicular to Y) $\geq$ 10 mm
- Range of motion in Z direction (perpendicular to print substrate surface) $\geq$ 10 mm
- Resolution (encoder or other sensor limit) $\leq$ 0.01 μm

- Minimum incremental motion ≤ 0.1 μm
- Positional inaccuracy (measured directly, or inferred from maximum of roll/pitch/yaw at 10 mm, as on-axis bi-idirectional repeatability, compensated backlash, or equivalent figure) ≤ 2 μm per 1 mm travel
- Controller/driver interface allows for direct, low-level commands (e.g., via command-line interface – note that a proprietary pipe from 3D modelling software does not meet this specification)
- Controller/driver interface specifications are compatible with real-time operation (e.g., RS–232 – note that USB may not meet this specification)
- Command set for controller/driver is well-documented and said documentation is made available
- Linux (Debian preferred) support for controller/driver – at a minimum, C libraries are provided
- Must be compatible with external hardware mounting of dispensing subsystem and printing substrate
- Must accept commands via same in-house-developed software as dispensing subsystem

Dispensing system requirements: A combination of dispensing hardware, dispensing verification sensors (e.g. camera), controller/driver electronics, and software, some or all of which may be integrated with each other, sufficient to allow commanded dispensing to the following specifications:

- Must dispense droplets of volume ≤ 50 pL to 100 pL
- Must have fluid reservoir of ≥ 25 μL
- Must reliably load and dispense fluids containing particulates ≥ 10 μm in diameter
- Must be compatible with fluids with the following properties: viscosity ≥ 0.9 mPa·s, temperature 5–40 °C
- Droplet throughput ≥ 5 Hz
- No bio-incompatible wetted parts
- Dispenser head empty/clean/reload cycle time ≤ 1 hr
- Must be controllable via direct interface (e.g., serial) or triggered via external signal (to allow for synchronization with positioning system timing)
- Command interface is compatible with real-time operation (e.g. RS–232 – note that USB may not meet this specification)
- Must be accept direct, low-commands to the following degree: trigger dispensing, query dispensing status, or dispensing complete signal
- Must be compatible with external hardware mounting of positioning subsystem and printing substrate
- Must accept commands via same in-house-developed software as positioning subsystem
- Must include droplet sensing/metrology system (e.g. focused optical feed to CCD) to allow in-house-developed software to perform droplet verification analysis and adjustment

There were very few options available on the microdispensing side; most systems we reviewed with droplet size resolution in the appropriate range were designed for pure liquids and their manufacturers could not or would not provide guidance on the system's anticipated performance with particulates (such as cells) in solution. Of those who did, only one, MicroDrop, made a system which provided low-level access to basic commands rather than requiring a proprietary software interface; since we needed the subsystem for integration into our prototype, this feature was a must-have. Our final solution was the MicroDrop MD-E–6010 system.

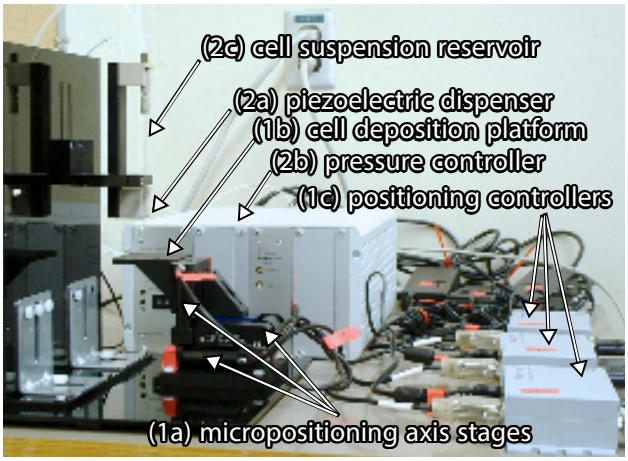

Figure 7.16: Our current hardware setup, with important components marked.

Having made our microdispensing subsystem selection considerably narrowed our choices for micro-positioning system, as the two subsystems needed to use the same type of software interface for us to be able to integrate their functions. We chose the Physik International C–863.11/M–111.1DG controller/ motor subsystem.

After receiving the commercial-off-the-shelf hardware, we needed hardware and software integration. We designed and built a laser-cut acrylic frame with adjustable spacing to mount the micropositioning stages and microdispenser head (Figure 7.16).

As shown in Figure 7.17 , the software written for this project takes realtime input from the user to fill and empty the dispenser head, and reads input files that describe the pattern to be printed. It then sends the appropriate commands to the bioprinter, with separate serial port connections for the dispensing system and the positioning system. These input files include the xyz locations where drops are to be deposited, the number of drops at each location, and the voltage and pulsewidth that the piezoelectric dispenser head will use. This software is written in C++ and runs on a Debian PC connected via RS–232 serial ports to the controllers for the positioning and dispensing systems. This software relies on raw user-supplied material patterns files, so a future step will be to upgrade it to allow it to read 3D file formats that are more standard.

7.4.2 Resolution & Cell Number

To optimize the print resolution, a range of voltages and pulsewidths were tested for the piezoelectric dispenser head, as shown in Figure 7.18 . Of the values tested, the maximum number of cells per drop was achieved with 150 V and a 150 microsecond pulsewidth. Lower voltages proved unreliable, in the tests referenced in Figure 7.18 as well as prior print tests: occasionally, no droplet dispensed at all at 50 V.

The parameters that maximize the number of cells per drop appear to be the most consistent in terms of standard deviation, and so to move toward reliable single-cell resolution, these same parameters (150 V, 150 µs) would be used with cell cultures that are more dilute than those at which this data were taken.

%

7.4.3 Cell Survival and Expression

The microdispensing system is a contactless piezoelectric system that works by sending a pressure wave through a thin glass tube containing our cell culture. We were concerned that this process might damage the cells. Typical results in the literature for similar systems have achieved cell survival rates as high as 90% [27, 58]; rates can be higher for systems which print multiple cells per drop [66], as the larger amount

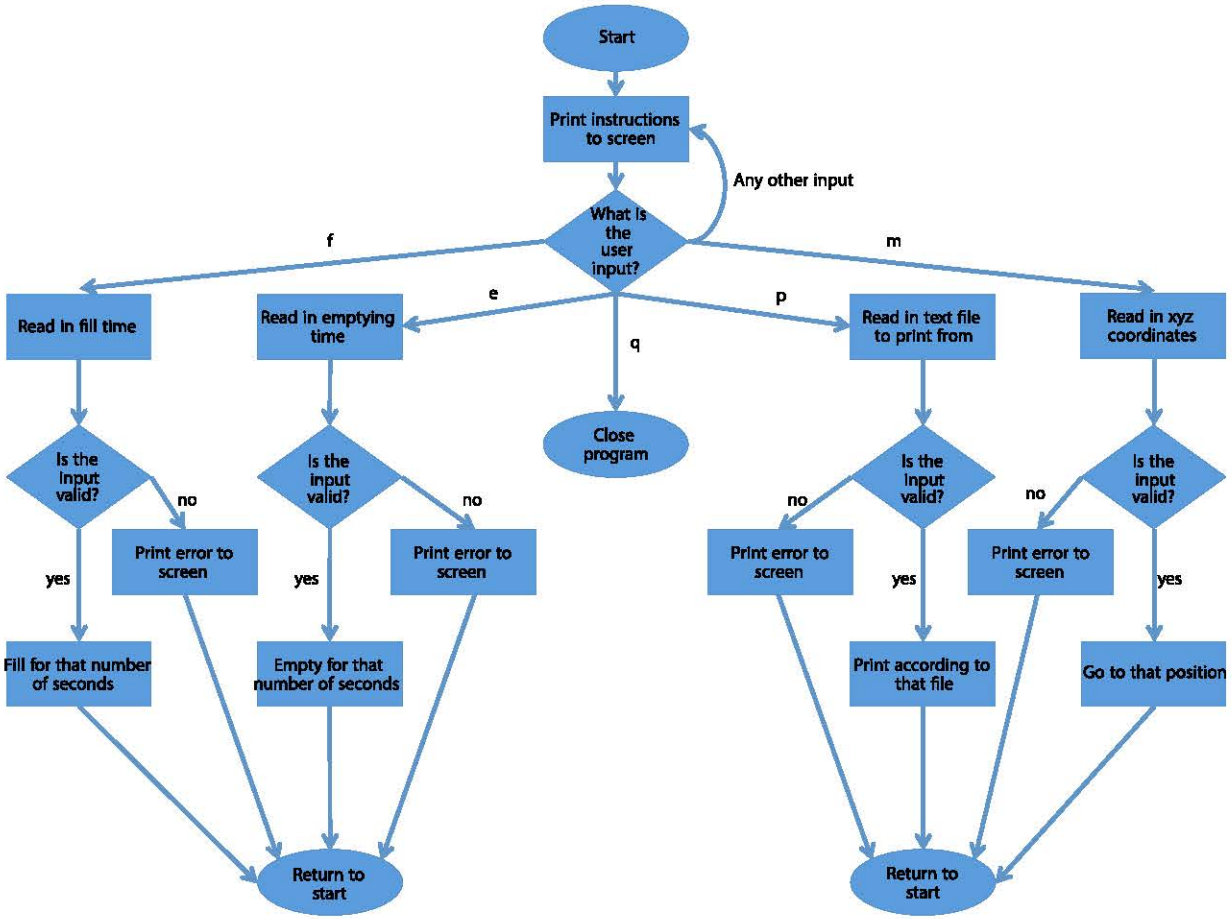

Figure 7.17: A flowchart for the software that controls the bioprinter, taking an input file that describes the print pattern and sending control signals to the positioning and dispensing systems.

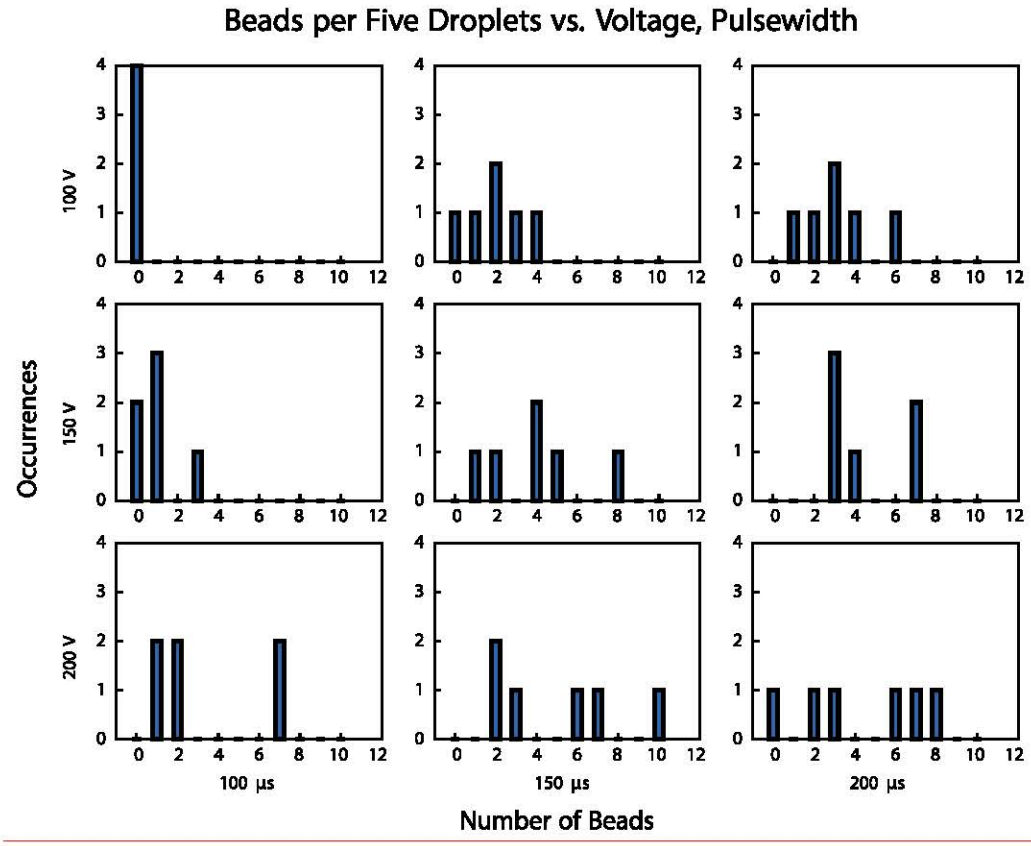

Figure 7.18: One of our plots showing the number of cells per print location for a range of dispenser head voltages and pulsewidths. Pulsewidths are in microseconds. We used a battery of these tests to determine the optimal printing parameters.

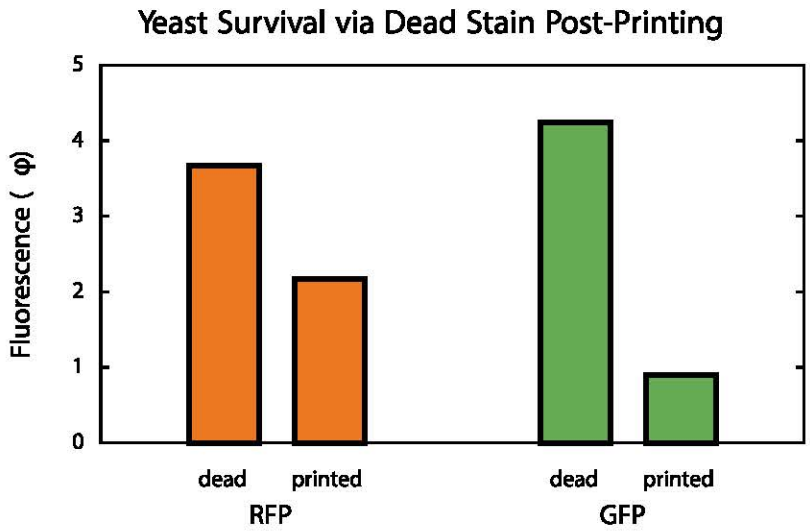

Figure 7.19: RFP and GFP cells were treated with a fluorescent dye that only stains dead cells. The fluorescence level resulting from staining printed cells were compared to staining an equivalent number of heat-killed cells to establish a floor for the number of cells killed by printing.

ofliquid present around each cell provides a protective effect.

We established a lower limit for the viability of dispensed cells by using SYTOX Green (Molecular Probes), a nucleic acid stain that can only enter cells with compromised membrane integrity (and thus generally non-viable). We created a 'killed control' by leaving a 1 mL aliquot of our cell strain suspended in PBS (a neutral salt buffer) in a 70–80 ⊠C water bath for 10 minutes. 25 µL of cell culture at the same density in the same buffer was then printed into a sample container. Both the printed cells and the killed control were stained with 5 µM SYTOX Green following the manufacturer's protocols. The entire 25 µL printed cell sample and 25 µL of the killed control were then each diluted into 200 µL of PBS to reduce background fluorescence. The 200 µL final samples were measured in a fluorometer (Figure 7.19) to determine the amount of bound fluorescence and then in a spectrometer to determine the cell density, allowing calculation of the amount of fluorescence present per cell (φ).

The results indicate a minimum survival rate of 40% for the RFP-expressing yeast and 60% for the GFP-expressing yeast. While the true rate is likely substantially higher, this is a sufficient demonstration to prove that enough cells survive to achieve our proof of concept.

7.5 Print Substrate

7.5.1 Substrate Composition Selection

The print substrate must keep the cells alive after printing; allow (in combination with the print medium) for a sufficiently low level of cell 'drift' post-printing; support the printed cells in an actively secreting state for long enough to allow a sufficient material yield; bind the secreted material so that it can be isolated; and allow removal (washing away) of the cells post-secretion.

Essentially all of the main print substrate components were determined by our earlier implementation choices (Figure 7.20). Agarose was chosen as a gelling base after we tested it against our RFP- and GFP-expressing cells and determined that it had acceptably low interference with fluorescence detection. Our choice of ura3 S. cerevisiae as a host strain meant that our substrate needed to contain a nitrogen base with selective amino acid supplements as a selective nutrient source. Our use of the pGAL1 for material stimulus control meant that the substrate had to contain galactose as a secretion expression stimulant. Our choice

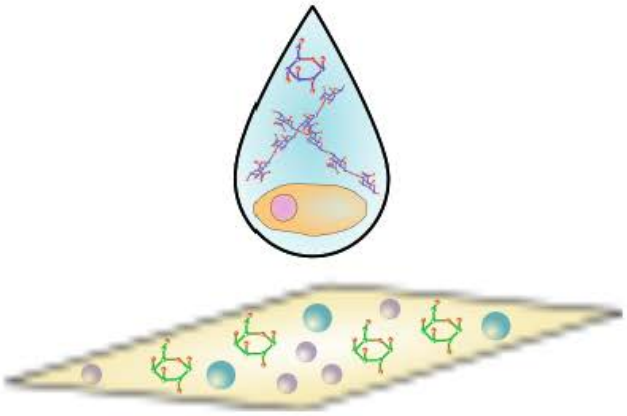

Figure 7.20: Many of the substrate components were determined by a priori choices, including the presence of nickel ions (for the affinity binding), galactose (to stimulate material production), calcium ions (to trigger gelling), and the yeast nitrogen base plus selective dropout supplements (to ensure the yeast remain active).

of gelled alginate as a biocompatible physical support meant that the substrate also had to contain calcium chloride, in order to cause contact gelling. The open-air nature of our print process means that ampicillin was necessary to prevent bacterial combination during the active material deposition phase. Our initial choice of polyhistidine tags as material binding sites meant that the substrate also needed to contain nickel ions.

7.5.2 Post-Printing Growth and Expression

To test that the cells would be able to produce sufficient amounts of material after printing, we conducted growth and fluorescence assays of cells manually deposited on our print substrate.

The first test simply compared growth in the presence of galactose to growth in the presence of dextrose (Figure 7.21). This showed a delay of growth due to the lower efficiency of galactose as a metabolic energy source, as expected, but no other ill effects.

The second test compared per-cell fluorescence Φ, as defined earlier, in two different concentrations of alginate at a variety of concentrations of calcium and nickel. As the alginate gels in the presence of calcium, these fluorescent readings show significant noise when compared to the readings taken in pure liquid cultures (Figure 7.22).

The fluorescence data from the full battery of tests is shown in Figure 7.23 . The presence of calcium appeared to have essentially no negative effect on material production. The presence of nickel, however, was clearly harmful at all but the lowest concentration. Interestingly, the higher concentration of alginate appears to offer some protective effect against the higher nickel concentrations; this may indicate that alginate, which takes up some of the calcium ions as part of the gelling process, also takes up nickel ions (which have the same charge) at a lower efficiency.

7.5.3 Material Binding and Washing

Polyhistidine tag binding tests for RFP and GFP were also run using the Dynabeads His-Tag Isolation and Pull-Down kit. The proteins were bound to the beads, washed, and then eluted, and the elution products were then run on an electrophoresis gel, the image of which is shown in Figure 7.24 . There are no bands for the lysis solutions because they were too diluted. There are bands for the flow-through that do not include a visible GFP or RFP band, and there are no visible bands for the wash solution. The elution products for GFP and RFP each include a band that does not appear for wild type yeast, and these additional bands

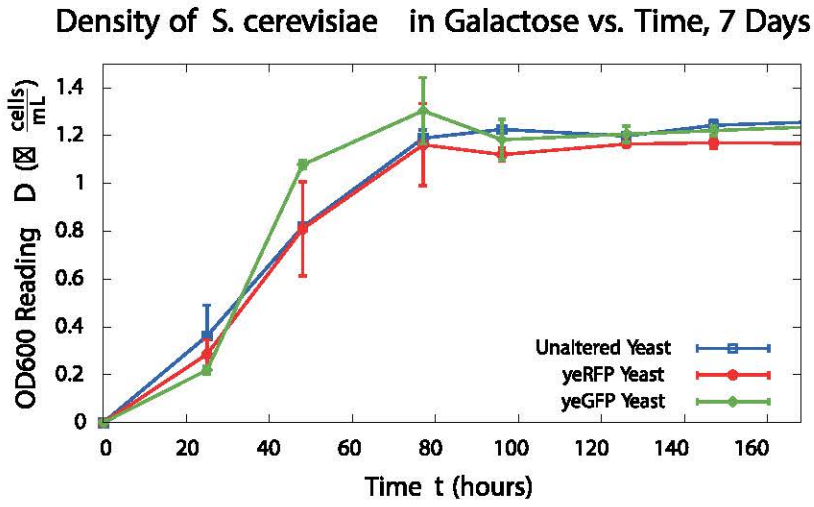

Figure 7.21: Cell density measured over a week for our unmodified host cell strain, our RFP-expressing cells, and our GFP-expressing cells in a galactose-containing medium. The modifications necessary to enable material production do not appear to affect cell growth when the cells are actively producing. Compared to Figure 7.14 , the use of galactose as a carbon source appears to slow cell growth, as expected, but allow for a slightly higher maximum population.

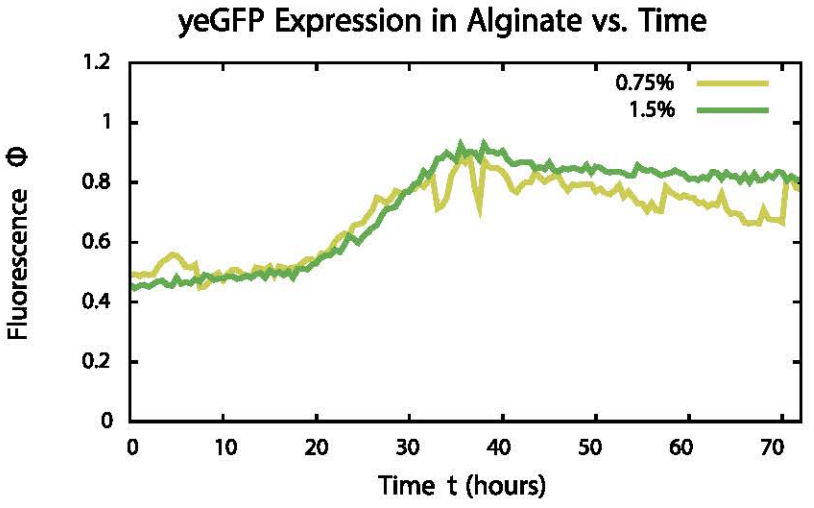

Figure 7.22: The normalized per-cell fluorescence Φ was measured over time to determine whether the presence of calcium and nickel in the substrate would reduce material production.

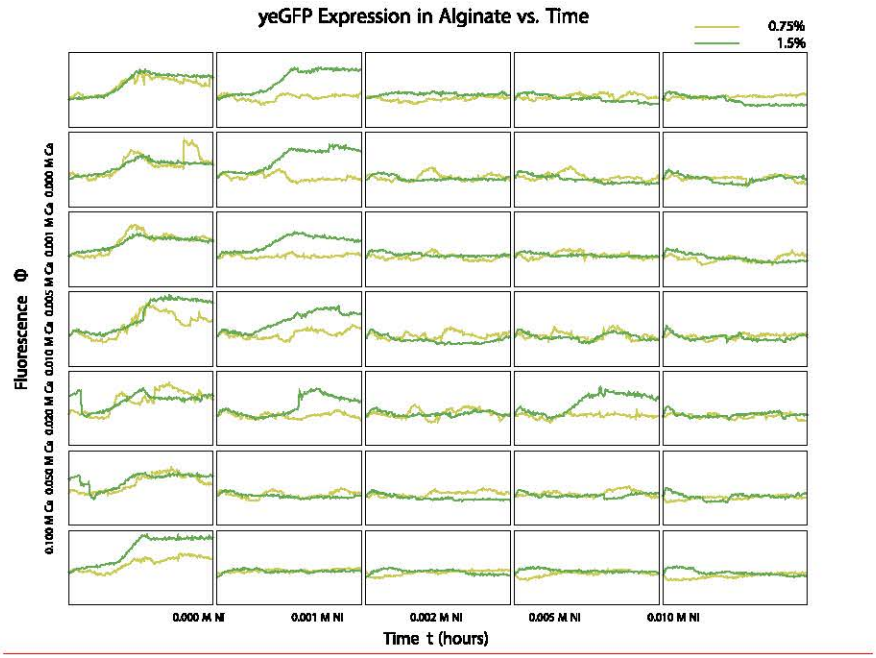

Figure 7.23: The normalized per-cell fluorescence Φ was measured over time at different concentrations of calcium and nickel.

are appropriately positioned relative to the ladder for the tagged RFP and GFP. This demonstrates that the combination of quantity of tagged material (protein) produced and the binding efficiency of the tags is sufficient for detection. However, the Dynabead kit uses cobalt as a binding substrate, and amount of cobalt needed in a print substrate for comparable binding is well above the toxicity threshold for our cells.

Thus, although this material demonstration is sufficient for our proof of concept, it also establishes that binding polyhistidine tags using metal (nickel or cobalt) ions are not a promising implementation for future development. We have begun investigation into two other possible alternatives, antibody-epitope pairs and protein-protein (or protein-polysaccharide) binding domains.

7.6 Material Template Selection

Our basic performance parameters, derived from the state of the art in related fields using similar technology (Section 5), are shown in Table 7.2. We designed a simple grid of five by five droplet locations to enable us to directly measure as many of our parameters as possible with simple microscopy. Since so many natural materials are composites (Table 4.1), we decided that our proof of concept should use two different materials. This yielded the two-material template shown in Figure 7.25.

7.7 Printing Demonstration & Performance Characterization

The first step in our proof of concept was to demonstrate the functionality of all the non-living parts, as the genetic engineering was by far the largest part of the Phase I work and would not be completed until relatively late in the process. This was accomplished by using 6 μm polystyrene beads (Polysciences) in two different colors to represent the two cell strains. The result is shown in Figure 7.25. These simulated print test runs were used to generate the print system performance metrics in Table 7.2.

Once the genetic engineering was completed for RFP and GFP expressing yeast, the two cultures were printed in the same alternating pattern as the beads, and micrographs of the resulting grid were taken on

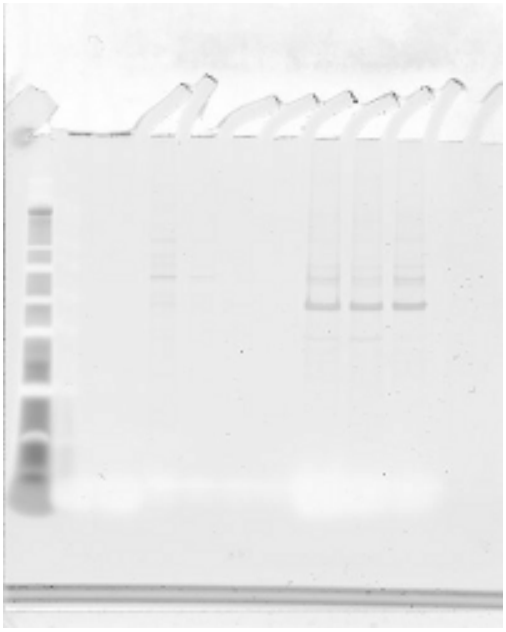

Figure 7.24: The protein bands resulting from a protein binding test using Dynabeads. The lanes are, from left to right: the SeeBlue Plus2 protein ladder, lysed cell solutions (RFP left of GFP), polyhistidine binding flow-through (RFP left of GFP), the used wash solution after the first wash (RFP left of GFP), and the elution products for RFP, GFP, and wild type yeast.

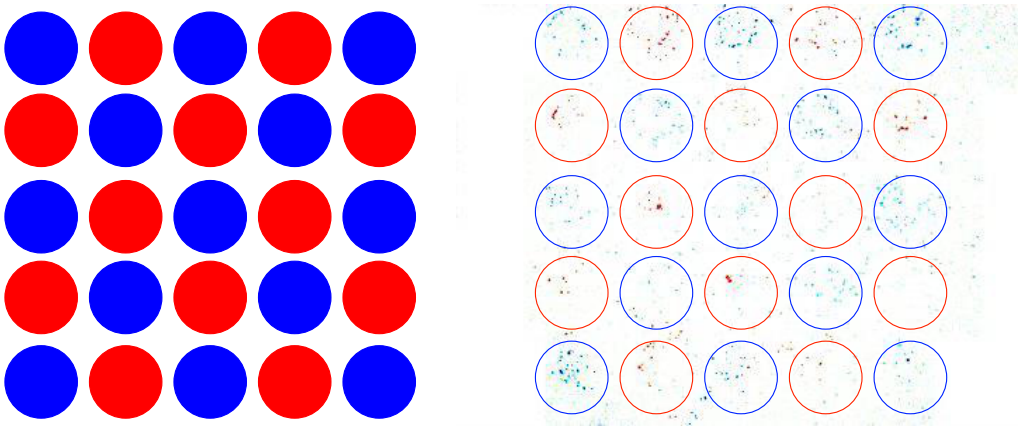

Figure 7.25: (r) The material template, printed in two colors to represent the two different cell types. The beads are 6 µm in diameter. (l) The results of the two-color grid print test with simulated cells, with the original material template overlaid. All locations received at least one 'cell' except for one, the farthest right red location in the second row from the bottom. Image magnification is 25x.

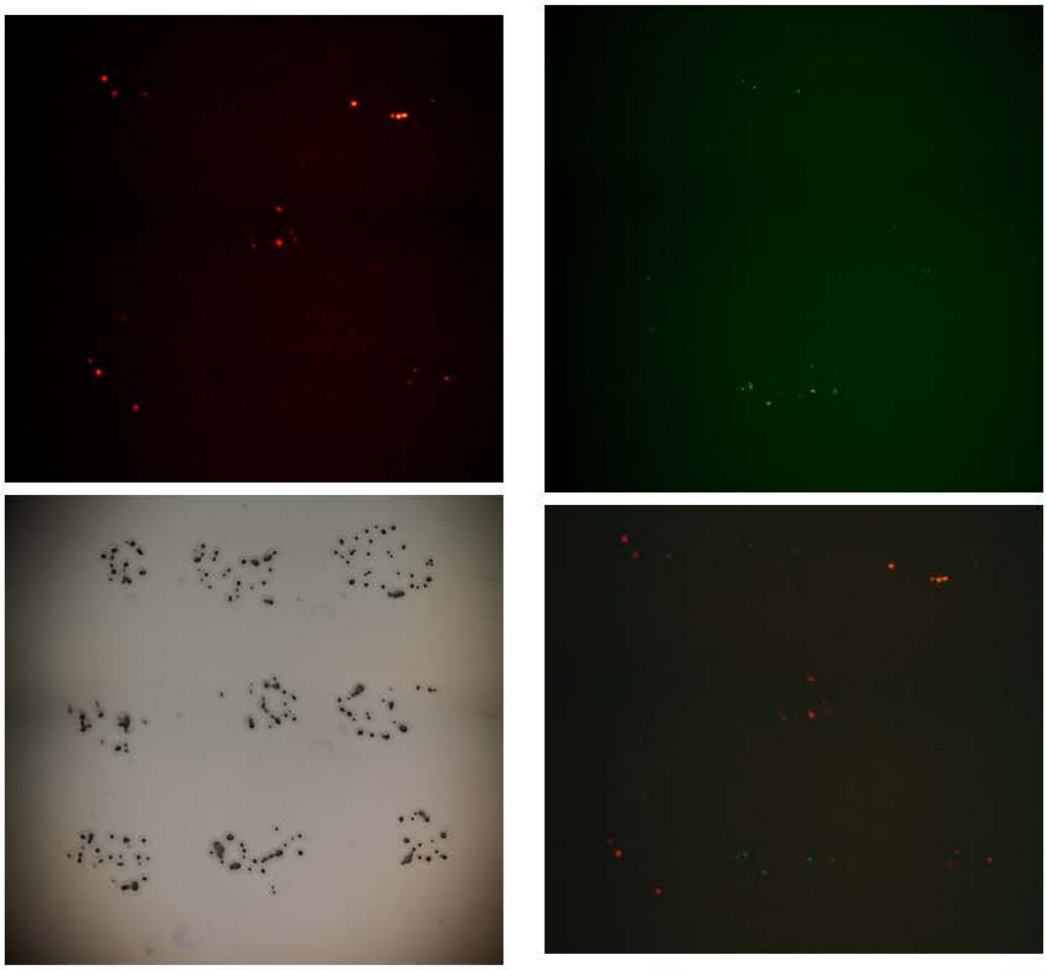

Figure 7.26: RFP-expressing yeast cells were printed in an alternating grid with GFP-expressing yeast cells. The droplets are placed at 0.4 mm increments for a 0.8 x 0.8 mm grid. (t) Grid imaged separately with red and green fluorescent filters. (b,l) Grid imaged with phase contrast. (b,r) Composite image of red and green fluorescence.

a fluorescence microscope using a different filter to view each fluorescent protein. The images taken using the two files are overlaid in Figure 7.26 so that the alternating pattern is apparent.

This, in combination with our print substrate washing tests (data shown in earlier sections), demonstrates critical end-to-end functionality of our proof of concept system.

7.8 Results & Discussion

We have clearly demonstrated that there is at least one complete biological 'chassis' that meets the performance requirements of this technique. Although many of our implementation choices can be fine-tuned in future work, when comparing our results to our originally derived metrics, we meet or exceed our minimum requirements in every case (Table 7.2).

The process of creating our proof-of-concept demonstration, as intended, brought to the forefront a number of needed answers and new questions about our technology concept. Perhaps the most powerful takeaway is the degree ofinterdependence between the different implementation decisions involved; nearly every

Table 7.2: Desired and current performance parameters.

Metric	Minimum	Desired	Current
positioning precision	1 cell diameter ☒ 10 µm	1 µm	2 µm
dispensing volume	≤ 1000 $\frac{\text{cells}}{\text{“voxel”}}$	☒ 1 $\frac{\text{cell}}{\text{“voxel”}}$	≤ 10 $\frac{\text{cell}}{\text{“voxel”}}$
“voxel” size	enc. 1000 cells = 1 nL	10 pL	20 pL
cell survival	50%	90%	☒ 50%
pattern completion	75%	95%	≥ 95%

choice we made substantially impacted our options at every other step. We have summarized the most important linkages in Figure 7.27 . We were aware prior to our Phase I work that the technical implementation of our concept would be application-dependent, but this work has clearly demonstrated the significant process-design effort involved in optimizing the approach for a given application. This is, in part, a consequence ofits interdisciplinary nature; each design decision has meaningful biological, chemical, physical and mechanical consequences that must be taken into account.

Another overall takeaway is the importance offunctional unification in process control. In our proof of concept, we were able to make the physical act of printing the trigger for material production, material delivery, substrate gelling and support, and material binding. Without this simplification, our demonstration would have been far more time-consuming to create. This combination of physical cues is something that needs to be taken into account very early in the implementation design process.

The individual component steps also yielded several key findings.

Although it may not be relevant in industrial or commercial application, for research purposes, detailed material analysis is an important additional step. Many of our choices were affected by the frequent need for immediate, low-cost material deposition verification (fluorescence microscopy). Future work will be necessary to determine if there is a need to monitor production rates this closely for structural material deposition – for example, for real-time feedback to stimulus control – or if this step can be eliminated once the technology has reached a more mature level.

The selection process for the material stimulus method led us to our insights regarding the relationship between stimulus type, spatial and temporal resolution, and material form factor (Table 8.2). This is a vital piece ofinformation for any future work in this area. Similarly, our material delivery method selection process led us to refine our original understanding of the link between delivery and material type, although this is a weaker determination.

Another realization of note was that the concept of a ‘voxel’, as the unit of three-dimensional printing, is a significant oversimplification of a parameter to use for our print metrics. Cell size, cell functional unit size (if different from cell size), material organization scale, dispensing droplet volume, ‘number resolution’ (the precision with which the number of cells in a droplet can be controlled), positioning accuracy, and stimulus spatial resolution are all part of the ‘resolution’ of our printing system. Although we defined our final print performance (Table 7.2) in terms of voxel resolution, since our original metrics were expressed in these terms, in future work we will likely develop more specific figures of merit.

Finally, implementing our proof of concept helped us observe that the time costs of our technology are not necessarily intuitive. As shown in Figure 7.15 , there is a certain amount of time (approximately 2 days) necessary for the cells to reach maximum material deposition. However, this time cost does not scale with the size of the material; once the cell array has been printed at the correct cell density, the delay for material deposition will always be 2 days, whether the cell array is millimeters or tens of meters in size. The time cost that scales with form factor and size is the printing time. Our current prototype prints approximately 1 mL of array in 1 hour with approximately 1 µm resolution; however, this ratio will be substantially improved for material and stimulus types that require a lower cell spacing resolution. Moving to a more parallelized

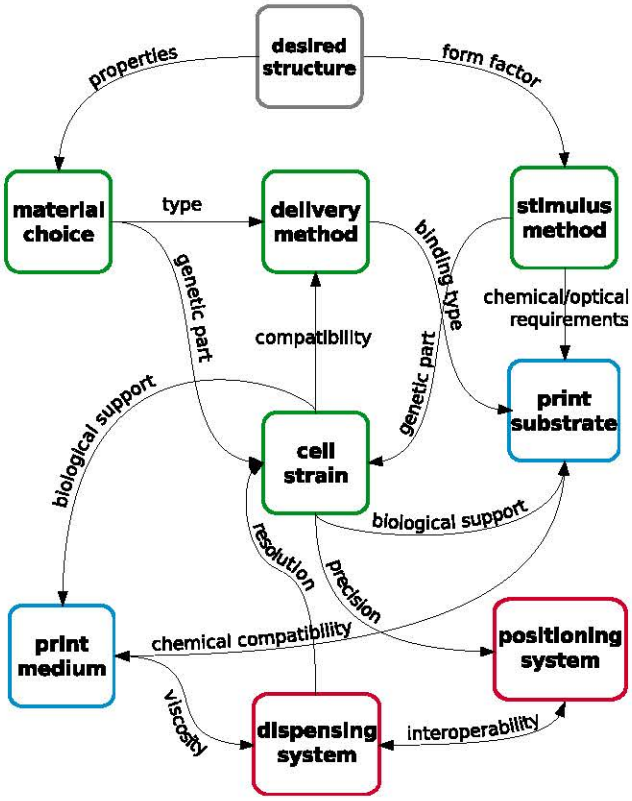

Figure 7.27: We have identified the linked decision-making pathways of each of our implementation choices. Understanding these interdependencies is key for future work on our technology concept.

print system (akin to having multiple jets in an inkjet print head), or one specialized for volume throughput, will also affect this part of the overall time cost.

These insights point to two primary outstanding needs in enabling technology. The first is for identification and characterization of genetic parts for new material types. This includes both existing structural biomaterials – especially those with multiple constituent materials – and, further in the future, *de novo* gene design. A particular need is for genetic tools to control delivery methods other than secretion; most of the most promising biomaterials have inorganic phases at least partially deposited outside of the cell, a mechanism currently outside the scope of synthetic biology. Being limited to secretion-related genetic parts, or else using a 'black box' approach to extracellular deposition without human-created controls, will prevent our technology concept from reaching its full potential.

The second key need is for better modelling and predictive tools for complex materials. Current technology is just beginning to scratch the surface of predictive functionality tools for protein folding; modelling properties and self-assembly of our materials will require understanding the interactions between several additional layers of structure beyond that. Such tools will need to be developed to, one day, allow *de novo* hierarchical material design.

8 Future Development Pathways

8.1 Introduction

Our third objective was to survey options and provide recommendations for hardware, biological, and material implementations for the next stages of technology development. This takes two forms. The first is short-term recommendations for follow-on work, particularly new or alternative potential implementations of the different components of our technology. The second is identifying longer-term needs, including advances in other fields, and describing pathways forward in those areas.

8.2 Short Term Implementations

8.2.1 Target Materials

Two primary factors determine the suitability of existing biomaterials for near-term future implementation. The first is how advantageous the material's mechanical properties are in comparison to existing engineering material choices. The second is the degree to which the genes and mechanisms responsible for material production have been identified. We surveyed both of these factors for a range of promising structural biomaterials in Table 6.2, Table 6.3, and Table 6.6.

Based upon our work here, we believe that the short list of materials to be considered for future implementation includes spider silk, silkworm silk, cellulose, mollusk shell, and crustacean shell. Of these, spider silk comes closest to having a pre-identified genetic part; one of its major constituent proteins has been cloned and expressed in *E. coli* [108]. Silkworm silk is a close second, as a significant percentage of its major proteins have had their corresponding genes sequenced [98, 115]. Cellulose, which is a polysaccharide, not a protein, is produced in plants by a complex arrangement of membrane-bound proteins formed by at least ten different genes [100]. Some bacteria produce a different form of cellulose [47]; though some of the genes responsible for the total synthesis pathway have been identified and cloned [48, 95], their full synthesis function has not been reproduced. The genetic bases for the formation of mollusk shell and crustacean shell are at a much lower state of knowledge.

A longer term avenue of investigation could be the investigation of empirical control of biomineralization by printed living mollusk or insect shell-lining cells; this would lose the precise control aspect of our technology concept, but might be a promising first step towards the most promising compressive materials. However, for the short term, we recommend that future work focus on either spider or silkworm silk, with cellulose as a fallback. We summarize these recommendations in Table 8.1.

Table 8.1: The potential materials proposed for immediate follow-on investigation, in order of implementation preference. They are ranked by whether the genetic parts responsible for their production have been identified (a necessary first step) and expressed in another organism (a second step towards standardization.)

Material	Identified	Expressed	Notes
spider silk	at least two major proteins	one protein	[34, 108]
silkworm silk	at least two major proteins	only partial sequences	[98, 99, 115]
cellulose (bacterial)	at least three genes in combination	no full synthesis function	[48, 95]

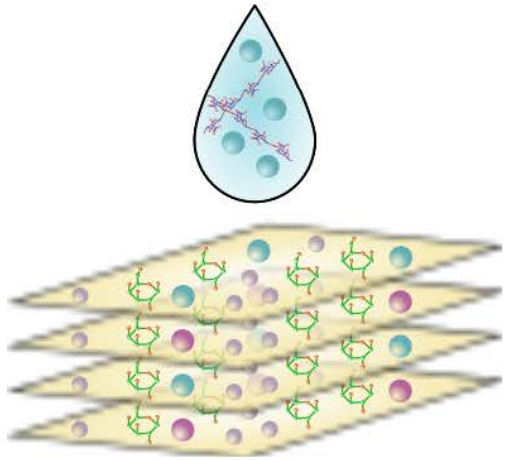

Figure 8.1: Combining printing the substrate, with differing chemical compositions, with printing the cells will allow us finer control over material production and deposition.

8.2.2 Support Medium & Substrate

New target materials will require new support media to provide the required raw materials for the engineered cells. In the case of mollusk shell, which is a composite of calcium carbonate with proteins and polysaccharides, the substrate would need to include the required calcium as well as the organic feedstock. As for cellulose, the compound itselfis a polysaccharide, so the organic feedstock should be sufficient to produce it, but to form a material with any structure, the cellulose would need to be embedded in a matrix of cross-linking glycans to for a macrostructure similar to the fibrils it forms in cell walls, or a different type of adhesive matrix to hold the cellulose strands together in a macro-scale structure. This matrix could be included in the print substrate and printed in alternating layers with the cellulose-secreting cells.

The first steps going forward would be to start with an alginate substrate prepared using cell growth media for use in initial tests to confirm that the new cell cultures can be printed effectively, survive printing, and grow. Then the additional substances, such as calcium in the case of mollusk shell, would be added to the media recipe, so that the expression of cells deposited on this media can be tested. Cellulose-producing cells should be able to express without additional raw materials in the print substrate, and layering with a matrix solution can be tested after the initial expression tests. The GAL1 promoter can be used the same as in this work, so that galactose in the print substrate will induce expression after printing, although alternative promoters can be investigated.

Once expression of printed cells is verified, alginate can be used in the print media so that printed droplets will gel on a substrate containing calcium ions, holding the cells in position until they have secreted measurable amounts of the desired material. This rapid gelling effect can also allow for multiple layers of cells to be printed on top of each other to create a three-dimensional structure as opposed to the two-dimensional proof-of-concept in this work. Depending on the type of matrix used with cellulose, alternating layers of cellulose-producing cells and the matrix solution may take the place of alginate in this process.

8.2.3 Production Stimulus

We have surveyed a number of potential material production control stimuli (Table 8.2). The primary factors to consider when choosing a control stimulus for future work are, firstly, how well the type of stimulus corresponds to the desired form factor, and secondly, whether there is an existing genetic part (promoter or other regulatory sequence) that corresponds to it.

Form factor matters because different types of stimuli have different spatial and temporal resolutions. Tem-

Table 8.2: Different material production stimuli match different form factors.

Stimulus	t resolution	$\vec{x}$ resolution	Form Factors
chemical	low	high	thick sheets, solid (deep) shapes
optical	high	high	thin sheets, fine surface structures
thermal	low	low	smooth density or composition gradients

perature is easy to control in a large gradient, either linear or exponential, but hard to change rapidly or over short distance scales. Chemical exposure can either be changed rapidly using fluidics, or achieve high spatial resolution if the substrate is printed with different compositions. Optical stimulus can achieve high spatial and temporal resolution over a 2D space at a low cost, but 3D spatial resolution within a partially opaque cell array becomes much more costly.

There are relatively simple heat-responsive eukaryotic promoters [91], and a wide variety of chemically sensitive ones that respond to salts, metal ions, sugars, and so on (e.g., [14, 73]). The optically sensitive regulatory systems that have been identified are substantially more complex, involving cascades of multiple mechanisms [88, 93].

Since much short-term work will likely focus on thin material sample sections, all three options are likely to be relatively inexpensive to produce in terms of process control. This leaves the labor cost of implementing the genetic engineering for a given stimulus as the determining factor. We therefore recommend chemical control for short-term work, with implementing optical stimulus as the next logical step.

As our immediate future work is therefore likely to rely on chemical stimulus, we should mention the possibility of 3D printing the substrate as well as the cells (Figure 8.1). Our printing hardware is compatible with our current print substrate, meaning that we only require multiple-material printing capability to be able to create spatial patterns of different chemical stimuli. We upgraded our printing hardware to this level as one of the last stages of our Phase I work, so it is likely we will be able to investigate this avenue in the near term as well.

8.2.4 Cell Positioning & Deposition

The bioprinters cell deposition setup and procedure can be updated to accommodate new cell types, and to improve the efficiency of the printing process. If cell types other than S. Cerevisiae are used to produce the desired materials, the voltage and pulsewidth used by the piezoelectric dispenser head to deposit the cells will need to be calibrated such that a number of cells are deposited per drop that is appropriate for the material pattern to be printed. If the size of the cells varies from that of S. Cerevisiae, a different size of dispenser head may be needed to accommodate the new cell diameter without clogging, while also keeping the minimum drop size and cells per drop as close to single-cell resolution as possible. Additionally, with multiple print heads, multiple cell types or solutions could be loaded into the bioprinter simultaneously, streamlining the process of printing materials with multiple components by eliminating the need to empty and fill a single print head with each new solution or cell culture.

In the longer term, other deposition methods are worth investigation. The deposition setup would need to be optimized for microgravity use if this technology is considered for the ISS, and that would involve adjusting droplet velocity and the distance from the dispenser head to the substrate, at a minimum. For the scenario of on-site construction on Mars, a deposition system integrated into a mobile platform that moves along the structure as it is constructed may be the most effective option.

It should be remembered that not all possible cell array construction approaches require full 3D printing capability. Another possibility is analogous to extrusion, in which a thin cross-section of cells is used to produce material that is continuously drawn away as it is deposited (Figure 8.2). Implementation of high spatial resolution stimuli might also lower the minimum cell printing resolution for certain types of mate-rials, although the strength of the effect will have to be determined experimentally.

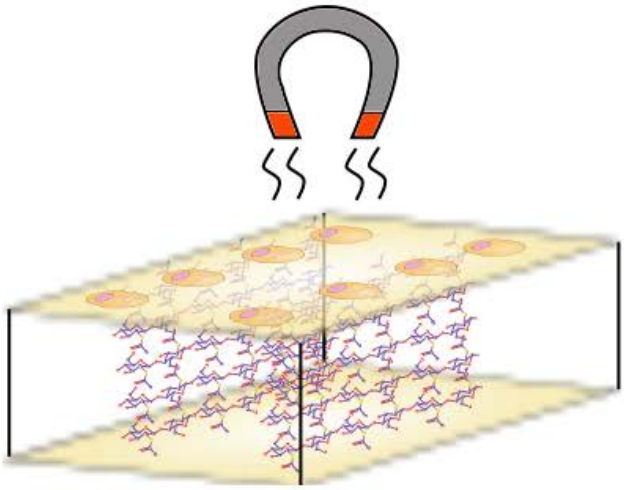

Figure 8.2: A hypothetical alternative approach to cell array construction: if either the cells are bound to a substrate, or the material is functionalized so that it can be subject to forces without affecting cell placement (e.g., through a magnetic tag), then a thin cross-section of cells could be used to produce a much larger piece of material that is continuously drawn away as it is deposited.

8.2.5 Material Delivery

We have surveyed a number of potential material delivery methods (Table 8.3). The primary factors to consider when choosing a delivery method for future work are, firstly, how well the type of delivery corresponds to the desired material type, and secondly, whether there is an existing genetic part (secretion tag or other pre-processing sequence) that corresponds to it.

The relationship between material type and delivery method have already been discussed in subsection 7.2.4 . Of the options we surveyed, by far the best studied and least controlled approach is cell lysing. Metal or inorganic salt sequestration and deposition is generally poorly understood, although it is often assumed to involve either secreted or surface-expressed proteins. We have included the entry 'extracellular(?)' in Table 8.3 to represent this class of mechanism. Secretion is, by comparison, well understood.

Implementation ofinorganic material integration is dependent on future work in other fields identifying the relevant biosynthetic mechanisms. We therefore recommend that short-term future work use secretion as a delivery method, with cell lysing as secondary option for materials unsuitable to known secretion tags.

8.2.6 Material Binding

The method of material binding to the print substrate, and to neighboring layers of cell-produced material, will depend on the material type. For proteins, the addition of a polyhistidine tag or a V5 epitope tag to one end of the protein can allow the protein to bind to nickel or V5 antibodies in the substrate, respectively. Cellulose, on the other hand, may need to be bound by the matrix solution that cross-links it into structures similar to fibrils.

Mollusk shell may need to simply bind to itselfin layers analogous to those found in nature, with the cells possibly held in place initially by gelled alginate, but the material itselfforming structural layers through the interaction of the calcium carbonate layers with the protein and polysaccharide layers. Due to their chemical properties, some materials will actually be self-assembling if the necessary environmental conditions are met. Examples of self-assembling materials are molecular crystals, lipid bilayers, and certain polymers [36].

Table 8.3: Different material delivery methods match different material types.

Method	Material Examples
secretion	proteins, some polysaccharides
sequestration	copper, iron, nickel, other metals
extracellular(?)	some polysaccharides, most inorganic biominerals
lysing	silk, cotton, other fibers, bioplastics

8.3 Long Term Approaches

Given that our technology is innovative, multidisciplinary, and extremely broad in potential scope, it is to be expected that a significant part of our TRL advancement in our Phase I work has been identifying specific unknowns relevant to our technology concept and investigating options to characterize them. In the previous section, we focused on immediate work that could be done to advance the proof of concept implementation. In this section, we list those longer-term questions identified by our Phase I work which must be answered to gain a complete understanding of this technology's potential costs and benefits.

- *Single-cell printing resolution.* We found that the only limiting factor in our cell array construction was the low repeatability of our microdispensing system. Although the droplet volume was very precise, the variability in the number of cells contained in each droplet causes to undesirably high variability in the number of cells placed at each location. Possible solutions include installing a monitoring system that can detect the number of cells printed in real time and re-print over the same location until the desired number is reached. This is not outside the scope of being added to existing commercial devices in the next few years, as the metrology system would essentially be a simplified flow cytometer.
- *Micropositioning resolution.* The minimum achievable resolution of DC-motor-based systems is in the 1 μm range, which exceeds the diameter of most eukaryotic cells. Finer resolutions can be achieved with piezo-based systems for work which requires prokaryotic cells; the limiting factor here, as discussed above, will be droplet resolution and repeatability.
- *Stimulus control.* Control of the stimuli used to regulate cell material production and structuring must be at a fine enough spatial and temporal scale. Chemical stimuli are limited only by droplet size, if the print substrate is pre-printed to include the stimulus. Optical stimulus can be over an order of magnitude more precise in space, and resolved on microsecond timescales, if technology comparable to that in a scanning laser microscope is used; however, opaque or semi-opaque supports or scaffolds will sharply limit the depth at which it can be used. Quantifying these limits will be important for determining the cost and potential benefit of implementing each.
- *Identification of new genetic parts corresponding to stimulus, delivery, and target materials.* Although rapid generation of libraries of characterized genetic parts is a common goal in synthetic biology, few existing efforts focus on genes related to structural materials. Fewer still focus on new control or delivery mechanisms related to material production. Although we can use 'black box' empirical techniques, such as growing the cells which natively express a material in close to their original environment, we will not be able to create material customization without real genetic tools at our disposal.
- *Design of new genetic parts. De novo* gene design and synthesis is still an emerging area. Ultimately, it will be necessary to develop these tools in order to create materials fully customizable down to the molecular level. It is likely fifteen to twenty years before this becomes a bottleneck for our technology concept; however, our technology will not achieve its full potential without it.
- In situ *resource extraction.* A strong selling point of our technology from an aerospace perspective is its ability to build a wide variety of materials from basic, locally extractable resources. This advantage is only magnified as *in situ* resource utilization technologies improve.
- *Compliant materials modelling tools.* The combination of compliant and rigid elements in natural bioma-

terials gives them their extreme toughness, resilience, and energy-dissipating ability. Existing material stress-strain modelling tools do not handle these properties well [11]. This is a current area of materials modelling research, due to its applications to emerging robotics and architectural concepts based on tensegrity.

- *Modelling tools for self-assembling materials.* Although this need shares some common ground with software tools such as predictive protein folding models and computational nanomaterials design, the many additional layers of structure in the most highly ordered biomaterials will require a specialized toolset. This is a novel requirement created by our technology concept.
- *Identification of biomaterial mechanical properties in a relevant environment.* This is a key unknown which can be addressed in the short term by materials testing under simulated space environments. However, in order to predict the performance of new materials created with out technology concept as part of the design and synthesis process, we will ultimately need to add this function to the proposed modelling tools referred to above.
- *Material properties for design tools.* Most structural design tools, such as finite element analysis software, assume essentially constant material properties and calculate maximum allowed loading conditions accordingly. To fully tap our technology concept's potential, this process has to be inverted; we need the ability to calculate fine-grained material properties to suit a given shape and load.

9 Complementary Advances

This highly interdisciplinary proposals is related to a suite of complementary technologies, and has the potential to interface with several. The field of bioprinting has focused primarily on tissue and organ printing with companies such as Organovo leading the way (reviewed in [50]). Recent successes in printing vascular tissue, heart valve, ears, skin and bone indicate the dawn of a new era in bioprinting. It should be noted that Organovo has recently partnered with Autodesk, the world's leader in 3D design, to develop an interface for 3D bioprinting. We have an excellent relationship with Autodesk in other projects, and we have started to investigate the use of their software for our bioprinting platform. While this work is complementary, the focus on tissue and organ bioprinting is to deliver functional cells in the correct conformation, whereas this proposal focuses on using the printed cells as a mean for "micromanufacturing" but having the cells secrete biomaterials which then go to form the finished product.

We are excited about the overlap between the materials produced under the proposed work and bioprinted fabrics. The microstructure and embedded capabilities that our technology can produce should revolutionize the production of flexible materials that could provide unique capabilities for human exploration, including habitat coatings and astronaut clothing. For example, just as we are proposing the seamless construction of materials that differ in rigidity and elasticity, so too could this construction be applied to a spacesuit or habitat cover.

The reduction in upmass of off-planet biological production systems is strongly linked with *in situ* resource utilization (ISRU). The development of the ISRU aspect is being explored elsewhere in our lab. Heterotrophic cells, such as yeast which we have used up to the this point, require organic inputs and metals. The former – most notably fixed carbon and nitrogen – can be provided by photosynthetic microbes. We have developed this concept since 2011 in a project we call "PowerCell", where cyanobacteria or algae will provide photosynthate that will feed heterotrophic "production organisms", which will generate food, fuel, and other materials, and oxygen, or in the case of the present project, biomaterials. The synthetic biology has been developed under the rubric of the 2011 Brown-Stanford iGEM team in our lab (http://2011.igem.org/Team:Brown-Stanford/PowerCell/Introduction), and the production cell system has been prototyped by the 2013 Stanford-Brown iGEM team (http://2013.igem.org/Team:Stanford-Brown/Projects/EuCROPIS). We have a unique opportunity to test this concept at microgravity, lunar and Martian gravity as a secondary payload of the German Aerospace Centers Eu:CROPIS satellite mission, due to be launched in late 2016. The data from this mission will allow us to better estimate the production capability of PowerCell at destination gravities, and thus the overall production capability of the NIAC biomaterials project.

Similarly, all living organisms need a source of metals. The 2012 Stanford-Brown iGEM team under Rothschild's supervision used synthetic biology to build an *E. coli* with the capability to bind metals to its flagellum (http://2012.igem.org/Team:Stanford-Brown/Biomining/Introduction). While the initial proof-of-concept was for copper binding, the potential exists to specifically bind any metal that can be bound by a protein with specificity. This work is currently being developed by a Ph.D. student in Rothschild's lab, Jesica Navarette, UC Santa Cruz.

10 Summary & Conclusions

The mission benefit analyses as described in our Phase I proposal (Objective #2, Section 6) are complete and contained in this report. As was appropriate for the information we had prior to the completion of the proof of concept, we focused on the benefits due to material subsitution and *in situ* resource utilization. These calculations alone show that our technology can save hundreds of kilograms of upmass for a potential human habit construction mission (a net mass savings of approximately one third per habitat module without ISRU, or mass savings including the full 240 kg per module if all materials are derived from ISRU). We have shown that continued advancement of this technology concept for use in a space mission environment is justified.

We completed the proof of concept described in our Phase I proposal (Objective #1, Section 7), a two-material array of non-structural proteins. We created an implementation of each step in our technology concept (Figure 7.1) and demonstrated its critical functionality (Table 7.2). Our current host cells are *S. cerevisiae*, a yeast, genetically engineered to secrete our target materials, fluorescent-tagged proteins, when exposed to galactose. Our current print medium and substrate are a glucose-containing alginate medium deposited onto a calcium- and galactose-containing agar surface. The calcium gels the alginate, and the introduction of galactose when the cells contact the substrate triggers the material secretion. This way, the act of printing is combined with the act of creating a physical support for the cells and providing the material production stimulus, greatly simplifying the end-to-end-process. The biological chassis and printing hardware we created as part of this work can be re-used for future work by inserting a material coding region upstream of the fluorescent tag. Overall, we showed that our technology concept is sound.

Our survey of future development pathways (Objective #3, Section 8) proved extremely informative in light of the lessons learned from our proof of concept work and mission scenario analyses. For example, we were able for the first time to distinguish between the levels of functionality provided by production of structural proteins, other polymers such as polysaccharides, and true organic-inorganic composites such as bone and mineralized shell. We were also able to survey the state of knowledge of the precise mechanisms involved in the formation of both non-protein-based structural materials, such as chitin and cellulose, and the inorganic phase of biominerals, and quantify our previously qualitative estimates of our technology concept's reliance on advances in other fields. Both of these analyses represent significant advances in formulating specific applications for our technology concept.

For Objective #4 (Section 9), we surveyed potential collaborations with other projects and synergies with enabling technologies that are developing, including labs at Stanford University and Drexel University, Organovo, and Autodesk. Collaboration with tissue engineers at Organovo would allow our technology to develop in parallel with tissue printing technology, and collaboration with Autodesk would speed the development of software to translate standard 3D model file formats into commands usable by the bioprinter. Finally, we have been in touch with the team behind the 2013 NIAC Phase II 'Super Ball Bot - Structures for Planetary Landing and Exploration' and are planning to develop our biomaterial printing technology with the goal of enabling tensegrity-based rovers such as theirs to use lighter, more robust materials.

A smooth transition from TRL 2 to TRL 3 assumes that the implementations of the technology concept which demonstrate critical functionality are also pathways for future development; while this is the case for most hardware or software projects, the multidisciplinary nature of our project, particularly the biological aspect of it, means that this is not always true. The most clear example of this in our Phase I work is the fact that our polyhistidine tag material binding method worked sufficiently well for a proof of concept demonstration, but is too cytotoxic for use in future work where we would need a much greater amount of the substrate to bind structural materials. Another, less obvious, example, is the case of genetic parts

for material production. We have determined as part of this work that although there are large number of known genetic parts that correspond to non-structural materials, such as the proteins we used in this work, sequences for structural organic proteins, let alone biomineralization pathways, are still far from standardization (Table 6.6). These realizations allowed us to further subdivide our concept into more detailed development areas, some of which are clearly established at TRL 3, others of which were newly identified sub-technologies moved from TRL 1 to TRL 2.

Similarly, although a single feasibility/benefit analysis is sufficient for advancement from TRL 2 to TRL 3, not all potential benefits to a technology concept as broad in scope as ours are apparent at TRL 2. Both our future pathways survey and our proof of concept work highlighted that the true mass savings potential of our technology concept cannot be quantified without modification of existing materials modelling tools to take into account the possibility of positional materials properties customization. Therefore, in our Phase I work, we have simultaneously both advanced one potential set of applications of our technology concept from TRL 2 to TRL 3 and also identified a previously unknown set of applications and advanced it from TRL 1 to TRL 2.

Our overall TRL advancement breakdown in shown in Table 3.2. Overall, we have moved the original formulation of our concept forward from TRL 2 to TRL 3, and the expanded formulation of it presented in this document has been advanced from a combination of TRL 1 and early TRL 2 to an overall late TRL 2, using the definitions in Table 3.1. We have also identified the key areas necessary for both short-term and long-term advancement, and made recommendations for specific future work in the most promising directions. With future work on a 1–2 year timeframe to continue advancement to overall TRL 3, we will be well positioned to begin work on a specific space mission technology insertion path.

11 References

[1] (1993) EVA Tools and Equipment Reference Book. National Aeronautics and Space Administration.

[2] Albrecht D, Underhill G, Wassermann T, Sah R, Bhatia S (2006) Probing the role of multicellular organization in three-dimensional microenvironments. Nature Methods 3: 369–375.

[3] Allen CC, Morris RV, Jager KM, Golden DC, Lindstrom DJ, et al. (1998) Martian Regolith Simulant JSC Mars-1. Proceedings of Lunar and Planetary Science XXIX pp. 1–2.

[4] Atala A, Kasper FK, Mikos AG (2012) Engineering complex tissues. Science Translational Medicine 4: 160rv12.

[5] Barron JA, Wu P, Ladouceur HD, Ringeisen BR (2004) Biological laser printing: a novel technique for creating heterogeneous 3-dimensional cell patterns. Biomedical Microdevices 6: 139–147.

[6] Bazylinski DA, Frankel RB, Heywood BR, Mann S, King JW, et al. (1995) Controlled Biomineralization of Magnetite (Fe_3O_4) and Greigite (Fe_3S_4) in a Magnetotactic Bacterium. Applied and Environmental Microbiology 61: 3232–3239.

[7] Bhatia SN, Balis UJ, Yarmush ML, Toner M (1998) Microfabrication of hepatocyte/fibroblast cocultures: role of homotypic cell interactions. Biotechnol Prog 14: 378–387.

[8] Bodde S, Meyers M, Mckittrick J (2011) Correlation of the mechanical and structural properties of cortical rachis keratin of rectrices of the Toco Toucan (*Ramphastos toco*). Journal of the Mechanical Behavior of Biomedical Materials 4: 723–732.

[9] Bond GM, Richman RH, McNaughton WP (1995) Mimicry of natural material designs and processes. Journal of Materials Engineering and Performance 4: 334.

[10] Boskey AL (1998) Biomineralization: conflicts, challenges, and opportunities. J Cell Biochem Suppl 30-31: 83–91.

[11] Brodland GW (1994) Finite element methods for developmental biology. International Review of Cytology 150: 95–118.

[12] Bruce J, Sabelhaus AP, Chen Y, Lu D, Morse K, et al. (2014) SUPERball: Exploring Tensegrities for Planetary Probes. International Symposium on Artificial Intelligence, Robotics and Automation in Space pp. 1–7.

[13] Cadogan D, Stein J, Grahne M (1999) Inflatable composite habitat structures for Lunar and Mars exploration. Acta Astronautica 44: 399.

[14] Cartwright CP, Li Y, Zhu YS, Kang YS, Tipper DJ (1994) Use of beta-lactamase as a secreted reporter of promoter function in yeast. Yeast 10: 497–508.

[15] Chang CN, Matteucci M, Perry LJ, Wulf JJ, Chen CY, et al. (1986) *Saccharomyces cerevisiae* secretes and correctly processes human interferon hybrid proteins containing yeast invertase signal peptides. Molecular and Cellular Biology 6: 1812–1819.

[16] Chen B, Peng X, Cai C, Niu H, Wu X (2006) Helicoidal microstructure of *Scarabaei cuticle* and biomimetic research. Materials Science and Engineering: A 423: 237–242.

[17] Chen B, Peng X, Wang W, Zhang J, Zhang R (2002) Research on the microstructure of insect cuticle and the strength of a biomimetic preformed hole composite. Micron 33: 571–574.

[18] Cho H, Jnsson H, Campbell K, Melke P, Williams JW, et al. (2007) Self-organization in high-density bacterial colonies: efficient crowd control. PLoS Biology 5: e302.

[19] Choi SU, Paik HD, Lee SC, Nihira T, Hwang YI (2004) Enhanced productivity of human lysozyme by pH-controlled batch fermentation of recombinant *Saccharomyces cerevisiae*. Journal of Bioscience and Bioengeering 98: 132–135.

[20] Choi YJ, Lee SY (2013) Microbial production of short-chain alkanes. Nature 502: 571–574.

[21] Clements JM, Catlin GH, Price MJ, Edwards RM (1991) Secretion of human epidermal growth factor from *Saccharomyces cerevisiae* using synthetic leader sequences. Gene 106: 267–271.

[22] Connell JL, Ritschdorff ET, Whiteley M, Shear JB (2013) 3D printing of microscopic bacterial communities. Proceedings of the National Academy of Sciences USA .

[23] Coradin T, Lopez PJ (2003) Biogenic silica patterning: simple chemistry or subtle biology? Chembiochem 4: 251–259.

[24] Cormack BP, Bertram G, Egerton M, Gow NA, Falkow S, et al. (1997) Yeast-enhanced green fluorescent protein (yEGFP): a reporter of gene expression in *Candida albicans*. Microbiology 143: 303–311.

[25] Corporation SET (2013) SpaceX: Capabilities. `http://www.spacex.com/about/capabilities`, accessed: June 1, 2014.

[26] Cui X, Breitenkamp K, Finn M, Lotz M, D'lima D (2012) Direct Human Cartilage Repair Using Three-Dimensional Bioprinting Technology. Tissue Engineering Part A 18: 1304–1312.

[27] Demirci U, Montesano G (2007) Single cell epitaxy by acoustic picolitre droplets. Lab Chip 7: 1139–1145.

[28] Derby B (2012) Printing and prototyping of tissues and scaffolds. Science 338: 921–926.

[29] Drake BG (2010) Human Exploration of Mars, Design Reference Architecture 5.0 - Addendum. National Aeronautics and Space Administration.

[30] Elowitz MB, Leibler S (2000) A synthetic oscillatory network of transcriptional regulators. Nature 403: 335.

[31] Engler C, Gruetzner R, Kandzia R, Marillonnet S (2009) Golden gate shuffling: a one-pot DNA shuffling method based on type IIs restriction enzymes. PLoS ONE 4: e5553.

[32] Falini G, Fermani S (2004) Chitin mineralization. Tissue Eng 10: 1–6.

[33] Fincham A, Luo W, Moradian-Oldak J, Paine M, Snead M, et al. (2000) Enamel biomineralization: the assembly and disassembly of the protein extracellular organic matrix. In: Teaford MF, Smith MM, Ferguson MWJ, editors, Development, Function and Evolution of Teeth, pp. 37–61, Cambridge.

[34] Gaines IV W, Marcotte Jr W (2008) Identification and characterization of multiple Spidroin 1 genes encoding major ampullate silk proteins in *Nephila clavipes*. Insect Molecular Biology 17: 465–474.

[35] Gibson I, Rosen DW, Stucker B (2010) Additive Manufacturing Technologies: Rapid Prototyping to Direct Digital Manufacturing. Springer.

[36] Gilroy JB, Gädt T, Whittell GR, Chabanne L, Mitchels JM, et al. (2010) Monodisperse cylindrical micelles by crystallization-driven living self-assembly. Nature Chemistry 2: 566–570.

[37] Girotti A, Reguera J, Rodríguez-Cabello JC, Arias FJ, Alonso M, et al. (2004) Design and bioproduction of a recombinant multi(bio)functional elastin-like protein polymer containing cell adhesion sequences for tissue engineering purposes. Journal of Materials Science: Materials in Medicine 15: 479–484.

[38] Gosline JM, Guerette PA, Ortlepp CS, Savage KN (1999) The mechanical design of spider silks: from fibroin sequence to mechanical function. Journal of Experimental Biology 202: 3295–3303.

[39] Haidar Z, Hamdy R, Tabrizian M (2009) Delivery of recombinant bone morphogenetic proteins for bone regeneration and repair. Part B: Delivery systems for BMPs in orthopaedic and craniofacial tissue engineering. Biotechnol Lett 31: 1825–1835.

[40] Hamid Q, Snyder J, Wang C, Timmer M, Hammer J, et al. (2011) Fabrication of three-dimensional scaffolds using precision extrusion deposition with an assisted cooling device. Biofabrication 3: 1–12.

[41] Häuplik-Meusburger S, Sommer B, Aguzzi M (2009) Inflatable technologies: Adaptability from dream to reality. Acta Astronautica 65: 841.

[42] Havemann SA, Foster JS (2008) Comparative characterization of the microbial diversities of an artificial microbialite model and a natural stromatolite. Applied and Environmental Microbiology 74: 7410–7421.

[43] He P, Sahoo S, Ng K, Chen K, Toh S, et al. (2012) Enhanced osteoinductivity and osteoconductivity through hydroxyapatite coating of silk-based tissue-engineered ligament scaffold. J Biomed Mater Res 101A: 555–566.

[44] Howard TP, Middelhaufe S, Moore K, Edner C, Kolak DM, et al. (2013) Synthesis of customized petroleum-replica fuel molecules by targeted modification of free fatty acid pools in *Escherichia coli*. Proceedings of the National Academy of Sciences USA 110: 7636–7641.

[45] Huang J, Wang X, Wang ZL (2008) Bio-inspired fabrication of antireflection nanostructures by replicating fly eyes. Nanotechnology 19: 5602.

[46] Huey DJ, Hu JC, Athanasiou KA (2012) Unlike bone, cartilage regeneration remains elusive. Science 338: 917–921.

[47] Iguchi M, Yamanaka S, Budhiono A (2000) Bacterial cellulose – a masterpiece of nature's arts. Journal of Materials Science 35: 261.

[48] Iyer PR, Liu Y, Deng Y, Mcmanus JB, Kao T, et al. (2013) Processing of cellulose synthase (AcsAB) from *Gluconacetobacter hansenii* 23769. Archives of Biochemistry and Biophysics 529: 92–98.

[49] Jakab K, Norotte C, Damon B, Marga F, Neagu A, et al. (2008) Tissue engineering by self-assembly of cells printed into topologically defined structures. Tissue Engineering Part A 14: 413–421.

[50] Jakab K, Norotte C, Marga F, Murphy K, Vunjak-Novakovic G, et al. (2010) Tissue engineering by self-assembly and bio-printing of living cells. Biofabrication 2: 022001.

[51] Jakosky BM, Nealson KH, Bakermans C, Ley RE, Mellon MT (2003) Subfreezing Activity of Microorganisms and the Potential Habitability of Mars' Polar Regions. Astrobiology 3: 343.

[52] Kennedy KJ, Alexander L, Landis R, Linne D, Mclemore C, et al. (2010) Human Exploration Destination Systems Roadmap .

[53] Keppler-Ross S, Noffz C, Dean N (2008) A new purple fluorescent color marker for genetic studies in *Saccharomyces cerevisiae* and *Candida albicans*. Genetics 179: 705–710.

[54] Ki CS, Um IC, Park YH (2009) Acceleration effect of sericin on shear-induced beta-transition of silk fibroin. Polymer 50: 4618–4625.

[55] Kim JB (2005) Three-dimensional tissue culture models in cancer biology. Seminars in Cancer Biology 15: 365–377.

[56] Komeili A, Li Z, Newman DK, Jensen GJ (2006) Magnetosomes are cell membrane invaginations organized by the actin-like protein MamK. Science 311: 242–245.

[57] Levingstone TJ, Matsiko A, Dickson GR, O'Brien FJ, Gleeson JP (2014) A biomimetic multi-layered collagen-based scaffold for osteochondral repair. Acta Biomaterialia 10: 1996–2004.

[58] Liberski AR, Delaney JT, Schubert US (2011) "One cell – one well": a new approach to inkjet printing single cell microarrays. ACS Combinatorial Science 13: 190–195.

[59] Liu H, Naismith J (2008) An efficient one-step site-directed deletion, insertion, single and multiple-site plasmid mutagenesis protocol. BMC Biotechnology 8: 91.

[60] Löwe J, Amos LA (2009) Evolution of cytomotive filaments: the cytoskeleton from prokaryotes to eukaryotes. The International Journal of Biochemistry & Cell Biology 41: 323–329.

[61] Luz GM, Mano JF (2009) Biomimetic design of materials and biomaterials inspired by the structure of nacre. Philos Trans A Math Phys Eng Sci 367: 1587–1605.

[62] Marin F, Luquet G, Marie B, Medakovic D (2008) Molluscan Shell Proteins: Primary Structure, Origin, and Evolution. In: vol. 80, pp. 209–275, Elsevier.

[63] Mayer G (2011) New toughening concepts for ceramic composites from rigid natural materials. Journal of the Mechanical Behavior of Biomedical Materials 4: 670–681.

[64] McConnell K, Slater J, Han A, West J, Suh J (2011) Microcontact printing for co-patterning cells and viruses for spatially controlled substrate-mediated gene delivery. Soft Matter 7: 4993.

[65] McKittrick J, Chen P, Tombolato L, Novitskaya E, Trim M, et al. (2010) Energy absorbent natural materials and bioinspired design strategies: A review. Materials Science and Engineering: C 30: 331–342.

[66] Merrin J, Leibler S, Chuang JS (2007) Printing multistrain bacterial patterns with a piezoelectric inkjet printer. PLoS ONE 2: e663.

[67] Meyer C (2003) Lunar Regolith. In: NASA Lunar Petrographic Educational Thin Section Set, pp. 46–48, National Aeronautics and Space Administration.

[68] Meyers MA, Chen PY, Lopez MI, Seki Y, Lin AY (2010) Biological materials: a materials science approach. Journal of the Mechanical Behavior of Biomedical Materials 4: 626–657.

[69] Meyers MA, McKittrick J, Chen PY (2013) Structural biological materials: critical mechanics-materials connections. science 339: 773–779.

[70] Miyako E, Sugino T, Okazaki T, Bianco A, Yudasaka M, et al. (2013) Self-assembled carbon nanotube honeycomb networks using a butterfly wing template as a multifunctional nanobiohybrid. ACS Nano 7: 8736–8742.

[71] Nowak PS, Sadeh WZ, Morroni LA (1992) Geometric modeling of inflatable structures for lunar base. Journal of Aerospace Engineering 5: 311.

[72] Olivera ER, Carnicero D, Jodra R, Miñambres B, García B, et al. (2001) Genetically engineered *Pseudomonas*: a factory of new bioplastics with broad applications. Environmental Microbiology 3: 612–618.

[73] Partow S, Siewers V, Bjørn S, Nielsen J, Maury J (2010) Characterization of different promoters for designing a new expression vector in *Saccharomyces cerevisiae*. Yeast 27: 955–964.

[74] Petrov GI, Park KS, Adams CM (2010) Optimization of Inflatable Spacecraft Interior Volume Using Constraints Driven Design Optimization of Inflatable Spacecraft Interior Volume Using Constraints Driven Design. American Institute of Aeronautics and Astronautics, 1-12 pp.

[75] Pirone D, Qi L, Colecraft H, Chen C (2008) Spatial patterning of gene expression using surface-immobilized recombinant adenovirus. Biomed Microdevices 10: 561–566.

[76] Porter D, Vollrath F, Shao Z (2005) Predicting the mechanical properties of spider silk as a model nanostructured polymer. The European Physical Journal E: Soft Matter 16: 199–206.

[77] Porter MM, Novitskaya E, Castro-Ceseña AB, Meyers MA, McKittrick J (2013) Highly deformable bones: Unusual deformation mechanisms of seahorse armor. Acta Biomaterialia 9: 6763–6770.

[78] Raabe D, Sachs C, Romano P (2005) The crustacean exoskeleton as an example of a structurally and mechanically graded biological nanocomposite material. Acta Materialia 53: 4281–4292.

[79] Ratner B, Hoffman A, Schoen F, Lemons J (2004) Biomaterials science: a multidisciplinary endeavor. Biomaterials science: An introduction to materials in medicine pp. 1–19.

[80] Ringeisen BR, Othon CM, Barron JA, Young D, Spargo BJ (2006) Jet-based methods to print living cells. Biotechnology Journal 1: 930–948.

[81] Sabelhaus A, Bruce J, Caluwaerts K, Chen Y, Lu D, et al. (2014) Hardware Design and Testing of SUPERball, a Modular Tensegrity Robot. World Conference of the International Association for Structural Control and Monitoring 6th: 1–11.

[82] Sadeh E, Sadeh ZW, Criswell M, Rice EE, Abarbanel J (2000) Inflatable Habitats of Lunar Base Development Inflatable Habitats of Lunar Base Development, vol. 462. European Space Research and Technology Centre, 301 pp.

[83] Sarikaya M (1999) Biomimetics: materials fabrication through biology. Proc Natl Acad Sci USA 96: 14183–14185.

[84] Séquin C (2005) Rapid prototyping: a 3D visualization tool takes on sculpture and mathematical forms. Communications of the ACM 48: 66–73.

[85] Serrano L (2007) Synthetic biology: promises and challenges. Mol Syst Biol 3: 158.

[86] Sethmann I, Wörheide G (2008) Structure and composition of calcareous sponge spicules: a review and comparison to structurally related biominerals. Micron 39: 209–228.

[87] Shimizu K, Cha J, Stucky GD, Morse DE (1998) Silicatein alpha: cathepsin L-like protein in sponge biosilica. Proceedings of the National Academy of Sciences USA 95: 6234–6238.

[88] Shimizu-Sato S, Huq E, Tepperman J, Quail P (2002) A light-switchable gene promoter system. Nature Biotechnology 20: 1041–1044.

[89] Shore SW, Unnikrishnan GU, Hussein AI, Morgan EF (2012) Bone Biomechanics. In: Winkelstein BA, editor, Orthopaedic Biomechanics, pp. 1–46, CRC Press.

[90] Singh V (2014) Recent advancements in synthetic biology: current status and challenges. Gene 535: 1–11.

[91] Slater MR, Craig EA (1987) Transcriptional regulation of an hsp70 heat shock gene in the yeast *Saccharomyces cerevisiae*. Molecular and Cellular Biology 7: 1906–1916.

[92] Song S, Choi J, Park Y, Hong S, Lee J, et al. (2011) Sodium alginate hydrogel-based bioprinting using a novel multinozzle bioprinting system. Artificial Organs 35: 1132–1136.

[93] Sorokina O, Kapus A, Terecskei K, Dixon L, Kozma-Bognar L, et al. (2009) A switchable light-input, light-output system modelled and constructed in yeast. Journal of Biological Engineering 3: 15.

[94] Sun J, Shao Z, Zhao H, Nair N, Wen F, et al. (2012) Cloning and characterization of a panel of constitutive promoters for applications in pathway engineering in *Saccharomyces cerevisiae*. Biotechnology and Bioengineering 109: 2082–2092.

[95] Sunagawa N, Fujiwara T, Yoda T, Kawano S, Satoh Y, et al. (2013) Cellulose complementing factor (Ccp) is a new member of the cellulose synthase complex (terminal complex) in *Acetobacter xylinum*. Journal of Bioscience and Bioengineering 115: 607–612.

[96] Szot CS, Buchanan CF, Freeman JW, Rylander MN (2011) 3D *invitro* bioengineered tumors based on collagen I hydrogels. Biomaterials 32: 7905–7912.

[97] Taboas JM, Maddox RD, Krebsbach PH, Hollister SJ (2003) Indirect solid free form fabrication of local and global porous, biomimetic and composite 3D polymer-ceramic scaffolds. Biomaterials 24: 181–194.

[98] Takasu Y, Yamada H, Tamura T, Sezutsu H, Mita K, et al. (2007) Identification and characterization of a novel sericin gene expressed in the anterior middle silk gland of the silkworm *Bombyx mori*. Insect Biochemistry and Molecular Biology 37: 1234–1240.

[99] Tatematsu K, Kobayashi I, Uchino K, Sezutsu H, Iizuka T, et al. (2010) Construction of a binary transgenic gene expression system for recombinant protein production in the middle silk gland of the silkworm *Bombyx mori*. Transgenic Research 19: 473–487.

[100] Taylor NG, Howells RM, Huttly AK, Vickers K, Turner SR (2003) Interactions among three distinct *CesA* proteins essential for cellulose synthesis. Proceedings of the National Academy of Sciences USA 100: 1450–1455.

[101] Trim MW, Horstemeyer M, Rhee H, El Kadiri H, Williams LN, et al. (2011) The effects of water and microstructure on the mechanical properties of bighorn sheep (*Ovis canadensis*) horn keratin. Acta Biomaterialia 7: 1228–1240.

[102] Vincent JF (2002) Arthropod cuticle: a natural composite shell system. Composites Part A: Applied Science and Manufacturing 33: 1311–1315.

[103] Vincent JF, Wegst UG (2004) Design and mechanical properties of insect cuticle. Arthropod Structure & Development 33: 187–199.

[104] Volfson D, Cookson S, Hasty J, Tsimring LS (2008) Biomechanical ordering of dense cell populations. Proceedings of the National Academy of Sciences USA 105: 15346–15351.

[105] Wegst U, Ashby M (2004) The mechanical efficiency of natural materials. Philosophical Magazine 84: 2167–2186.

[106] Wegst UG (2011) Bending efficiency through property gradients in bamboo, palm, and wood-based composites. Journal of the Mechanical Behavior of Biomedical Materials 4: 744–755.

[107] Weiss IM, Kirchner HO (2011) Plasticity of two structural proteins: alpha-collagen and beta-keratin. Journal of the Mechanical Behavior of Biomedical Materials 4: 733–743.

[108] Xia XX, Qian ZG, Ki CS, Park YH, Kaplan DL, et al. (2010) Native-sized recombinant spider silk protein produced in metabolically engineered Escherichia coli results in a strong fiber. Proceedings of the National Academy of Sciences USA 107: 14059–14063.

[109] Xu H, Cao B, George A, Mao C (2011) Self-assembly and mineralization of genetically modifiable biological nanofibers driven by beta-structure formation. Biomacromolecules 12: 2193–2199.

[110] Xu T, Kincaid H, Atala A, Yoo J (2008) High-throughput production of single-cell microparticles using an inkjet printing technology. Journal of Manufacturing Science and Engineering 130: 020601.1–024503.5.

[111] Xu T, Petridou S, Lee E, Roth E, Vyavahare N, et al. (2004) Construction of high-density bacterial colony arrays and patterns by the ink-jet method. Biotechnol Bioeng 85: 29–33.

[112] Yang M, Shuai Y, Zhang C, Chen Y, Zhu L, et al. (2014) Biomimetic Nucleation of Hydroxyapatite Crystals Mediated by *Antheraea pernyi* Silk Sericin Promotes Osteogenic Differentiation of Human Bone Marrow Derived Mesenchymal Stem Cells. Biomacromolecules 15: 1185–1193.

[113] Zhang K, Chou CK, Xia X, Hung MC, Qin L (2014) Block-Cell-Printing for live single-cell printing. Proceedings of the National Academy of Sciences USA 111: 2948–2953.

[114] Zhang W, Zhang D, Fan T, Gu J, Ding J, et al. (2008) Novel photoanode structure templated from butterfly wing scales. Chemistry of Materials 21: 33–40.

[115] Zhou CZ, Confalonieri F, Medina N, Zivanovic Y, Esnault C, et al. (2000) Fine organization of *Bombyx mori* fibroin heavy chain gene. Nucleic Acids Research 28: 2413–2419.

[116] Ziauddin J, Sabatini DM (2001) Microarrays of cells expressing defined cDNAs. Nature 411: 107–110.

[117] Zsebo KM, Lu HS, Fieschko JC, Goldstein L, Davis J, et al. (1986) Protein secretion from *Saccharomyces cerevisiae* directed by the prepro-alpha-factor leader region. Journal of Biological Chemistry 261: 5858–5865.

A Press & Publications

The project has received significant publicity. We have received requests for collaboration from other institutions, including labs at Stanford University and Drexel University; we will propose to work with at least one of these potential collaborators in our Phase II proposal. We have also received visits from industry, including Organovo, a tissue engineering company, and Autodesk, a major 3D and materials design software company.

The project has also been featured in the popular press. A partial list of publications includes:

- TechCrunch (http://techcrunch.com/2014/02/09/how-nasa-prints-trees/)
- VICE's Motherboard
- ENGINEERING.com (http://www.engineering.com/3DPrinting/3DPrintingArticles/ArticleID/7132/NASA-Research-Aims-to-Print-Wood-in-Space.aspx)
- 3Ders.org (http://www.3ders.org/articles/20140210-nasa-to–3d-print-wood-in-space.html)
- Newsweek (http://www.newsweek.com/2014/05/30/recycling-mars–251740.html)

A New Technology Report (ARC–17157–1) was submitted for this project in March 2013 and is currently in review for patentability at the Patent Counsel Office at NASA Ames Research Center.

B Recipes, Protocols and Sequences

B.1 Plasmid Maps

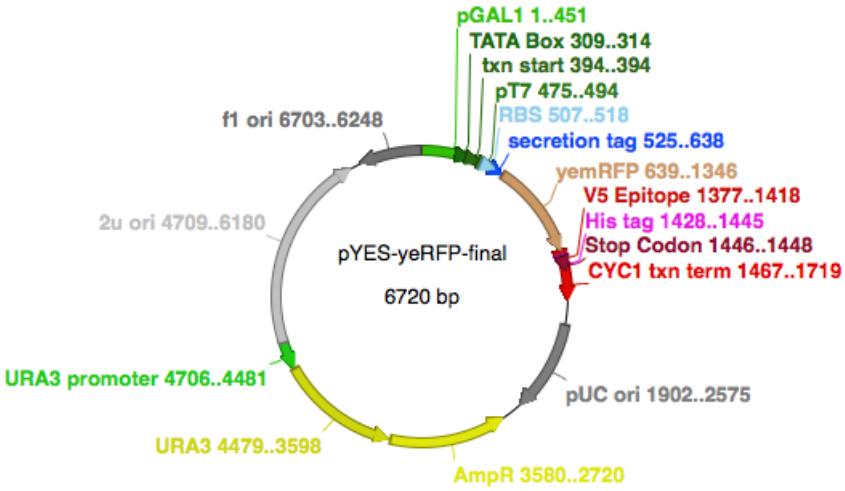

Figure B.1: The plasmid backbone used for our RFP-producing yeast cells.

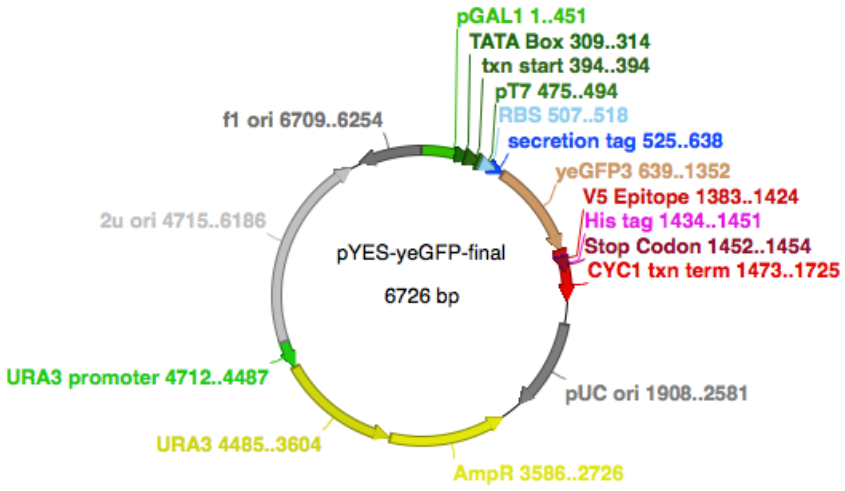

Figure B.2: The plasmid backbone used for our GFP-producing yeast cells.

B.2 Print Medium Composition

The print medium we developed and tested for this work, as described in the main body of the report, is detailed below. This recipe is for dextrose as the sugar type; galactose is substituted at a 1–1 ratio for stimulus control. For a 300 mL final volume:

1. Combine:
    - 2.01g yeast nitrogen base
    - 0.576 g yeast synthetic drop-out medium (uracil deficient)
    - If any other additives are required for the specific experiment, add them now unless they will not survive the autoclave.
    - DI water to a total of 270 mL
2. Autoclave the mixture.
3. After cooling until the flask is safe to touch, add:
    - 30 mL of a sterile 20% dextrose solution (2% sugar final concentration)
    - 300 μL of a 1000x concentrated ampicillin solution (1x final concentration)
    - any experiment-specific additives that would not have survived the autoclave, which must have been sterilized by other means
4. Store at 4 °C.

B.3 Print Substrate Composition

The print substrate we developed and tested for this work, as described in the main body of the report, is detailed below. For a 300 mL final volume:

1. Combine:
    - 2.01g yeast nitrogen base
    - 0.576 g yeast synthetic drop-out medium (uracil deficient)
    - 9g agarose
    - (If any other additives are required for the specific experiment, add them now unless they will not survive the autoclave.)
    - DI water to a total of 270 mL
2. Autoclave the mixture.
3. After cooling until the flask is safe to touch, add:
    - 30 mL of a sterile 20% galactose solution (2% sugar final concentration)
    - 300 μL of a 1000x concentrated ampicillin solution (1x final concentration)
    - any experiment-specific additives that would not have survived the autoclave, which must have been sterilized by other means
4. In a sterile environment, pour into petri dishes, and once the agar has gelled, store at 4 °C.